Influence of large-scale climate variability on upwelling regimes off the Namibian coast: implications for past and future climates

Dissertation

zur Erlangung des Doktorgrades
an der Fakultät für Mathematik, Informatik und Naturwissenschaften
im Fachbereich Geowissenschaften der Universität Hamburg

vorgelegt von

Nele Tim

Hamburg

2015

Tag der Disputation:
Freitag, 04.12.2015

Folgende Gutachter empfehlen die Annahme der Dissertation:

Dr. Eduardo Zorita
Prof. Dr. Kay-Christian Emeis

Abstract

Detecting the atmospheric drivers of an upwelling system is essential to understand its present variability and its past and future changes. This thesis presents a statistical analysis of the upwelling simulated in several climate simulations, with the main focus placed on the Benguela upwelling system. The simulations are two high-resolution ocean-only simulations driven by observed atmospheric fields over the last 60 years and 13 years with the aim of identifying the large-scale atmospheric drivers of Benguela upwelling variability and trends. The simulations are found to reproduce well the seasonal cycle of upwelling intensity, with a maximum in the austral winter season (June–August) in North Benguela and in the austral summer season (December–February) in South Benguela.

The statistical analysis of the interannual variability of upwelling focuses on its relationship to atmospheric variables (sea level pressure, 10 m-wind, and wind stress). The relationship between upwelling and the atmospheric variables differ somewhat in the two regions, but generally the correlation patterns reflect the common atmospheric pattern favouring upwelling: southerly wind/wind stress, strong subtropical anticyclone, and an ocean-land sea level pressure gradient.

In addition, the statistical link between upwelling and large-scale climate variability modes is analysed. Among the various climate modes, the El Niño-Southern Oscillation and the Antarctic Oscillation exert some influence on austral summer upwelling velocities in South Benguela. North Benguela seems to be slightly influenced by the tropical Atlantic indicating the possible impact of warm water intrusions of equatorial origin (Benguela Niños). The El Niño-Southern Oscillation may also contribute to extreme events in upwelling due to changes in the Walker circulation, and changes in the strength of the trade winds.

The decadal evolution and the long-term trends of simulated upwelling and of the ocean-land sea level pressure gradient do not agree with Bakun's hypothesis that anthropogenic climate change should generally intensify coastal upwelling. This hypothesis has been further tested, also in the three other Eastern Boundary Upwelling Systems (Peru, California, and Morocco), by the use of ensemble simulations of two Earth System Models simulating the last millennium. On this centennial time scale the imprint of external forcing cannot be seen in the upwelling, too. The internal variability of the atmospheric circulation is so large that the imprint of the external forcing is not detectable. Furthermore, for future climate, a significant change could be detected for the next 100 years only with the scenario of the most drastic increase of greenhouse gas concentrations. Nevertheless, the direction of these changes differ among the four upwelling regions. Thus, the future development of upwelling systems in the eastern boundary currents of the ocean seems to be not easily predicted

and not closely connected to anthropogenic climate forcing.

The conclusions of this study depend on the realism of the atmosphere and ocean models analysed. Their spatial resolution, limited by computing requirements, may in some cases still be too coarse. Future studies with higher-resolution models should confirm the conclusions presented here.

Zusammenfassung

In dieser Arbeit wird der atmosphärische Antrieb des Benguela Auftriebsgebiets untersucht. Dies ist von essentieller Bedeutung, um die Variabilitäten und Änderungen des Auftriebs vor der Küste Angolas, Namibias und Südafrikas in der Vergangenheit und Zukunft zu verstehen. Diese Doktorarbeit beinhaltet eine statistische Analyse zweier Ozeansimulationen der letzten 60 bzw. 13 Jahre mit dem Ziel die großkaligen atmosphärischen Antriebsmuster, Variabilitäten und Trends zu identifizieren. Die simulierten Jahresgänge decken sich mit beobachteten und zeigen für Nordbenguela ein Maximum im Südwinter (Juni–August) und für Südbenguela ein Maximum im Südsommer (Dezember–Februar).

Die statistische Analyse des atmosphärischen Antriebs fokussiert sich auf den Luftdruck, den 10 m-Wind und den Windstress. Nicht nur der Jahresgang, sondern auch der Einfluss der atmosphärischen Variablen unterscheidet sich zwischen Nord- und Südbenguela. Im Allgemeinen zeigt sich aber, dass ein verstärktes Südatlantik-Hoch, starke südöstliche Passatwinde/Windstress und ein starker Luftdruckunterschied über dem Ozean und dem angrenzenden Land den Auftrieb verstärken.

Zusätzlich wird der statistische Zusammenhang zwischen einigen Klimaindizes und dem Auftrieb untersucht. Die El Niño-Southern Oscillation und die Antarktische Oszillation haben einen stärkeren Einfluss auf den Auftrieb in Südbenguela im Südsommer als auf den Auftrieb in Nordbenguela. Nordbenguela ist zudem vom tropischen Atlantik beeinflusst. Sogenannte Benguela Niños sind Extremevents wenn äquatoriales warmes Wasser außerordentlich weit nach Süden entlang der Westafrikanischen Küste transportiert wird. Die El Niño-Southern Oscillation scheint auch zu Extrema im Auftrieb durch die Änderungen in der Walker-Zirkulation beizutragen und dadurch entstehende Änderungen in der Stärke der Passatwinde.

Dekadische und langfristige Trends im Auftrieb und im Ozean-Land Luftdruckunterschied stimmen nicht mit der Hypothese Bakuns überein, dass anthropogener Klimawandel den Küstenauftrieb verstärkt. Diese Hypothese wurde zudem anhand zweier Erdsystemmodellsimulationen, die das letzte Jahrtausend abdecken, untersucht. Auch auf diesen Zeitskalen hat das externe Klimaforcing keinen signifikanten Einfluss auf den Auftrieb, weder im Benguela Auftriebsgebiet noch in den anderen Ostrandstrom-Auftriebsgebieten (Peru, Kalifornien und Marokko). Die interne Variabilität der atmosphärischen Zirkulation ist so groß, dass der Einfluss des externen Forcings nicht zu erkennen ist. Auch in den Szenarien des 21. Jahrhunderts zeigt sich nur bei dem Szenario mit dem drastischsten Treibhausgasanstieg ein Einfluss auf den Auftrieb. Allerdings variiert die Richtung der Änderung mit den Auftriebsregionen. Deshalb scheint die zukünftige Entwicklung des Auftriebs in den Ostrandströmen nicht ohne weiteres vorhersagbar und nicht linear an das anthropogene

Klimaforcing gekoppelt zu sein.

Die Schlussfolgerungen dieser Arbeit hängen von der Qualität der Ozean- und Atmospärenmodelle ab. Deren horizontale Auflösung mag in einigen Fällen zu gob sein. Zukünftige Studien mit Modellen mit höher Auflösung sollten die Ergebisse bestätigen.

Contents

<div align="right">

Chapter 1

Introduction

</div>

1.1 Upwelling systems

The world ocean presents distinct regions where vertical mass transport from the deeper layers towards the surface is specially intense. These areas are important from the climate point of view because they provide a way by which temperature and salinity of the deeper layers can mix with water masses close to the surface in an ocean that is in general terms stratified. On the other hand, upwelling transports nutrient rich water masses into the biologically more active layers where primary production takes place. They are, therefore, important for the global geochemical and biogeochemical cycles.

Upwelling regions can be generally classified in two types, open ocean upwelling and coastal upwelling. Persistent open ocean upwelling takes place in equatorial regions and in the centre of low pressure systems in subpolar regions due to the Ekman transport. The Coriolis force, directed to the right of the velocity in the Northern Hemisphere and to the left of the velocity in the Southern Hemisphere, induces a surface divergence by a net surface water transport. Coastal upwelling occurs mainly in the subtropical trade wind regions. In coastal upwelling regions, the alongshore trade winds induce the upward transport of cold and nutrient-rich water of deeper layers to surface layers by the offshore transport of water directed perpendicular to the wind stress forcing (Fig. 1.1). In these subtropical regions, the direction of the wind associated to the semi-permanent subtropical high-pressure systems is roughly parallel to the meridional orientation of the coastal profiles and thus the intensity of the subtropical highs impacts the intensity of subtropical coastal upwelling. This thesis deals with coastal upwelling. Therefore, hereafter, the term upwelling corresponds to coastal upwelling.
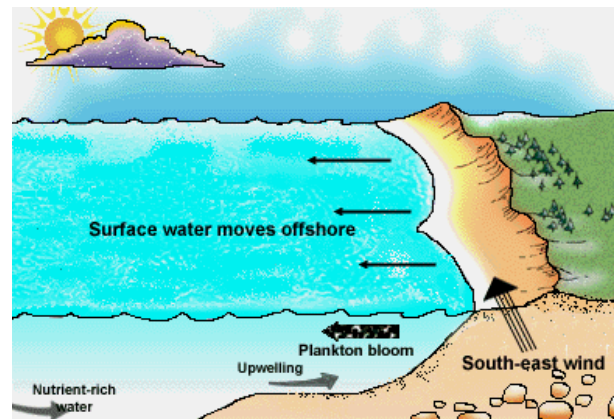
Figure 1.1: Schematic picture of southern hemisphere coastal upwelling. Source:
$http://disc.sci.gsfc.nasa.gov/education-and-outreach/images/Benguela\_upwelling.gif$.

The four major coastal upwelling regions are the Eastern Boundary Upwelling Systems (EBUSs), located in the subtropics at the eastern side of the Atlantic and Pacific Ocean. These EBUSs are the California upwelling system off California and Oregon, the Humboldt upwelling system off Peru and Chile, the Canary upwelling system off the Canary Islands and Northwest Africa, and the Benguela upwelling system off Angola, Namibia, and South Africa (Chavez and Messié, 2009) (Fig. 1.2). These four regions cover around 1 % of the worlds ocean but contain 25 % of its biological productivity (Pauly and Christensen, 1995). Coastal upwelling in the EBUSs are mainly driven by the trade winds (Bakun and Weeks, 2004), forced by the high pressure systems over the subtropical open ocean, adjacent to the upwelling system (Mackas et al., 2006). Coastal upwelling is generally strongest in the summer of the respective hemisphere, with stronger seasonality at higher latitudes (Chavez and
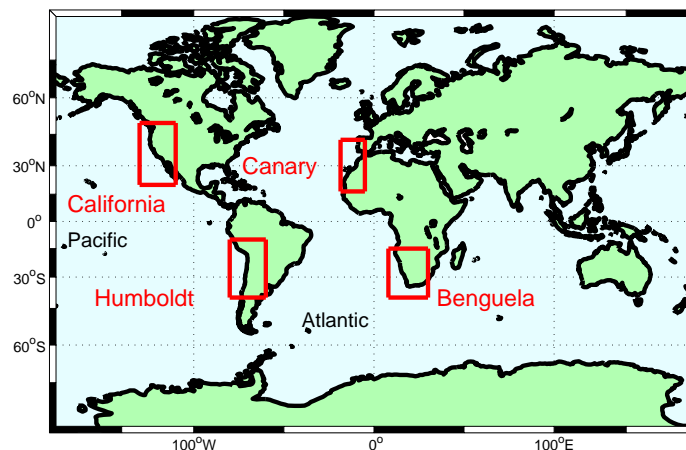
Figure 1.2: Map of the four Eastern Boundary Upwelling Systems (red boxes). In the Atlantic Ocean, there are the Canary upwelling system (Northern Hemisphere) and the Benguela upwelling system (Southern Hemisphere). In the Pacific Ocean, there are the California upwelling system (Northern Hemisphere) and the Humboldt upwelling system (Southern Hemisphere).

Messié, 2009). Due to its high productivity, these regions are of major importance
to fisheries and thus to the economy of adjacent countries. Therefore, variabilities
and trends of these regions are of large interest not only to researchers but also to
policy makers with respect to environmental and economic issues.

1.2   The Benguela upwelling system

The Benguela upwelling system (BUS) is located off Angola, Namibia, and South
Africa (Blanke et al., 2005). This region is characterised by the Benguela Current,
a cold current along the west coast of southern Africa that flows northward until
around 15° S (Hutchings et al., 2009), fed by the South Atlantic Current and Ag-
ulhas rings (Gordon et al., 1992) (Fig. 1.3). The Benguela Current is the eastern
boundary current of the South Atlantic and the eastern branch of the subtropical
gyre. The uniqueness of the BUS is that it has warm currents at its boundaries, the
Angola Current and the Agulhas Current (Hutchings et al., 2009). The Angola Cur-
rent reaches the Benguela region from the north. The Agulhas Current flows from
the Indian Ocean westward around South Africa and reflects south of Cape Town
at the Agulhas retroflection. Therefore, the BUS is characterised by water masses
with strong differences in their characteristics. The South Atlantic Central Water
(SACW) is transported by the Angola Current from the tropics towards Benguela.
This water mass is warm, nutrient-rich, and oxygen-poor. The Eastern South At-
lantic Central Water (ESACW) forms at the southern boundary of the BUS, in the
Cape regions, and is oxygen rich and nutrient poor. The oxygen concentration on
the shelf depends on the relative contribution from these two water masses, which
in turn is driven by the strength of the local currents (Mohrholz et al., 2008).
The climate over the Benguela region and the adjacent countries (as described by
Rathmann (2008)) is strongly influenced by the subtropical high pressure system,
the extratropical westerlies and the previously described ocean currents. The sea-
sons are better defined by precipitation rather than by temperature. Precipitation
and temperature reach their minimum in austral winter, with lowest precipitation
values in the Namib and Kalahari desert, an exception being the region around Cape
Town where precipitation amounts are high in austral winter due to the westerlies
in the south of the continent. The subtropical high, the St. Helena high, reaches its
southernmost position in February and its northernmost position in May, when it
is strongest. Its position and intensity impact the trade winds and in particular the
southeasterly trades, which dominate the Benguela region. This wind system causes
Ekman transport in the Benguela region which leads to the upwelling of nutrient-rich
cold water of deeper layers (Tomczak and Godfrey, 2003). The trade-wind-induced
upwelling takes place between the Angola-Benguela front, the northern boundary
of the BUS (Shannon and Nelson, 1996), Cape Agulhas, the southern boundary
(Shannon and Nelson, 1996), and Port Elizabeth, the eastern boundary (Shannon
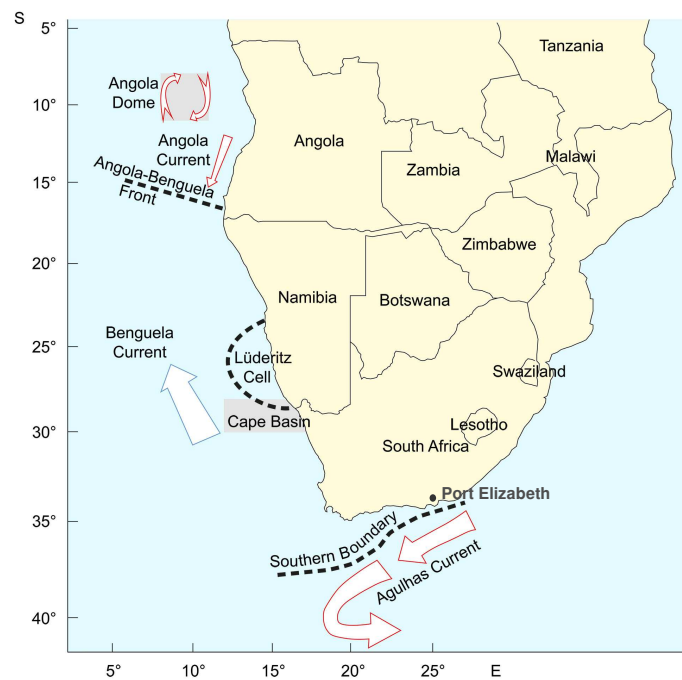
Figure 1.3: Map of the Benguela upwelling system (BUS). The BUS is located off Angola, Namibia, and South Africa with the strongest upwelling cell, the Lüderitz cell, in its middle. The northern boundary is the Angola-Benguela front, the southern boundary is just south of the African continent at Port Elizabeth. The dominant ocean current in the BUS is the Benguela Current.

and O'Toole, 2003) (Fig.1.3).

Strongest upwelling occurs at Lüderitz (~28° S) where upwelling takes place all year round (Shannon and Nelson, 1996). This upwelling cell is often used as a boundary between the North Benguela upwelling system and the South Benguela upwelling system. Both upwelling systems behave quite differently in their seasonality (Tim et al., 2015). In the north, upwelling is strongest in austral winter and spring when the subtropical high is at its northernmost position (Rathmann, 2008) and the trade winds are strongest in this region (Hutchings et al., 2009). In contrast, in the south the upwelling is strongest in austral summer when the subtropical high has moved to its southernmost position (Rathmann, 2008) and winds are upwelling-favourable there (Hutchings et al., 2009).

1.2.1   Atmospheric drivers of the Benguela upwelling system

Upwelling is strongly driven by the atmosphere. The large-scale sea level pressure (SLP) field with the subtropical high and the continental low lead to alongshore wind at the coast (Bakun and Weeks, 2004) and induce a wind stress curl further offshore (Fennel and Lass, 2007). Therefore, when investigating the variability and trends of the upwelling system, it is essential to analyse the variability and trends

of the atmospheric drivers.

Additionally, climate modes influence the Benguela upwelling and its strength on interannual or decadal time scales (e.g. Shannon et al., 1986; Jones and Widmann, 2004; Dufois and Rouault, 2012). For the BUS, there are the following climate modes that seem to impact the upwelling:

The St. Helena Island Climate Index (HIX) is an index of the strength of the St. Helena high, the subtropical high over the South Atlantic Ocean (Hagen et al., 2005). The index is the first mode of the Empirical Orthogonal Function (EOF) Analysis of air temperature, SLP, and precipitation (Hagen et al., 2005). Due to its positive correlation with the southeasterly trades, it possibly modulates the strength of the upwelling (Hagen et al., 2005). As described before, the position of the subtropical high has a substantial influence on the upwelling by defining its seasonality.

The Antarctic Oscillation (AAO), also called Southern Hemisphere Annular Mode (SAM), seems to modulate the upwelling in the BUS as well (Jones and Widmann, 2004). It is calculated as the SLP difference between mid and high latitudes of the Southern Hemisphere and is thus related to the strength and the position of the circumpolar westerly flow (Jones and Widmann, 2004). During the positive phase, when westerlies are located more closely to Antarctica, upwelling is in favour (Tim et al., 2015).

Coupled modes of atmosphere-ocean variability are also thought to influence Benguela upwelling, although the mechanisms are not totally understood, and the magnitude of their influence is still debated. The most prominent climate mode, the El Niño Southern-Oscillation (ENSO), is thought to modulate the Benguela upwelling on interannual time scales (Shannon and Nelson, 1996; Rouault et al., 2010). During its positive phase, the warm El Niño phase, upwelling is reduced while during the negative phase, the cold La Niña phase, upwelling is intensified (Rouault et al., 2010). The ENSO signal would enter the BUS via atmospheric teleconnections (Dufois and Rouault, 2012). The time lag until the ENSO signal reaches the South Atlantic is around six months (Latif and Grötzner, 2000; Rodríguez-Fonseca et al., 2009) or one season (Colberg and Reason, 2006).

Similar to ENSO are the Atlantic Niños, the Atlantic counterpart to the dominant climate mode in the Pacific. More frequently but less intense than the tropical Pacific (Shannon et al., 1986), the tropical Atlantic may unusually warm due to reduced equatorial trades (McCartney, 1982). This warm water anomaly is transported by Kelvin waves eastward along the equator (Rouault et al., 2007). Less frequently than the Atlantic Niños, the so-called Benguela Niño may also occur (Hardman-Mountford et al., 2003). This happens when the warm water anomaly is further transported southward along the west coast of Africa by the Angola Current reaching more far south than normally, south to Lüderitz (Shannon et al., 1986). Richter et al. (2010) mentioned that this happens due to a relaxation of the alongshore winds in the BUS because of a weakening of the St. Helena high. This may explain why the signal of such extreme events could be seen not only in the sea

surface temperature (SST) but also in the wind and the upwelling itself.
Understanding the atmospheric drivers of the upwelling and analysing their vari-
ability and contribution to long-term trends in upwelling is one main subject of this
thesis. Two ocean-only simulations, together with observational-based atmospheric
reanalysis data, give an insight into the response of the upwelling system to atmos-
pheric forcing. Furthermore, investigating the mechanisms of the ocean-atmosphere
interactions leading to extreme events in upwelling is subject of this thesis. This
understanding may contribute to predict a few month in advance events of intensive
or weak upwelling which could cause local changes in fish stock, precipitation, and
temperature.

1.2.2   Trends of the Benguela upwelling system

The investigation of the recent and long-term trends of the BUS are the other main
part of this thesis. The main hypothesis of the present and future long-term evo-
lution under increasing external climate forcing was put forward in an often cited
paper by Bakun (1990), who stated that upwelling will intensify due to anthro-
pogenic climate change. The hypothesis behind this is that due to the increase in
greenhouse gas concentrations the surface temperature over land will heat up more
rapidly than over the ocean and this increasing temperature contrast should inten-
sify the subtropical oceanic highs as well as the continental lows. This enhanced
SLP gradient would cause an intensification of upwelling-favourable alongshore trade
winds over the upwelling regions (Bakun, 1990). The intensification of long-term
trends in upwelling in the present climate turned to be challenging due to the limited
direct observations available. Later, Bakun et al. (2010) relativised his hypothesis
to account for the lack of long-term upwelling trends in some of the EBUSs and
proposed that the positive trend caused by to rising greenhouse gas concentrations
may be masked by the recent strong ENSO events, which have an impact on the
global tropical climate system.
Recent studies have identified upwelling trends in the Benguela region that support
but also contradict Bakun's hypothesis (Tab. 1.1). Narayan et al. (2010) found a
positive trend in observed meridional wind stress at Lüderitz over 1960–2000. In
agreement, Demarcq (2009) detected a positive trend in upwelling-favourable winds
in Benguela for 2000–2007 in observations and Sydeman et al. (2014) found positive
trends over the last 60 years poleward of 20° S in several wind data sets. In contrast,
the study of Narayan et al. (2010) shows no trend over 1960-2000 when analysing
reanalysis data (ERA40).
Using SST as indicator for the upwelling, no trend (Demarcq, 2009), positive trends
(Narayan et al., 2010; Santos et al., 2012), and a negative trend (Narayan et al.,
2010) for upwelling in Benguela or around Lüderitz have been detected, depending
on the analysed period as well as the data set used.
Two studies, Feistel et al. (2003) and Hagen et al. (2005), indicate a weakening of

Table 1.1: Upwelling trends in the Benguela upwelling system

Author(s)	Trend	Variable	Time period	Region
Bakun (1990)	+	wind stress	1950–1986	EBUSs (excl. Benguela)
Narayan et al. (2010)	+	wind stress	1960–2000	Lüderitz
Demarcq (2009)	+	wind	2000–2007	Benguela
Sydeman et al. (2014)	+	wind	up to last 60 years	poleward of 20° S
Demarcq (2009)	no trend	SST	1998–2007	Benguela
Narayan et al. (2010)	+	SST	1871–2006	Lüderitz
Narayan et al. (2010)	–	SST	1960–2006	Lüderitz
Santos et al. (2012)	+	SST	1970–2009	20–35° S
Hagen et al. (2005)	–	HIX	1930–1985	St. Helena
Feistel et al. (2003)	+	SLP	1893–1999	St. Helena
Pardo et al. (2011)	+	Ekman transport	1948–2009	central Benguela
Pardo et al. (2011)	–	Ekman transport	1948–2009	northern and southern limits of Benguela
Wang et al. (2015)	+	upwelling	1950–2099	EBUSs
Blamey et al. (2015)	–	fish stock	last years	Benguela

the St. Helena high. However, Pardo et al. (2011), after analysing reanalysis data (NCEP/NCAR), mentioned that Ekman transport seems to have intensified in central Benguela, but weakened at the northern and southern limits of the upwelling region.

On centennial time scales of the past, sediment cores are sometimes used as proxy for upwelling due to the lack of direct observations, satellite or reanalysis data. However, the proxies derived from sediment cores are usually an indicator of water temperatures and not a direct indicator of upwelling velocities. The usual interpretation of the sediment cores located in upwelling regions is that colder temperatures are linked to stronger upwelling. This interpretation may be challenged on the basis that external climate forcing can also cause large-scale temperature changes that regionally may be unrelated to upwelling. Regarding the future, possible trends of upwelling in future scenarios of climate models have been recently analysed by Wang et al. (2015), who found that under a strong increase of greenhouse gases the upwelling would intensify, in accordance with Bakun's hypothesis.

Fish stock studies generally indicate a decrease over the last years. This seems to be mainly due to overfishing but could partly also be caused by climate factors (Blamey et al., 2015), so that it is difficult to establish a direct connection between the variability and trend in fish stocks and upwelling.

Overall, recent studies do not agree whether there is already an ongoing trend in upwelling, nor do they agree on its sign. The result of the trend analysis depends on the type of data set used, the temporal coverage and variable used as indicator for upwelling. Therefore, in this thesis, the trend of modelled upwelling is analysed in a high-resolution ocean simulation for a relatively long period, the past six decades. This simulation has been driven by global meteorological reanalysis and, therefore, the simulated temporal evolution should ideally mimic the real evolution of the ocean over this period. In addition, a set of simulations with two coupled climate models is used to detect the influence of the external forcing on upwelling over the past mil-

lennium, in the last 150 years, and in the 21st century. Using a set of simulations is
a beneficial way of addressing the question whether variabilities and possible trends
are driven by external forcings, such as greenhouse gas concentrations. If the exter-
nal forcing imposes trends on simulated upwelling, the trends should be similar in
all simulations. If, in contrast, there is no clear agreement in the temporal evolution
simulated in the different members of the simulation ensemble, these variabilities
or trends are more likely due to internal climate variability. For local fisheries, it
is of major importance to know how internal variability and anthropogenic-induced
climate changes impact the ecosystem in the Benguela region. Even if the fishing
pressures may presently be the strongest driver of fish stock (Blamey et al., 2015),
anthropogenic climate change may bring about profound changes in the upwelling
ecosystem due to ocean acidification, caused by the increase in carbon dioxide in the
atmosphere, deoxygenation, rising water temperatures and wind changes. It is the
objective of this thesis to quantify and disentangle the upwelling variability that can
be attributed to the forcing of the atmospheric circulation at different time scales
and estimate to what extent the increase of the external radiative forcing linked to
rising concentrations of greenhouse gases in the atmosphere may change the wind
regimes that presently sustained coastal upwelling in the EBUSs.

1.3   Thesis Objective

This thesis is conducted within the second phase of the GENUS Project, the Geo-
chemistry and Ecology of the Namibian Upwelling System Project, funded by the
BMBF (Federal Ministry of Education and Research) of Germany. The first phase
ran from March 2009 to April 2012. The subsequent second phase ended in April
2015 and had the topic: Impact of climate change on biogeochemical cycles and
ecological processes in the shelf region of the South Atlantic. This interdisciplinary
project was carried out by several German research institutions covering atmosphe-
ric and oceanic science, physical, biological, chemical, and biogeochemical aspects
of the Namibian upwelling system.
This thesis is part of the Sub-Project 1 of GENUS II. Sub-Project 1 had the goal
to examine statistically long-term observational time series as well as global and re-
gional model runs with regard to imprint of external influences on internal patterns
of the Benguela upwelling system, to detect climatological changes of the system,
and processes driving the ecosystem status. Due to the lack of long-term observa-
tional data sets, I focused on regional and global model outputs, as well as reanalysis
data.
To address the aims of the project, I raised the following five research questions and
tried to answer them in my thesis. The first three focus on the Benguela upwelling
system, whereas the last two cover all four EBUSs for comparison reasons and due
to the global scale of climate change.

- What are the atmospheric drivers of the Benguela upwelling system?

- Are there any multi-decadal trends in the Benguela upwelling?

- How do years of extreme upwelling in Benguela differ from the climatological mean with regard to their drivers and oceanic responses?

- How did upwelling in the Eastern Boundary Upwelling Systems change in the last thousand years and how sensitive it is to external forcing, especially anthropogenic forcing due to greenhouse gas concentrations?

- How might the upwelling in the Eastern Boundary Upwelling Systems change in the future under global climate change?

1.4   Thesis Outline

The thesis contains four main chapters, chapter 2 to chapter 5. Two of them have been published or prepared for peer-reviewed publication. A short presentation of the chapters content is given in the following. The data sets used in this thesis are described in table 1.2

In chapter 2, I present a statistical analysis of a high-resolution (0.1 deg) ocean-only simulation (STORM), driven by observed atmospheric fields over the last 60 years. My aim was to identify the large-scale atmospheric drivers of upwelling variability and trends in the Benguela upwelling system. The seasonal cycle of upwelling intensity is reproduced well by the simulation, showing a maximum in the June–August season in North Benguela and in the December–February season in South Benguela. The statistical analysis of the interannual variability of upwelling focuses on its relationship to atmospheric variables (SLP, 10 m-wind, and wind stress). The relationship between upwelling and the atmospheric variables is slightly different in the two regions, but generally agrees that southerly wind/wind stress, strong subtropical anticyclone, and a strong ocean-land SLP gradient all favour upwelling in the Benguela region. Furthermore, the statistical link between upwelling and large-scale climate variability modes is analysed. The El Niño-Southern Oscillation and the Antarctic Oscillation have an influence on upwelling velocities in austral summer in South Benguela. The Bakun hypothesis that anthropogenic climate change should generally intensify coastal upwelling is not supported by the decadal evolution and the long-term trends of simulated upwelling and of the ocean-land SLP gradient.

In chapter 3, I provide a companion of the study in chapter 2 by analysing another high-resolution ocean-only simulation, a regional one, that includes the biogeochemistry and brackets the last 13 years (GENUS-MOM). This simulation was conducted within the GENUS project (Sub-Project II) with the aim of detecting interactions

Table 1.2: Description of the data sets used in this thesis

Acronym	Data description	Time period	Grid [°]
NCEP/NCAR	reanalysis data	1948–2011	2.5
ERA-Interim	reanalysis data	1979–2010	0.70
HadISST1	global gridded observations	1870–2012	1
STORM	global ocean-only simulation/model MPI-OM	1950–2010	0.1
GENUS-MOM	regional ocean-only simulation	July 1999–May 2012	0.07
MPI-ESM past1000	global coupled Earth System Model simulation	850–1850	1.9 (atm.), 1 (ocean)
MPI-ESM historical	global coupled Earth System Model simulation	1850–2005	1.9 (atm.), 0.4 (ocean)
MPI-ESM future	global coupled Earth System Model simulation	2006–2100	1.9 (atm.), 1 (ocean)
MPI-ESM pre-industrial	global coupled Earth System Model simulation	1850–3005	1.9 (atm.), 1 (ocean)
CESM-CAM5 past1000	global coupled Earth System Model simulation	850–1850	2 (atm.), 1 (ocean)
CESM-CAM5 historical	global coupled Earth System Model simulation	1850–2005	2 (atm.), 1 (ocean)
CCSM4 past1000	global coupled Earth System Model simulation	850–1850	1 (atm., ocean)
CCSM4 pre-industrial	global coupled Earth System Model simulation	800–1300	1 (atm., ocean)
MEI	Multivariate ENSO (El Niño-Southern Oscillation) Index	1950–2012	
AAO	Antarctic Oscillation	1957–2012	
ATL-3	tropical Atlantic SST (HadISST1, STORM)	1870–2012 and 1950–2010	1 and 0.1
AMM	Atlantic Meridional Mode	1948–2012	
HIX	St. Helena Island Climate Index	1892–2012	
QBO	Quasi-Biennial Oscillation	1979–2012	
AVHRR	pathfinder 5.0, remote-sensed SST	1985–2009	0.04
QuikSCAT	satellite based observations	August 1999–October 2009	1

between oceanic physics and biogeochemical parameters as well as to provide a continuous time series of data to compare it with the observations measured on cruises with research vessels. Both simulations, the STORM simulation and the GENUS-MOM simulation, agree on the annual cycle, the main atmospheric drivers of the upwelling, and the impact of ENSO and the AAO, but differ in the connection of upwelling to SST.

In chapter 4, I describe my analysis of the extrema in upwelling and its predictability. Here I use the Earth System Model of the Max Planck Institute for Meteorology (MPI-ESM) past1000 simulation as well as the Community Climate System Model version 4 (CCSM4) and the STORM simulation for comparison. In extreme years of upwelling, the season preceding the main upwelling season shows upwelling-unfavourable conditions in wind stress and positive anomalies in SSTs. The same is found when looking at the years of extreme weak upwelling, when in the season previous to this event wind stress is upwelling-favourable and the SST shows negative anomalies.

In chapter 5, the impact of external climate forcing, such as greenhouse gases and solar activity, on the four EBUSs is presented. Under increased radiative forcing, surface temperature should warm faster over the land than over the oceans, resulting in an intensification of the subtropical continental lows and the oceanic highs and a strengthening the upwelling-favourable winds. However, coastal upwelling simulated in two ensembles of climate simulations with two Earth System Models (MPI-ESM and CESM-CAM5) over the past millennium do not show any imprint of external forcing. The ensemble of future scenarios of the MPI-ESM indicate that the imprint of external forcing on upwelling is only detectable under an extreme increase of greenhouse gas concentrations. These results undermine the claimed connection between upwelling and external forcing, strongly suggesting that chaotic

internal variability has dominated upwelling intensity in major upwelling regions over the past centuries and will further dominate unless the anthropogenic forcing dramatically increases.

<div style="text-align: center">

Chapter 2

Decadal variability and trends of the Benguela upwelling system as simulated in the high-resolution ocean simulation STORM [1]

</div>

2.1 Introduction

The Benguela upwelling system (BUS; North Benguela and South Benguela) is one of the four major Eastern Boundary Upwelling Systems (EBUSs) of the world (Shannon, 1985; Leduc et al., 2010) and among the most productive oceanic regions (Bakun et al., 2010; Leduc et al., 2010). Nutrient-rich coastal upwelling in the EBUSs are mainly driven by wind patterns that cause offshore Ekman transport that cannot be balanced by the horizontal advection of water (Bakun and Weeks, 2004). Further offshore, the wind stress curl causes upwelling by Ekman pumping. These areas are thus rich in pelagic fish biomass and important for coastal fisheries (Bakun et al., 2010). The BUS, off Angola, Namibia, and South Africa (Blanke et al., 2005), has its northern boundary at the Angola-Benguela front (between 14° and 17° S) (Shannon and Nelson, 1996; Veitch et al., 2010). The southern boundary of the BUS is defined by the Agulhas retroflection at the southern tip of the continent where Agulhas Current water penetrates into the southern Benguela at 37° S (Shannon and Nelson, 1996). The main driver of the BUS is thought to be

---

the wind stress off southwestern Africa (Nelson and Hutchings, 1983) while north of the front the upwelling is more strongly related to the larger-scale equatorial upwelling (Hardman-Mountford et al., 2003). The strongest upwelling takes place near Lüderitz (27° S) (Shannon and Nelson, 1996), resulting in intense cold sea surface temperatures (SSTs) that persist throughout the year (Parrish et al., 1983). This upwelling cell naturally divides the BUS into a northern and a southern part (Shannon and Nelson, 1996; Hutchings et al., 2009). In the southern Benguela the upwelled water occurs near the coast, whereas in the northern Benguela it extends farther off the coast, westward up to about 150–250 km (Shannon and Nelson, 1996; Fennel et al., 2012).

The upwelling intensity is highly seasonal in the temperate latitudes (30–34° S), with generally higher intensity in boreal spring and summer, but more uniformly distributed across seasons in regions closer to the Equator (15–30° S) (Parrish et al., 1983; Mackas et al., 2006; Chaigneau et al., 2009; Chavez and Messié, 2009). However, a clear picture of the upwelling seasonality is not established yet. Bakun and Nelson (1991) stressed that the strongest upwelling takes place in the austral summer seasons, Blanke et al. (2005) widened this seasonal frame from October to March. In contrast, Hagen et al. (2001) and Hagen et al. (2005) argued that the main upwelling season is rather the austral winter to spring. Veitch et al. (2010) clarified that upwelling peaks in the southern Benguela in austral spring and summer, whereas in the north, with weaker seasonal variations, it does in austral autumn and spring. Central Benguela upwelling near Lüderitz does not show a clear seasonal cycle (Shannon and Nelson, 1996). This distinction supports the division in two distinct regimes (Shannon, 1985) and highlights the complex nature of the BUS, which warrants a closer look at the large-scale climate drivers.

The Benguelan upwelling is thought to be driven by several factors. The coastal topography and the climatological winds frame the areas of upwelling (Shannon, 1985; Chavez and Messié, 2009). The region is dominated by southerly and southeasterly winds (Hagen et al., 2001; Risien et al., 2004) that are influenced by the high pressure system over the South Atlantic, by the cyclones moving westward over the southern Benguela, and by the pressure over southern Africa (Shannon and Nelson, 1996; Risien et al., 2004). Seasonal trade winds also influence the dynamics of the upwelling (Shannon, 1985; Chavez and Messié, 2009). In addition, the BUS displays some particular characteristics, compared to other EBUSs, determined by its geophysical boundaries: the Agulhas retroflection, the Angola-Benguela front, and the passage of westerly winds in the south (Shannon and Nelson, 1996). Zooming more closely into the BUS, Lachkar and Gruber (2012) characterised the Benguela subregions as having a shallow mixed layer depth, but with central Benguela dominated by strong upwelling (net primary production) due to a wide shelf and low eddy activity, whereas southern Benguela is characterised by weaker upwelling, a wide shelf, and moderate to high eddy activity. In the northernmost Benguela, the upwelling is moderate in a narrow shelf and with moderate to high

eddy activity.

The upwelling intensity is not constant, but presents intraseasonal variations. In general, the variability of the Benguela system is dominated by the intraseasonal (eddy) variability (Chavez and Messié, 2009) and coastal-trapped waves (Rouault et al., 2007). Lachkar and Gruber (2012) identified factors that inhibit the net primary production and thus have indirectly been linked to upwelling dynamics, namely strong eddy activity, a narrow continental shelf, and a deep mixed layer. These factors help to provide a spatial characterisation of the Benguela system and its spatial heterogeneity (Lachkar and Gruber, 2012).

From a larger-scale climatic perspective, climate modes seem to have an impact on the interannual variability of upwelling through modulation of the local conditions. Hagen et al. (2001) mentioned a possible influence of the Quasi-Biennial Oscillation (QBO), a mode of variability that describes quasi-oscillations of low stratospheric winds. The St. Helena Island Climate Index (HIX, first mode of the empirical orthogonal function (EOF) analysis of air temperature, sea level pressure (SLP), and precipitation) is positively correlated with the southeasterly trades and thus should modulate the strength of the upwelling (Hagen et al., 2005). Furthermore, the Antarctic Oscillation (AAO), which is related to the strength of the circumpolar westerly flow (Jones and Widmann, 2004), could also influence the upwelling intensity.

In addition to the mentioned climate modes, the impact of El Niño-Southern Oscillation (ENSO) on the Benguela upwelling could, according to some authors (e.g. Dufois and Rouault, 2012), be of major importance, even stronger than the one of the AAO (Rouault et al., 2010). According to this study, El Niño and La Niña events tend to weaken and strengthen upwelling, respectively. The proposed physical mechanism is related to an equatorward shift in the high pressure over the southern Atlantic which leads to weaker upwelling-favourable trades (and conversely for La Niña events) (Dufois and Rouault, 2012). The results obtained by Shannon and Nelson (1996) support this by identifying the relation to ENSO as the most significant one on interannual time scales. Deutsch et al. (2011) also presented changes in the upwelling intensity and the depth of the thermocline associated with ENSO.

Some authors (e.g. Huang et al., 2005) suggest that ENSO, affecting the whole tropical belt around the Earth, also has an influence on the so-called Benguela Niños. These extreme events are a type of Atlantic Niños that reach the BUS when warm waters extend into the eastern Atlantic around 600 km further south than usually (Shannon et al., 1986). The Benguela Niño events have been explained by two different causal chains. According to the first, SST anomalies along the southwest African coast develop due to zonal wind anomalies in equatorial South America and the equatorial western Atlantic (McCartney, 1982; Wang, 2006). Kelvin waves crossing the basin are induced due to the relaxation of the trades along the Equator (Rouault et al., 2007). The unusual sea surface height reaches

the Angola-Benguela front which leads to increased intrusion of tropical water into the Angola-Benguela upwelling system (McCartney, 1982; Rouault et al., 2007). According to a second scenario (Richter et al., 2010), the main drivers of Benguela Niños are alongshore wind anomalies, which occur due to the weakening of the subtropical high that develops 2–3 months in advance of Benguela Niños and 5–6 months before the Atlantic Niños. Furthermore, they found that Kelvin waves had an insignificant influence on the Benguela Niño event in 1995. Most past major warming events, which usually occurred between February and May and lasted a few months, were related to the Atlantic Niño state and cooling events to Atlantic Niña state, but the relationship does not seem to be linear (Rouault et al., 2010; Dufois and Rouault, 2012). The warming events have been found to be weaker and less frequent than the Pacific ENSO (Shannon et al., 1986; Latif and Grötzner, 2000). In contrast, Hardman-Mountford et al. (2003) estimated a much higher frequency of warm events in the Atlantic than in the Pacific, but these authors found that the warming events penetrate more rarely into the Benguela system. For this to occur, southerly winds at the Equator are required to blow simultaneously with the southward water flow (Hardman-Mountford et al., 2003). Shannon et al. (1986) found that, in any case, the effect on the southern Benguela is small, whereas in the northern Benguela the intrusions of warm water persist for at least 6 months, leading to extreme events in precipitation in Namibia and Angola (Rathmann, 2008), and a weaker or shorter (about 2 months) upwelling season (Hagen et al., 2001). Hagen et al. (2001) found a periodicity of the occurrence of Benguela Niños of around every 11 years (1909–1963) and between 1974 and 1999 every 5 years, and interpreted this shift as a tendency of these extreme events to occur more often.

Another ongoing discussion hints to a more complex interaction from the tropical Pacific into the tropical Atlantic as a simple unidirectional influence from the Pacific to the Atlantic. Rodríguez-Fonseca et al. (2009) mentioned that ENSO events are preceded by Atlantic events of opposite sign and that the Atlantic could strengthen ENSO. Ham et al. (2013) agree and explain that easterlies over the equatorial far-eastern Pacific are considerably weaker under Atlantic Niña conditions. The same study adds that the northern tropical Atlantic is more strongly connected with the Pacific ENSO than with the Atlantic Niño. In contrast, Wang (2006) detected no correlation between both El Niños (Pacific and Atlantic) but found that anomalous SSTs of the two equatorial oceans can induce an inter-Pacific-Atlantic SST gradient that leads to anomalies in surface zonal wind over parts of both oceans and equatorial South America. These anomalies of the zonal wind constitute the bridge conveying the interaction between the two oceanic basins. Wang (2006) stated that the SST gradient between the equatorial Pacific and Atlantic is of higher importance than the individual ocean SST anomalies as driver of the atmospheric circulation across northern South America. Contrasting to the results of Rodríguez-Fonseca et al. (2009), Latif and Grötzner (2000)

mentioned that the equatorial Atlantic responds to ENSO with a lag of 6 months, this time being needed by the equatorial Atlantic to adjust to low-frequency wind stress variations. Also Colberg and Reason (2006) found that ENSO-induced wind anomalies play a major role in driving upper South Atlantic temperatures by an atmospheric teleconnection with a lag of one season. Thus, even if the direction of teleconnection is unclear, the influence of ENSO and the Benguela Niños on the Benguelan upwelling could be of major importance when investigating the atmospheric drivers due to their effects on the Benguelan ecosystem.

The long-term trend of the Benguela upwelling brought about by anthropogenic climate change is another important reason to identify its large-scale atmospheric drivers. In his landmark paper, Bakun (1990) put forward his hypothesis that can be summarised as follows: as a consequence of rising greenhouse gas concentrations, the surface temperature over the continents warm faster than oceans. This leads to a strengthening of the continental lows and oceanic highs. The land-sea pressure gradient is thereby enhanced, causing a strengthening of alongshore winds and enhancing upwelling. In addition, the warming ocean surface results in more humidity in the otherwise very dry atmosphere over land, which reinforces the greenhouse gas effect (Bakun, 1990). Observations do indicate that over south-western Africa surface temperatures over land have increased more rapidly than over the ocean from 1980 onwards, although in previous periods the statistical significance of the trend is compromised due to a poorer data quality (Hartmann et al., 2013, Fig. 2.22). In agreement to Bakun's hypothesis, Narayan et al. (2010) found decreasing trends in coastal SSTs in four major EBUSs over 1960–2000 and attributed them to meridional wind stress intensification. This was supported by Demarcq (2009), who found a positive trend in southerly winds in the Benguela EBUS for 2000–2007. In addition, Rathmann (2008) reported an intensification of the trade winds due to SLP trends. However, Narayan et al. (2010) recognised the spread in estimation of the wind stress trend using different data sets (reanalyses and observations) and Belmadani et al. (2014) could not identify the mechanisms linking the land-sea thermal contrast and upwelling-favourable winds in the Peru upwelling system in future climate model simulations. Bakun et al. (2010) also expressed some doubts about the robustness of the estimated upwelling trends in Benguela. To explain this apparent lack of clear upwelling trends in BUS, Bakun et al. (2010) later reasoned that the influence of ENSO on atmospheric humidity in Benguela, combined with the succession of recent strong ENSO events may have stifled a long-term intensification of upwelling that should have occurred as a result of the anthropogenic greenhouse effect. However, climate models still give an unclear picture about the long-term effect of anthropogenic greenhouse gas forcing on ENSO (Vecchi and Wittenberg, 2010), but at least 9 of 22 models of the Coupled Model Intercomparison Project phase 5 (CMIP5) show an increasing trend in ENSO amplitude before 2040 and a decreasing trend thereafter (Kim et al., 2014). In addition, global climate models still display clear systematic errors in simulating

the SST in the eastern ocean basins (Richter and Xie, 2008; Echevin et al., 2012; Grodsky et al., 2012), the origin of these errors still being under investigation.

Against the backdrop of these competing hypotheses about the role of large-scale climate modes on Benguela upwelling and the long-term evolution of upwelling itself, the purpose of this chapter is to analyse the atmospheric drivers of the interannual variability and the long-term trends of upwelling in the BUS as simulated in a high-resolution (about 0.1° lon-lat) ocean simulation with the ocean model MPI-OM developed at the Max Planck Institute for Meteorology in Hamburg, and spanning the last 6 decades driven by the NCEP/NCAR (National Centers for Environmental Prediction/National Center for Atmospheric Research) meteorological reanalysis.

The focus of this analysis lies on the longest time scales possible for such high-resolution simulations. This focus requires a trade-off between a possibly higher quality atmospheric forcing data provided by most recent meteorological reanalysis, on the one hand, and the period covered by those data sets, on the other hand, which is considerably shorter than those of the NCEP/NCAR reanalysis. Although the ocean simulation was driven by the NCEP/NCAR reanalysis, some analyses were confirmed with the more recent and higher-resolution ERA-Interim reanalysis. However, through this study, it has to be borne in mind that the conclusions obtained may be dependent on the realism and homogeneity of the NCEP/NCAR product. The resolution of the wind stress provided by this meteorological reanalysis may be too coarse to fully represent the effect of the atmospheric forcing on the ocean dynamics. The results of this simulation must, therefore, be considered as conditional on the realism of this wind forcing and should be contrasted against future simulations that will eventually use higher-resolution atmospheric forcing. For the time being, however, due to the high computational costs required for a high-resolution atmosphere, other simulations to estimate the recent and future evolution of upwelling have also used either meteorological reanalysis or atmospheric models of comparable horizontal resolution (Serazin et al., 2015; Wang et al., 2015). It has to be kept in mind that the results of this analysis are based on a simulation and that it is very difficult to establish the reliability of simulations when the direct observations are fragmentary and other gridded observation data sets are themselves based on models. Therefore, this study does not claim to represent the truth, but rather my goal is to use a state-of-the-art model simulation and compare the conclusions that can be derived from it with predictions about long-term environmental changes based in more general principles like Bakun's hypothesis. This approach should contribute to improve the understanding of those changes and also of possible model deficiencies in situations in which long-term observations are incomplete.

Table 2.1: Description of the data sets used in this chapter.

Acronym	Data description	Time period	Grid [°]
NCEP/NCAR	reanalysis data	1948–2011	2.5
ERA-Interim	reanalysis data	1979–2010	0.70
HadISST1	global gridded observations	1870–2012	1
STORM	global ocean-only simulation/model MPI-OM	1950–2010	0.1
MEI	Multivariate ENSO (El Niño-Southern Oscillation) Index	1950–2012	
AAO	Antarctic Oscillation	1957–2012	
ATL-3	tropical Atlantic SST (HadISST1, STORM)	1870–2012 and 1950–2010	1 and 0.1
AMM	Atlantic Meridional Mode	1948–2012	
HIX	St. Helena Island Climate Index	1892–2012	
QBO	Quasi-Biennial Oscillation	1979–2012	
AVHRR	pathfinder 5.0, remote-sensed SST	1985–2009	0.04

2.2 Data and methods

For this study I analyse climate variables derived from observational data sets, atmospheric data from meteorological reanalyses, and from a high-resolution global ocean-only simulation. A summary of the characteristics of these data sets is presented in table 2.1.

2.2.1 Gridded observational data

Atmospheric variables (10 m-wind, wind stress, and SLP) were obtained from the NCEP/NCAR reanalysis 1. This data set is available from 1948 onwards with a horizontal resolution of 2.5° (Kalnay et al., 1996). Monthly means were downloaded and averaged to seasonal means of the area 50° W–40° E, 0–50° S. An analysis of the gradient of the SLP field is performed with the SLP of the ERA-Interim reanalysis (available from 1979 onwards) (Dee et al., 2011) as well as of the NCEP/NCAR reanalysis 1. Here I choose a region over the ocean (20° W–10° E, 15–35° S) and one over land (12–25° E, 10–20° S), subtract the SLP over the land from the SLP over ocean, calculate its trend and the significance of the trend (p value), and correlate it with the upwelling indices derived from the vertical velocity (described in Sect. 2.2.3). The chosen regions are identified as most closely correlated to the upwelling (Fig. 2.1). Furthermore, these regions cover the ocean subtropical high and the continental low. Selecting slightly different regions does not change the results of the analysis of the SLP gradient.

In addition to the reanalyses data, the observational gridded sea surface temperature data set HadISST1 with a grid spacing of 1° and data between 1870 and 2012 (Rayner et al., 2003) are used in this study for the validation of the model output. For the same purpose, remotely sensed SST at 4 km resolution from the advanced Very High Resolution Radiometer (AVHRR; Casey, 2010) version 5.0, a radiometer onboard the National Oceanic And Atmospheric Administration (NOAA) satellites,
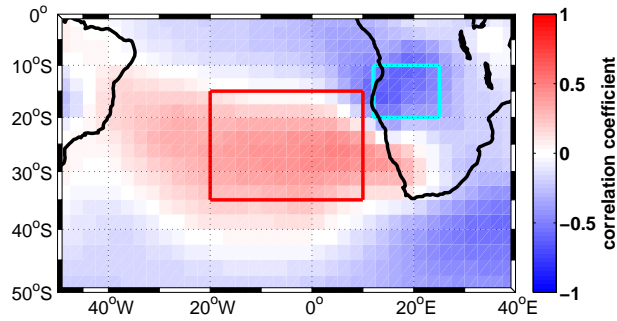
Figure 2.1: Correlation pattern of the sea level pressure field of NCEP/NCAR reanalysis and the upwelling index of North Benguela of the STORM simulation in austral winter (JJA) in the period 1950–2010. The boxes indicate the regions used for calculating the sea level pressure difference between ocean (red) and land (cyan).

is used to detect the possible SST bias of the model data described in the following. However, it is known that this version of pathfinder has a warm bias of up to 5 °C close to the coast in austral summer in the southern Benguela (Dufois et al., 2012).

2.2.2   Model data

The ocean simulation analysed here is a global simulation (hereafter denoted STORM) with a high-resolution version of the state-of-the-art model MPI-OM (Marsland et al., 2003) covering the period 1950–2010 driven by the global NCEP/NCAR meteorological reanalysis (von Storch et al., 2012; Li and von Storch, 2013). The horizontal resolution of this model version is 0.1° and it has 80 levels. The model is driven in this simulation by fluxes of heat, fresh water, and momentum derived from the meteorological reanalysis. Note that in this stand-alone simulation, there is no feedback of the simulated state of the ocean onto the driving fluxes. In particular, the prescribed wind stress flux does not consider the effect of the simulated ocean currents.

2.2.3   Upwelling indices

To identify the large-scale atmospheric drivers, an upwelling index has first to be defined. The definition may depend on the available data, since not always are direct data of the vertical water mass transport readily available. Chen et al. (2012) defined an index derived from the SST and mentioned that it represents well the upwelling intensity in terms of the spatial variation while the index defined derived from the offshore Ekman transport represents the temporal variations. The same study found that the index constructed from the SST is not able to correctly provide the upwelling intensity during warm water intrusions of the Angola Current.
In general, SSTs are not only affected by upwelling but also by a complex interaction

between horizontal ocean advection, ocean-atmosphere heat fluxes, and vertical mixing (McCabe et al., 2015). Therefore, the simulated vertical mass transport at $52\,\mathrm{m}$ depth, close to the modelled mixed layer depth in the Benguela region, is used as upwelling index. All data sets are seasonally averaged using the standard seasons definition: December–February (DJF), March–May (MAM), June–August (JJA), and September–November (SON). Previous studies (Shannon and Nelson, 1996; Hutchings et al., 2009) suggested that there exists a strong difference in the behaviour of the upwelling in the northern and southern Benguela. Thus, the area is divided into two regions with the border at Lüderitz ($28°\,\mathrm{S}$) (Fig. 2.2a, b). The South Benguela region covers around 2.7 times the oceanic region of North Benguela, because the south coast of South Africa with the Indian Ocean is included too. There, upwelling takes place as well (Shannon and O'Toole, 2003). Thus, the region denoted by South Benguela contains the southern BUS and additionally the south coast upwelling. My results are not sensitive regarding the chosen upwelling region. A southern Benguela region restricted close to the coast does not change the results of this chapter.

2.2.4   Climate indices

The upwelling indices are not only correlated with the atmospheric variables but also with climate indices. The influence of the Multivariate ENSO Index (MEI; Wolter and Timlin, 1993), the Antarctic Oscillation (AAO; Marshall, 2003), and the tropical Atlantic (ATL-3, $20°\,\mathrm{W}$–$0°\,\mathrm{E}$, $3°\,\mathrm{N}$–$3°\,\mathrm{S}$; Rodríguez-Fonseca et al., 2009) are investigated, as well as the impact of the Atlantic Meridional Mode (AMM; Chiang and Vimont, 2004), the St. Helena Island Climate Index (HIX; Feistel et al., 2003), and the Quasi-Biennial Oscillation (QBO; Labitzke and van Loon, 1988) on the upwelling off southern Africa are examined. The ATL-3 values are calculated with the data sets of HadISST1 and STORM.

For the analysis of the statistical significance of the long-term trends in the upwelling indices and the linear correlations between the indices, a two-sided significance level of $p = 0.05$ is adopted. The p value of the correlation and of the trend significance indicates the significance of the correlation (or trend) under the usual assumption applied in ordinary least-squares regression of serially uncorrelated and normally distributed regression residuals. The series of upwelling in North Benguela clearly display decadal variability, so that the test of significance of a linear trend is not correct using the usual assumptions of uncorrelated regression residuals. This is why I additionally use another, more sophisticated, method based on Monte Carlo generation of surrogate series by resampling the original series and on phase randomisation to preserve the autocorrelation structure of the original series (Ebisuzaki, 1997). Using this method, the estimated linear trend in North Benguela is no longer statistically significant.

If no explicitly stated, all correlations have been calculated with long-term detrended series.
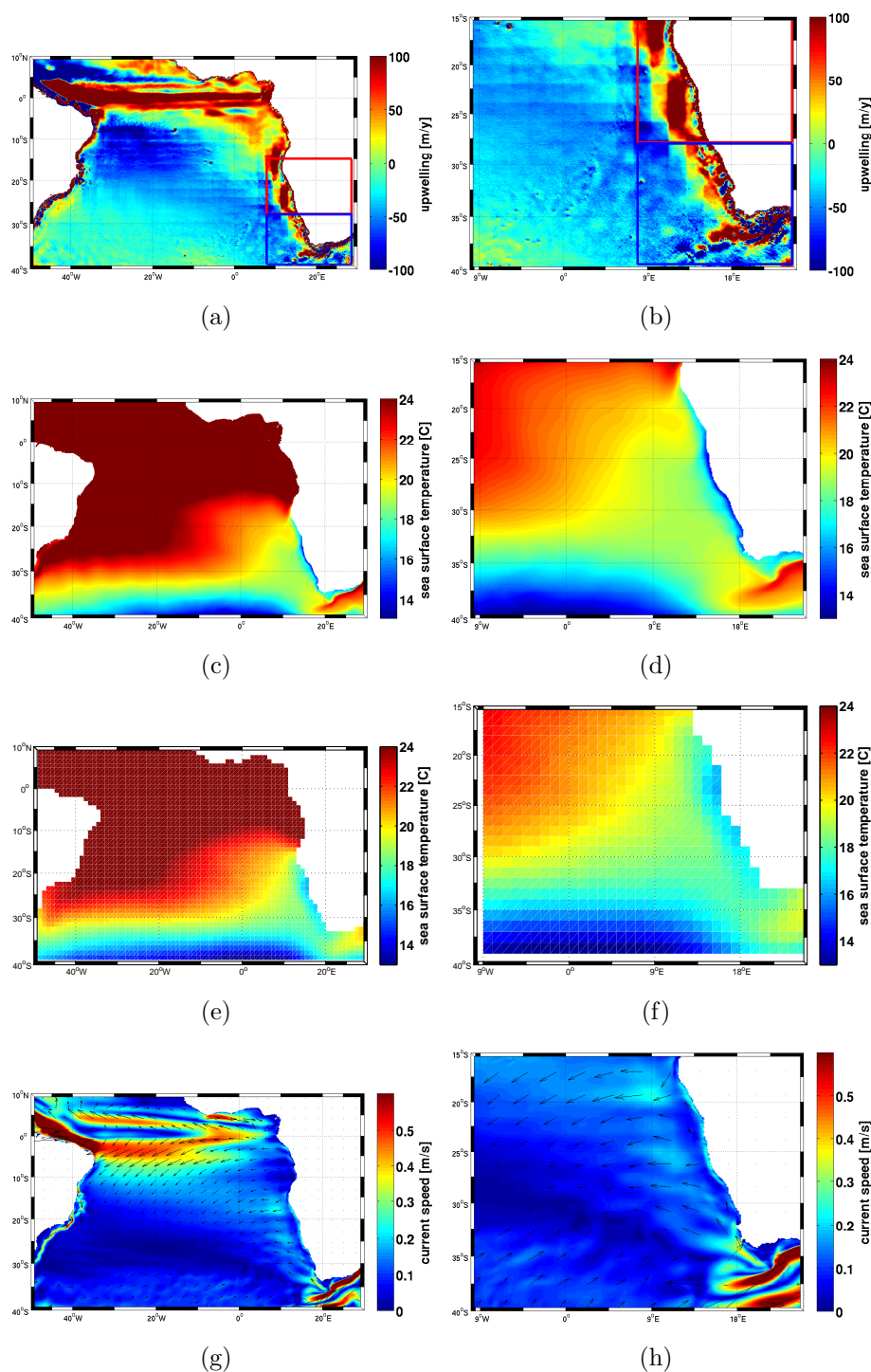
Figure 2.2: Long-term mean of the annual mean upwelling velocity at 52 m depth of the STORM simulation (1950–2010) for two regions in the South Atlantic (a, b), the boxes indicate the regions used for the upwelling index of North Benguela (red) and South Benguela (blue). The long-term annual mean simulated sea surface temperature of the STORM simulation (1950–2010) (c, d) and of the long-term mean annual sea surface temperature of HadISST1 (1870–2012) (e, f), and the simulated long-term annual mean surface currents of the STORM simulation at 6 m depth (1950–2010) (g, h).

2.3   Long-term means, annual cycle, and link between upwelling and SST

Figure 2.2 shows the long-term annual means of some important variables obtained from the STORM simulation in the South Atlantic and in the southeast Atlantic: the vertical velocity at 52 m depth, SST (compared to the corresponding fields derived from HadISST1), and surface currents. Figure 2.2a and b display the upwelling cells at the western and southern coast of southern Africa. The SST pattern of STORM (Fig. 2.2c, d) and HadISST1 (Fig. 2.2e, f) look very similar, with colder SST at the coast due to upwelling. The SST of the STORM simulation shows lower values than the observational data set HadISST1. This may be due to relatively coarse resolution of the HadISST1. In figure 2.2g and h one can see the realistic representation of the equatorial currents, the Agulhas Current, Benguela Current, and the westward drift along the west coast caused by the trade winds.
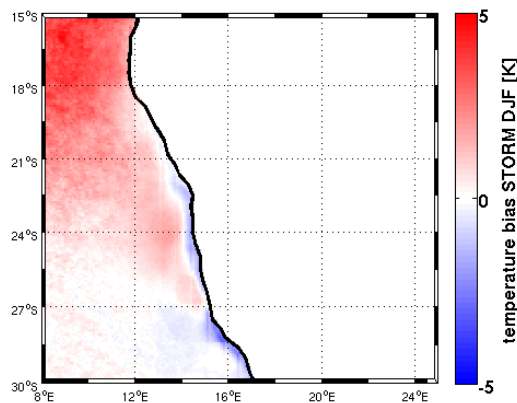
Figure 2.3: Long-term difference between the simulated sea surface temperature of the STORM simulation (1950–2010) and the AVHRR-derived (1985–2009) sea surface temperature in austral summer (DJF).

The simulated SST in STORM compared to that of AVHRR is shown in figure 2.3. To have the same spatial resolution in both data sets, the AVHRR data set are spatially smoothed by averaging two grid points in both spatial directions. If the two grid-points include one missing value, the missing value is ignored in the mean. The STORM data set is interpolated onto the grid of AVHRR. The STORM simulation displays a warm bias in the upwelling region, as it is well-known for general circulation models. The issue of SST bias in climate models is being vigorously investigated, since it is pervasive across many climate models and may be related to the global climate sensitivity as well. The reason is not clear, as it has been recently reviewed by Richter (2015). Both atmospheric and oceanic processes may be involved: stratiform clouds in the boundary layer, too weak winds, and remote oceanic influence from the tropics. The cold bias located along the coast may be also

(a)

(b)

(c)

(d)

(e)
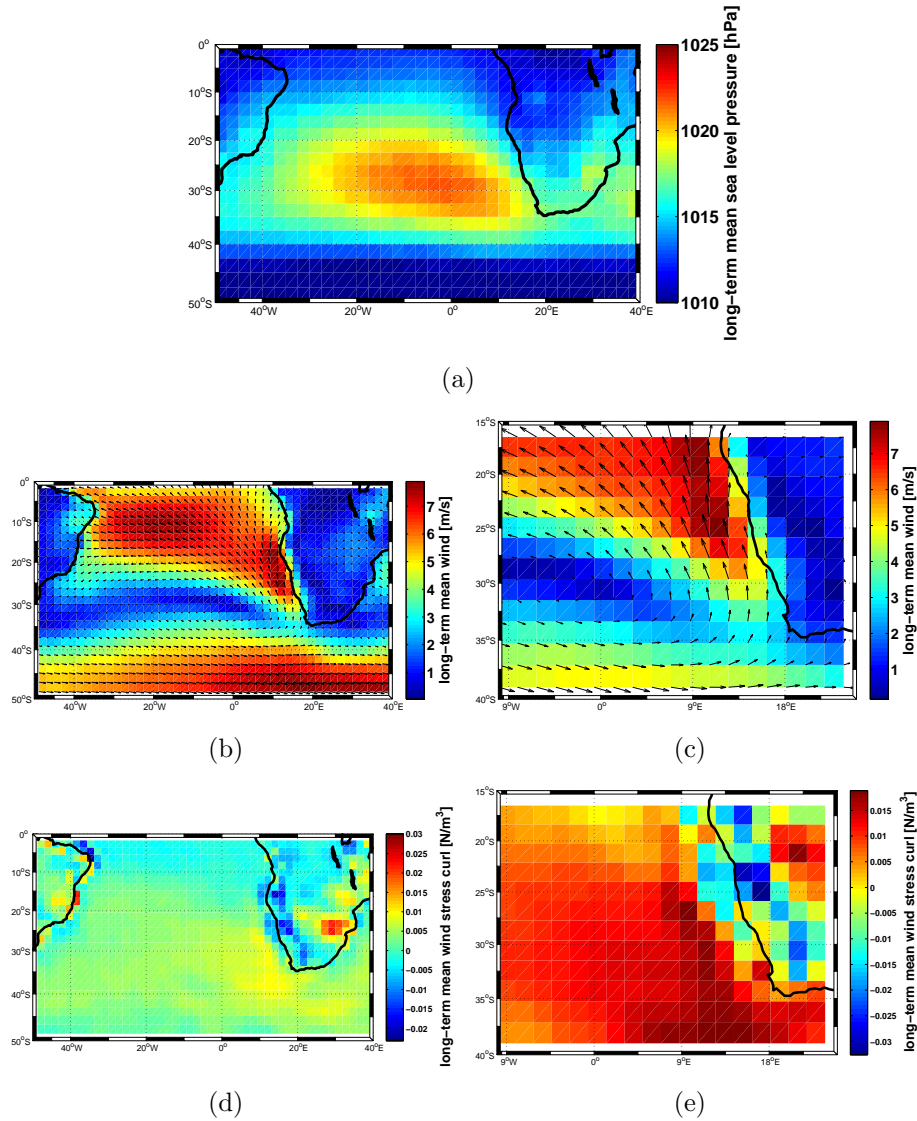
Figure 2.4: Long-term mean of sea level pressure (a), wind (b, c), and wind stress curl (d, e) of NCEP/NCAR reanalysis in the period 1948–2011.

partially caused by the bias of the AVHRR data mentioned by Dufois et al. (2012). The stronger bias of AVHRR underlines the more realistic cold SSTs simulated by STORM along the coast compared to HadISST1.

A presentation of NCEP/NCAR reanalysis is displayed in figure 2.4. The climatology of the alongshore wind stress, the wind stress curl, and SLP show a realistic pattern for the South Atlantic Ocean and the Benguela region. Nevertheless, cyclonic wind stress curl takes place in the wind drop-off zone near the coast. This contribution to the coastal upwelling might be under-represented in the NCEP/NCAR reanalysis data set due its coarse resolution (Chelton et al., 2004). The long-term trends of NCEP/NCAR reanalysis winds over the whole simulation period are small and not significant (Fig. 2.5). The validation of these trends is more problematic due to the lack of in situ observations in this area. Comparing NCEP/NCAR reana-
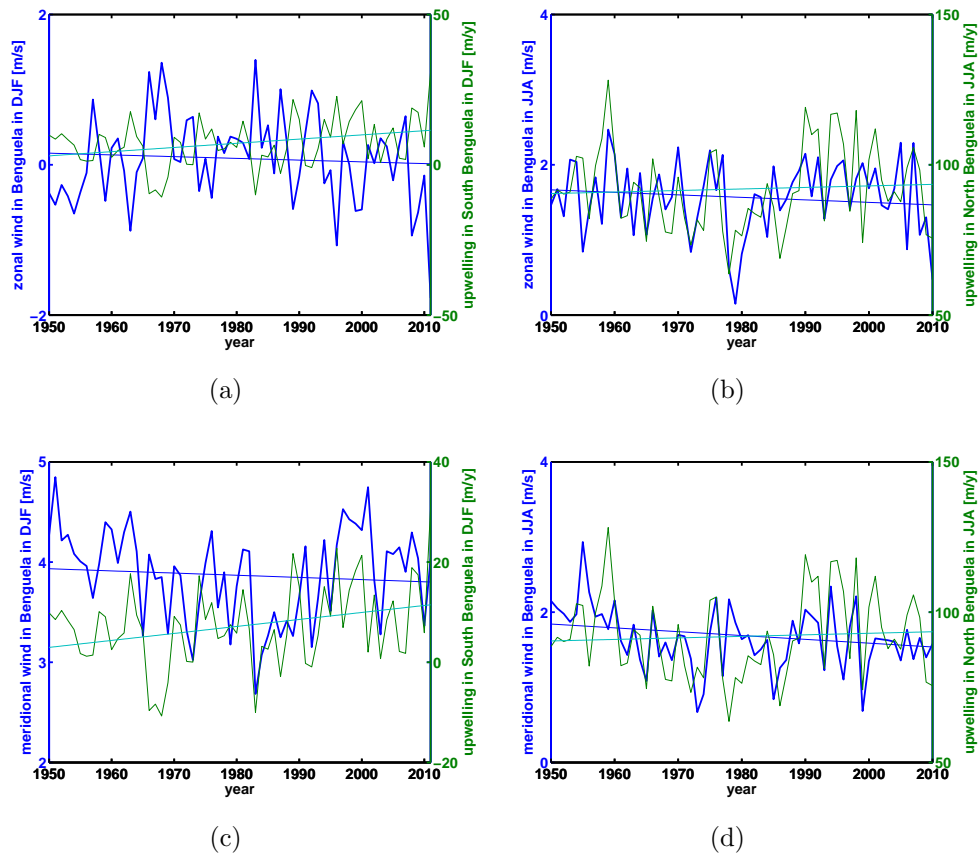
Figure 2.5: Time series of wind components of NCEP/NCAR reanalysis over the ocean (8–30° E, 15–40° S) and North and South Benguela upwelling and their trends in austral summer (DJF) (a, c) and austral winter (JJA) (b, d) in the period 1950–2010.

lysis to the World Ocean Circulation Experiment (WOCE) shows an underestimation of the pressure systems in my regions and thus of the near-surface winds (Smith et al., 2001). The comparison of NCEP/NCAR reanalysis to QuikSCAT displays the deficits of NCEP/NCAR reanalysis in capturing small-scale features of the wind stress (Risien and Chelton, 2008), although it is difficult to assess whether these limitations also influence the long-term trends in the wind stress. The results of the STORM simulation are admittedly conditional on the quality of the NCEP/NCAR reanalysis forcing, but unfortunately there are no clear alternatives for the study of the long-term variability of the atmospheric forcing. Satellite data as well as more recent reanalyses with higher resolution surely represent an improvement compared to NCEP/NCAR reanalysis but the longer temporal coverage is a key element for my analysis, and this is missing in the higher-resolution data sets.

The annual cycle of the upwelling index in North and South Benguela is displayed in figure 2.6. The upwelling index in South and North Benguela display clear differences. Whereas in the north upwelling shows a broad maximum in JJA, in South Benguela it tends to be stronger in DJF, due to the position of the subtropical Atlantic high (Mackas et al., 2006). This is in broad agreement with observations,

considering the discrepancies already indicated in the introduction (Sect. 2.1).

The relationships between the upwelling index and the SST are displayed in figure 2.7 as a map of the correlation coefficient between the upwelling index and the SST in each model grid cell. These correlations are negative near the coast and more pronounced in North Benguela. The correlations between the upwelling index of South Benguela and the SST field in STORM are negative along the entire coast in DJF, with stronger correlations in the south. In JJA the correlations are negative only at the southern coast of South Africa.
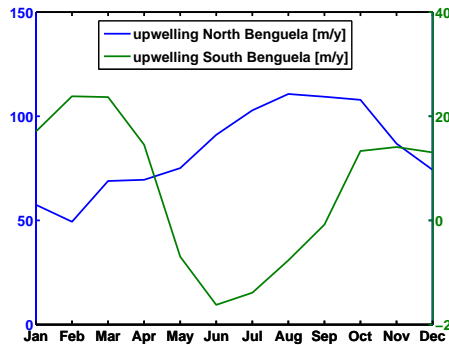
Figure 2.6: Annual cycle of the upwelling indices of the STORM simulation derived from the simulated vertical velocity at 52 m depth in North and South Benguela in the period 1950–2010.

2.4   Simulated upwelling over the last decades

2.4.1   Linear trends and variability of upwelling over the last 50 years

Table 2.2 summarises the main findings of the analysis of the upwelling index in the STORM simulation, including the estimated linear trends (and their two-sided 95 % uncertainty ranges) expressed as the change of upwelling intensity over the period 1950–2010 relative to their long-term mean. The long-term mean values themselves may depend on the depth, area, and quite presumably on model resolution, but they are in the reasonable range of tens of metres per year, which agrees with estimations using simplified models of upwelling dynamics (Rykaczewski and Checkley, 2008).

The time evolution of the upwelling indices (deviations from their long-term mean) through the period of the STORM simulation (Fig. 2.8) indicates that the variations of upwelling in the north and in the south do not go hand in hand. The significant linear correlation between the upwelling in North and South Benguela is 0.30 in DJF and −0.52 in JJA, indicating that the interannual variations of upwelling during JJA (the season with maximum upwelling in North Benguela) is out of phase in both regions. These results strongly suggest that the Benguelan upwelling cannot
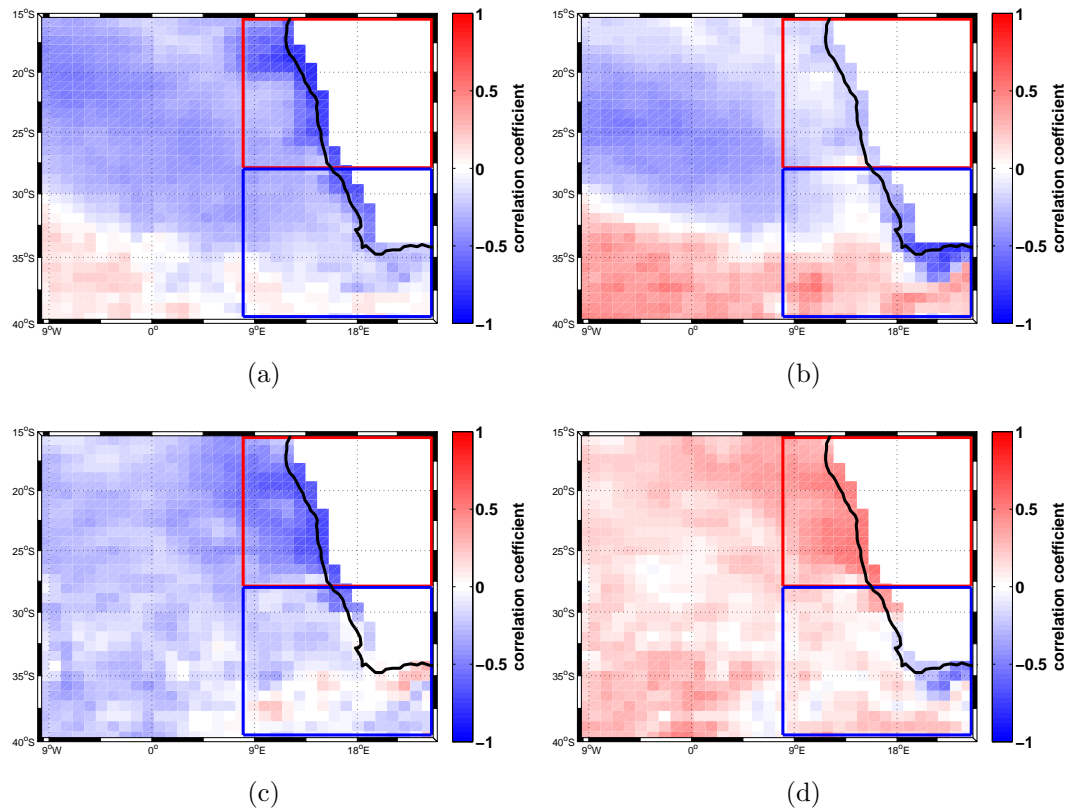
Figure 2.7: Correlation patterns between upwelling indices derived from the vertical velocity and the sea surface temperature field of the STORM simulation (1950–2010) in austral summer (DJF) (North Benguela (a), South Benguela (b)), and in austral winter (JJA) (North Benguela (c) and South Benguela (d)). Boxes indicate the regions used for the upwelling index of North Benguela (red) and South Benguela (blue).

be considered as a homogeneous system, in accordance with previous observational studies (see Sect. 2.1).

The linear trends of the upwelling indices in the STORM simulation are positive in North Benguela in MAM, JJA, and DJF and positive in South Benguela in MAM, SON, and DJF (Tab. 2.2). Upwelling in North Benguela is about twice as intense as in South Benguela (Fig. 2.6, Fig. 2.8) and it is less variable relative to its long-term mean (Tab. 2.2). The interannual standard deviation (SD) of the long-term mean is lower in the north than in the south (Tab. 2.2). The second characteristic is that the decadal variations are much more coherent across seasons in the north than in the south (Fig. 2.8). There is obviously some persistent factor in the tropical upwelling region that coherently drives the upwelling decadal variability in all seasons. In the south, in contrast, the seasonal upwelling indices display a more incoherent behaviour across the four seasons. In addition, the time scales of variations are longer in the north than in the south, as it will be more clearly shown later with a spectral analysis of these indices.

The analysis of the significance of the trends shows that only in North Benguela

Table 2.2: Coefficients of variation (CV, ratios between interannual SD, and long-term mean, in %) and trends in upwelling intensity over the period 1950–2010 as simulated in the STORM simulation. The magnitude of the trends is expressed as total linear changes over the period 1950–2010 relative to the long-term mean. The numbers in parenthesis bracket the nominal 95 % uncertainty range in the trend estimation, assuming uncorrelated and Gaussian-distributed trend residuals.

	North Benguela CV	North Benguela trends	South Benguela CV	South Benguela trends
MAM	+24	+26 (+05, +46)	+84	+15 (−62, +91)
JJA	+15	+03 (−11, +17)	−72	−09 (−75, +56)
SON	+16	−11 (−25, +03)	+81	+38 (−35, +110)
DJF	+29	+31 (+10, +52)	+48	+39 (−03, +82)
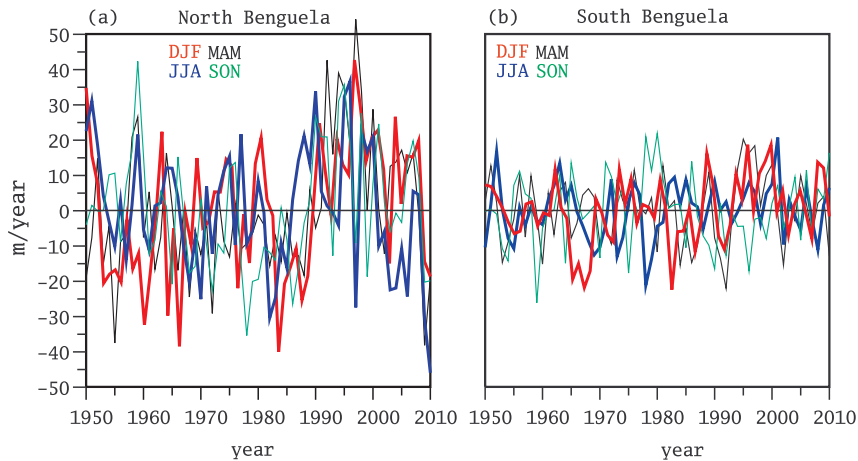
Figure 2.8: Time evolution of the seasonal upwelling indices (deviations from their long-term mean) in North Benguela (a) and South Benguela (b) derived from the vertical velocity of the STORM simulation in the period 1950–2010.

the positive trends in MAM and DJF are nominally significant (i.e. assuming Gaussian and serially uncorrelated trend residuals; see confidence intervals in table 2.2). However, figure 2.8 clearly shows that a linear trend in the north is not a good description of the long-term evolution of upwelling. In general, upwelling intensity remains stable from 1950 to 1985 and undergoes a decadal surge and subsequent slowdown until the end of the simulation. This behaviour is not what one would expect from a steady increase in external climate forcing over the second half of the 20th century. These long-term changes over the whole simulation period are of the same order as the coefficients of variation (standard deviation divided by the long-term mean), if not weaker, which further confirms that the decadal variations are dominating the temporal variability. A more sophisticated analysis of the statistical significance considering the serial correlation of the trend residuals (see Sect. 2.2.4) indicates that both trends are not significant at the 95 % level. In the south, the trend in DJF is close to the $p = 0.05$ significance level, but the long-term evolution,

as displayed in figure 2.8, does show a steady, albeit weak, increase through the simulation. The trend residuals are in this case not serially correlated. The central estimate of the trend in South Benguela upwelling in DJF implies a linear increase of about 40 % from the start through the end of the simulation. I will return to this point when discussing the connection of upwelling to the large-scale climate modes.

2.4.2 Correlations with large-scale climate fields

Correlations with atmospheric fields are calculated for the upwelling indices. Figure 2.9 depicts the correlation patterns between the upwelling index and wind stress (defined as positive when directed into the ocean) for DJF and JJA. This figure not only illustrates the expected relationship between upwelling and wind stress but also the seasonality in this relationship. In North Benguela, wind stress variability is more important for upwelling during JJA – the season with stronger upwelling – whereas in South Benguela the seasonality is not very marked. In both regions, the direction of upwelling-favourable winds does not change with season. These wind stress correlation patterns can also explain the mutual correlations between the north and south upwelling indices. As indicated before, the correlation between the interannual variations in upwelling in both regions in JJA is negative ($r = -0.52$). North Benguela upwelling is statistically connected to winds south of the southern tip of Africa that actually inhibit upwelling in South Benguela, and vice versa. In DJF, by contrast, this does not happen, and North Benguela upwelling is statistically linked to winds south of South Africa that are also upwelling-favourable for South Benguela, and vice versa, explaining the weak but positive correlation between both upwelling indices in this season. In the STORM simulation, upwelling is strongly correlated with upwelling-favourable wind stress in North Benguela. South Benguela upwelling in DJF is strongly driven by wind stress at the southern coast and not so pronouncedly by the wind stress at the southern west coast. This could be due to my definition of the region chosen as South Benguela, which includes parts of the coast of the Indian Ocean as well.

Figure 2.10 shows the corresponding correlation patterns to the wind stress curl. The patterns also display the expected negative correlation between upwelling in the boxes defining North and South Benguela and the wind stress curl, as the Coriolis parameter is negative. The exception here is North Benguela in the DJF season, when upwelling is weakest. However, further away from the coast, the correlation with the wind stress curl changes sign for both regions and both seasons, indicating that near-coastal upwelling driven by the wind stress curl and upwelling further offshore in the ocean would include anticorrelated contributions. Widening the geographical boxes in which regional upwelling is defined to include more open-ocean regions would thus lead to smaller upwelling variability than in the coastal and open-ocean regions considered individually.

Summarising, the upwelling in North Benguela is driven mainly by the expected wind pattern. In contrast, the correlations with South Benguela show upwelling-favourable wind stress that is more pronounced at the south coast than at the west coast south of Lüderitz. The correlation pattern with the SLP supports this with a positive pressure anomaly south of the continent instead of an intensified subtropical high located in the central South Atlantic (not shown here).
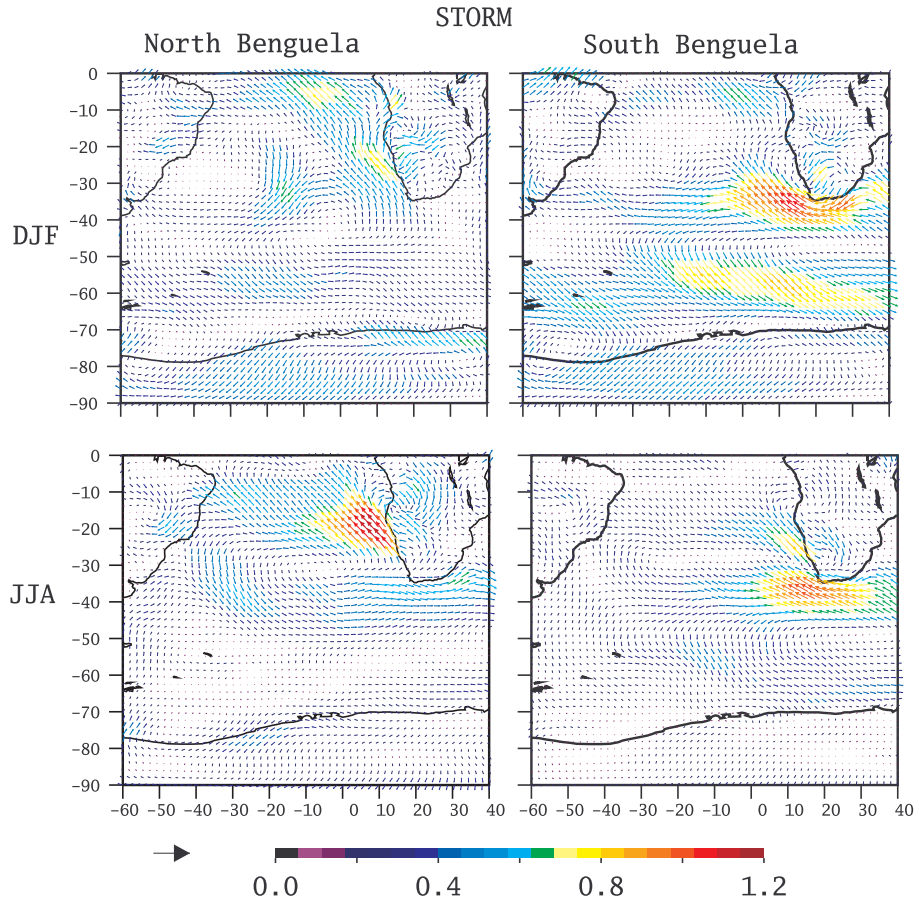
Figure 2.9: Correlation patterns between the simulated upwelling indices of the STORM simulation and the NCEP/NCAR reanalysis wind stress for North and South Benguela and for austral summer (DJF) and austral winter (JJA) in the period 1950–2010. The zonal and meridional components of the arrows represent the correlation with the corresponding component of the wind stress. The colours code the square root of the sum of these zonal and meridional correlations squared.

2.4.3   Correlations with climate modes

To identify the connection between climate modes and the upwelling index, the correlations of this index with ENSO (MEI), the AAO, the ATL-3, HIX, the QBO, and
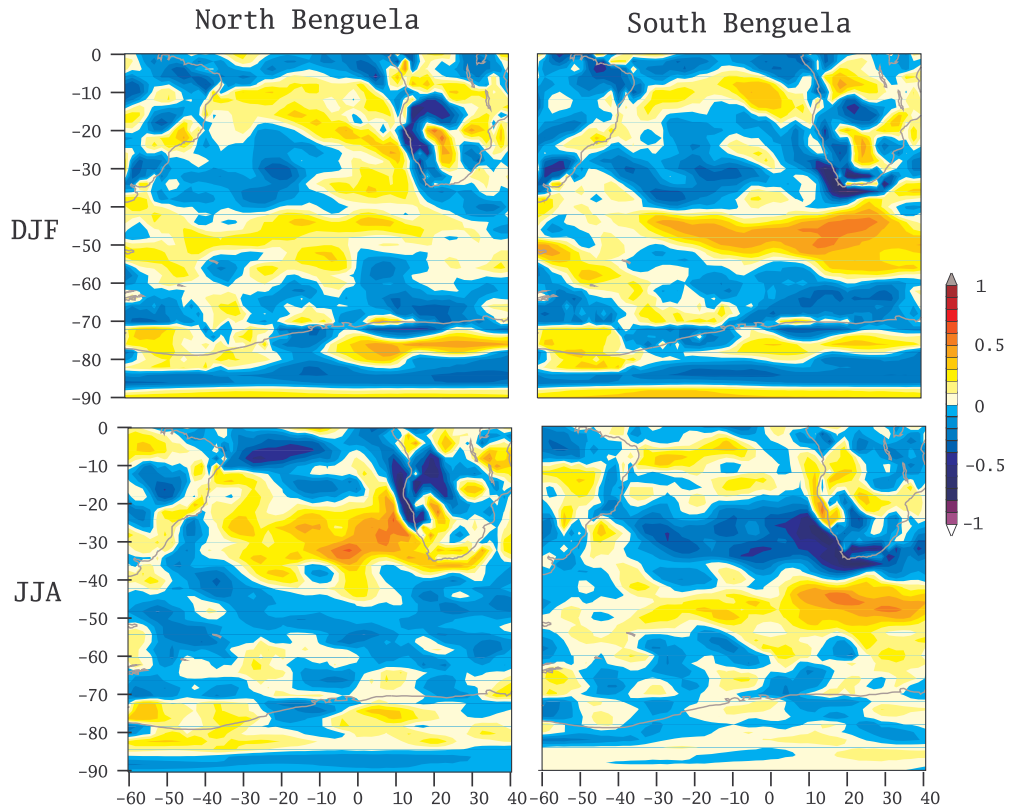
Figure 2.10: Correlation patterns between the simulated upwelling indices of the STORM simulation and the NCEP/NCAR reanalysis wind stress curl for North and South Benguela and for austral summer (DJF) and austral winter (JJA) in the period 1950–2010. The colours code the correlation coefficient.

the AMM are also calculated (Tab. 2.3).

The upwelling in North Benguela in STORM is significantly positively correlated with MEI in MAM, with the AAO in MAM and DJF, and with HIX in DJF. Significant negative correlations were found with AAO in JJA and ATL-3 in DJF (Tab. 2.3). In contrast, the upwelling in South Benguela is significantly negatively correlated with ENSO in MAM and DJF and positively with AAO in all four seasons and AMM in DJF (Tab. 2.3). The correlations with the QBO are all insignificant. The correlation pattern between wind stress and the ENSO index in DJF (Fig. 2.11) clearly explains the stronger negative correlations with South Benguela upwelling and the negligible correlation in the north. The wind stress anomalies associated with ENSO tend to weaken the climatological winds in the south and are very small in the north. The pattern of wind stress anomalies related to ENSO have a large-scale character, spanning almost the whole South Atlantic at midlatitudes, being clearly strongest in South Benguela. The correlation between ENSO and wind stress in North Benguela is quite weak, consistent with the weak correlation found between ENSO and North Benguela upwelling. The wind stress correlation pattern

Table 2.3: Correlation coefficients of the upwelling indices derived from the vertical velocity of the STORM simulation of North Benguela and South Benguela with ENSO, AAO, ATL-3 of HadISST1, ATL-3 of STORM, HIX, AMM, and QBO, significant correlations are highlighted by **.

	ENSO	AAO	ATL-3 (HadISST1)	ATL-3 (STORM)	HIX	AMM	QBO
North Benguela:							
MAM	+0.26**	+0.27**	−0.16	−0.21	+0.06	+0.08	−0.04
JJA	−0.13	−0.31**	+0.02	+0.00	+0.22	+0.14	−0.16
SON	−0.21	+0.06	+0.01	−0.19	+0.18	−0.02	−0.14
DJF	+0.01	+0.29**	−0.04	−0.32**	+0.33**	+0.17	−0.02
South Benguela:							
MAM	−0.26**	+0.40**	+0.04	−0.06	+0.07	+0.05	+0.19
JJA	+0.17	+0.37**	+0.03	−0.05	−0.06	−0.07	+0.07
SON	+0.23	+0.32**	−0.06	−0.15	+0.01	+0.01	+0.14
DJF	−0.46**	+0.61**	+0.13	−0.02	+0.05	+0.28**	+0.04

indicates that, if anything, ENSO may contribute to drive upwelling anomalies in South Benguela but not in the north. Even if the correlation is weak, the wind stress pattern favoured by ENSO shows the upwelling-unfavourable influence of a positive phase of ENSO. I suggest that these correlation patterns, which display systematically large values at midlatitudes and very small values in the tropical regions, arise as a result of a large-scale dynamical teleconnection with ENSO via the midlatitudes, rather than due to a tropical bridge between the tropical Pacific and the tropical Atlantic, as can be seen in figure 2.11. Also, a link between ENSO and Benguela upwelling resulting from the modulation of smaller-scale humidity dynamics in the Benguela region, as discussed by Bakun et al. (2010), does not seem to be required, since the correlation patterns display a large-scale teleconnection structure.

Similarly, the AAO index displays suggestive teleconnection patterns with the wind stress field in DJF and JJA (Fig. 2.11). These patterns indicate that the influence of the AAO is more pronounced in South Benguela and suggests the reason why the correlation between the North Benguela upwelling and the AAO is weaker. In both seasons, the AAO is associated with upwelling-favourable winds in South Benguela, and this link is somewhat stronger in DJF.

2.4.4   Spectral analysis

To identify the more important time scales for upwelling variability, we perform spectral analyses on the upwelling indices.

The spectra of the indices (Fig. 2.12) highlight their different behaviour in North and South Benguela. In the north, the spectra are red through the whole frequency range, with some superimposed broad and weak peaks. In the south, the spectra flatten for frequencies lower than 2×10^{-1} (periods longer than 5 years). The uncer-
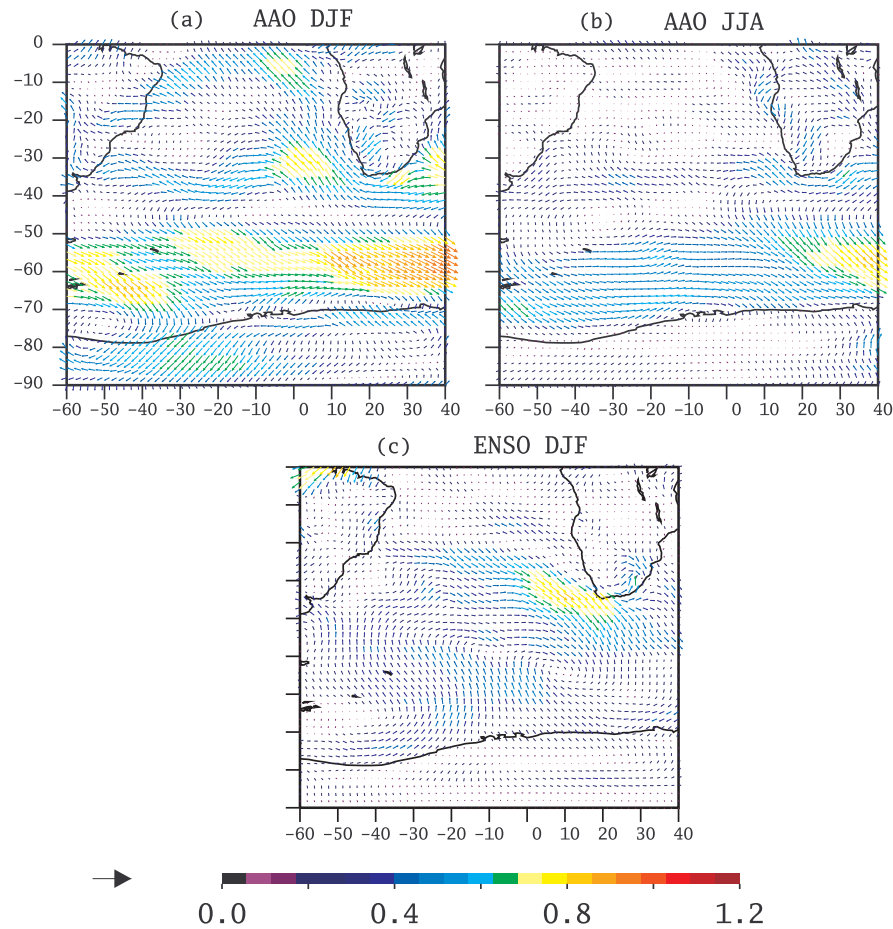
Figure 2.11: Correlation patterns between the downward wind stress from the NCEP/NCAR reanalysis and the Antarctic Oscillation (AAO) index in austral summer (DJF) (a) and austral winter (JJA) (b) and the Multivariate ENSO Index (MEI) in austral summer (DJF) (a) in the period 1950–2010. The zonal and meridional components of the arrows represent the correlation of MEI and accordingly AAO with the zonal and meridional component of the wind stress, respectively. The colours code the square root of the sum of these zonal and meridional correlations squared.

tainty range in the estimation of the spectral density (Jenskins and Watts, 1968) is also included in the figure panels. In both regions the spectra show some enhanced variability that is not strictly statistically significant, but which are nevertheless documented here as it supports some of the results of the correlation analysis and as it can be useful for future analysis with longer simulations in which these signals may be better revealed with a larger sample size.

The upwelling index of North Benguela of the STORM simulation (Fig. 2.12) displays a very broad spectral peak at periods of around 5 years in the season DJF and 4 years in JJA. In the season SON, the variabilities with periods of 3 years are slightly enhanced, whereas in MAM this occurs for slightly shorter periods of 2.5 years. In South Benguela, the spectra hint at an enhanced variability in the period range of
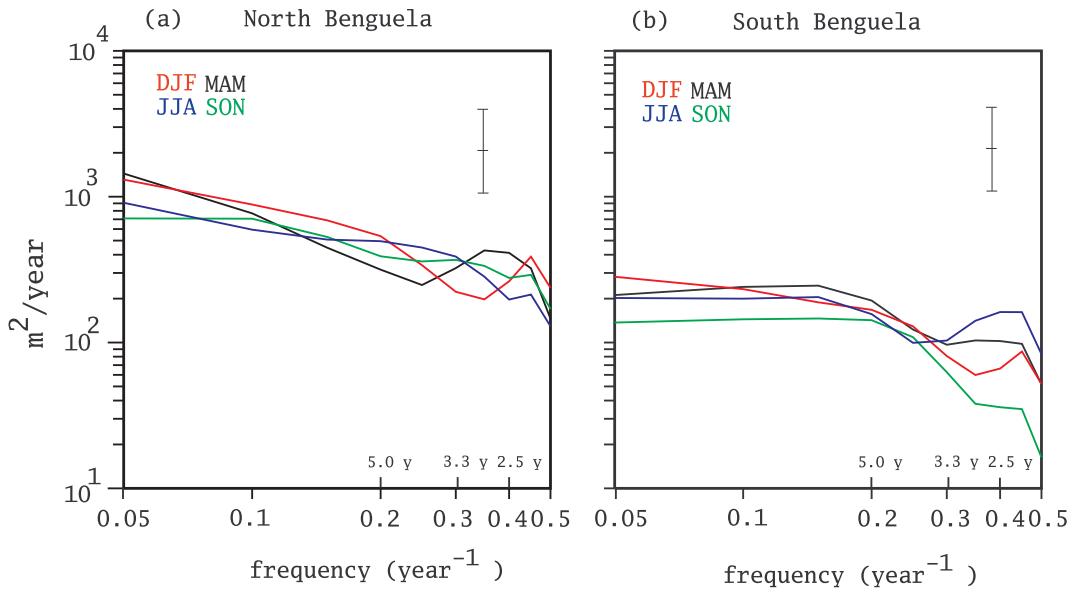
Figure 2.12: Spectral density of the upwelling indices derived from the vertical velocity of the STORM simulation in North Benguela (a) and South Benguela (b) in the period 1950–2010. The vertical black lines indicate the 90 % confidence interval.

3–5 years, with other maxima at 2.5 years. However, whereas the spectra of the upwelling index in both North and South Benguela display enhanced variability at the typical ENSO periodicities, correlations to the ENSO index differ between the two regions (Tab. 2.3). The index in North Benguela shows mainly weak correlations to ENSO. The index in the south displays stronger and significant correlations in DJF and MAM.

In summary, the red spectral background in the north is probably a result of tropical dynamics, whereas the more white spectra in the south may reflect the atmospheric forcing at midlatitudes, which generally has a flatter spectrum itself. Both upwelling spectra display enhanced variability at periods of around 2.5, 3.3, and 5 years. The periods of 5 years in the DJF season suggest a link to ENSO, as it was found in the correlation analysis between the upwelling index of South Benguela and the ENSO index. The 2.5-year period could indicate an influence of the QBO. However, the QBO and the upwelling of the STORM simulation are insignificantly correlated (Tab. 2.3). Possible reasons for these variations have to be further investigated.

2.5   SLP gradient and long-term trends in up-welling

Bakun (1990) postulated a long-term intensification of coastal upwelling driven by the increasing greenhouse gas concentration. This hypothesis would formally agree

with the positive trend found here in the North Benguela upwelling, although the upwelling evolution cannot be well described by a steady linear trend. In the south, the long-term evolution is described by a linear trend better than in the North, but its magnitude lies just below the 95% significance level. The mechanism proposed by Bakun (1990) involves a stronger increase of near-surface temperatures over land than over the ocean, which would lead to an intensification of the continental thermal low pressure relative to the ocean SLP. Consequently, the SLP gradient between land and ocean would tend to increase, the SLP difference between ocean and land becoming more positive, leading to a strengthening of the upwelling-favourable wind and hence to an increase of upwelling. I test Bakun's hypotheses concerning the link between the SLP gradient and upwelling in the framework of the ocean simulation (STORM) in Benguela, and concerning the long-term trend in upwelling in this simulation.
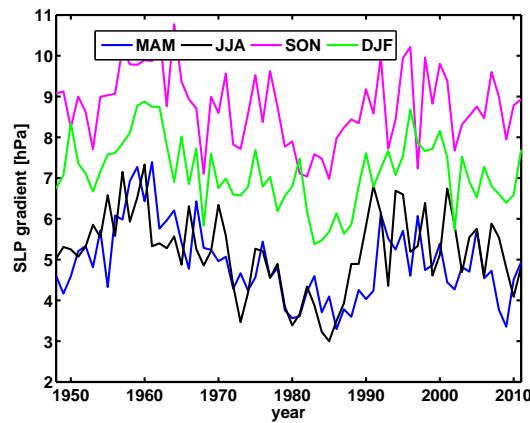
Figure 2.13: Time evolution of the sea level pressure (SLP) gradient over the Benguela upwelling system (SLP over ocean (20° W–10° E, 15–35° S) minus SLP over land (12–25° E, 10–20° S)), derived from the NCEP/NCAR reanalysis data in the period 1948–2011.

I define two regions, one over land (12–25° E, 10–20° S) and one over ocean (20° W–10° E, 15–35° S), and calculate the difference (ocean minus land) of their respective area-averaged SLP. Analysing the trend of this SLP difference in NCEP/NCAR reanalysis and ERA-Interim reanalysis does not support Bakun's hypothesis in this region. Bakun's hypothesis would predict a positive trend in this difference – land SLP decreasing relative to ocean SLP – whereas the NCEP/NCAR and ERA-Interim reanalyses SLP provide significantly negative trends for the MAM seasons (Fig. 2.13, Tab. 2.4), with the trend in other seasons being not significant.
The trends of the SLP over land and over ocean are positive for both data sets and all seasons, except for the SLP in MAM of NCEP/NCAR reanalysis (Tab. 2.4). This could indicate a missing imprint of increasing greenhouse gas concentrations on the SLP, especially over land, which might be due to the relatively short temporal period covered by the reanalyses data or the reanalyses data itself.
The correlation at interannual time scales yields a clear relationship between the

Table 2.4: Trends of the sea level pressure over land, over ocean, and its gradient (ocean: 20° W–10° E, 15–35° S; land: 12–25° E, 10–20° S) in hectopascals per year and the correlation coefficients between the gradient and the upwelling indices of the STORM simulation, significant correlations and trends are highlighted by **.

	SLP (NCEP/NCAR)			SLP (ERA-Interim)		
Trend:	Gradient	Land	Ocean	Gradient	Land	Ocean
MAM	−0.02**	+0.02**	−0.001	−0.03**	+0.03**	+0.00007
JJA	−0.01	+0.01	+0.003	−0.01	+0.01	+0.01
SON	−0.01	+0.02**	+0.01**	+0.004	+0.01	+0.01
DJF	−0.01	+0.02**	+0.01**	−0.02	+0.01**	+0.01
North Benguela:						
MAM	+0.69**			+0.57**		
JJA	+0.72**			+0.65**		
SON	+0.42**			+0.56**		
DJF	+0.51**			+0.65**		
South Benguela:						
MAM	+0.27**			+0.23		
JJA	−0.32**			−0.33		
SON	+0.14			+0.07		
DJF	+0.28**			+0.17		

upwelling intensity and the ocean-land SLP gradient. Bakun's hypothesis, applied at interannual time scales, predicts a positive correlation between upwelling and this gradient. The correlations with the upwelling index are positive and significant in North Benguela in all four seasons (with NCEP/NCAR and ERA-Interim reanalyses). South Benguela upwelling is significantly correlated with the SLP difference in MAM, JJA, and DJF calculated from the NCEP/NCAR reanalysis SLP gradient, but in no season when correlating with the ERA-Interim reanalysis SLP gradient. This is probably due to the relatively short period covered by the ERA-Interim reanalysis. The ERA-Interim reanalysis covers only 32 years, whereas NCEP/NCAR reanalysis spans twice that period. Although the strength of the correlation is similar in both data sets, the smaller sample size in ERA-Interim reanalysis renders the correlation not statistically significant.

Therefore, the SLP difference between ocean and land derived from these two meteorological reanalyses do not support Bakun's hypothesis of a long-term intensification due to increasing greenhouse gas concentrations, although there is a relationship at interannual time scales as Bakun (1990) and Bakun et al. (2010) envisaged. The lack of a significant trend does not necessarily indicate that Bakun's hypothesis is not correct. The reason could lie in insufficient quality of the reanalysis SLP in this region to identify long-term trends or that the long-term trend in the SLP gradient over the last decades is still overwhelmed by other factors and therefore has not emerged from the background noise yet. Bakun et al. (2010) indicated that this possible factor which blurs the long-term trend in upwelling in BUS is its relation-

ship to ENSO, to which I briefly direct my attention now.

According to the results of the correlation between upwelling and climate modes, and the correlation patterns between the climate modes ENSO and AAO with the wind stress, it appears that the influence of both climate modes is more pronounced in South Benguela than in North Benguela. I attempt to estimate the contribution of ENSO and the AAO to the long-term trend in upwelling in South Benguela in DJF, the season in which the interannual correlations are stronger and the wind stress patterns also display a clearer signal. For this, I set up a linear regression model between upwelling as predictand and ENSO and the AAO as predictors:

$$\text{upwelling}(t) = \alpha_{\text{enso}}\text{ENSO}(t) + \alpha_{\text{aao}}\text{AAO}(t) + \epsilon, \qquad (2.1)$$

where upwelling represents the upwelling index in South Benguela in the DJF, t represents the year, α_{enso} and α_{aao} are the regression coefficients, and ϵ represents the unresolved variance in upwelling. Using the data from the period covered by all three data sets (ENSO, AAO, and STORM, 1957–2010) we can estimate the values of α_{enso} and α_{aao}. The contribution of ENSO and AAO to the long-term upwelling trend is then estimated as

$$\alpha_{\text{enso}}\text{trend}_{\text{enso}}$$
$$\text{and} \qquad\qquad\qquad\qquad\qquad\qquad\qquad (2.2)$$
$$\alpha_{\text{aao}}\text{trend}_{\text{aao}},$$

respectively, where $\text{trend}_{\text{enso}}$ and $\text{trend}_{\text{aao}}$ are the long-term trends in the ENSO and AAO indices, respectively. It turns out that the ENSO trend in DJF is by far not statistically significant, whereas the AAO trend in DJF is positive and clearly statistically significant over the $p = 0.05$ level. The South Benguela upwelling in the STORM simulation increases linearly over 1957–2010 by 39 % of its long-term mean value. The estimated contribution of ENSO to the long-term trend in upwelling in South Benguela in DJF is -3 % of the mean upwelling and the estimated contribution of the long-term trend in the AAO is 41 % of the mean upwelling. This means that, under the assumptions of this simple statistical analysis, the trend in upwelling in South Benguela in DJF simulated in the STORM simulation could be almost entirely explained by the long-term trend in the AAO, with the ENSO contribution remaining negligible.

2.6   Discussion

The large-scale atmospheric drivers of Benguela upwelling in this ocean-only simulation were identified using an upwelling index based on the vertical velocity.

An important result is the disagreement between my analysis of the SLP gradient and the hypothesis of Bakun (1990). There are several possibilities for this

disagreement. The results of the correlation analysis between the upwelling indices and the SLP gradient do show the expected relation of wind forcing driving the upwelling on interannual scales, but neither the upwelling nor its drivers, the upwelling-favourable winds and the SLP gradient show significant trends (except the SLP gradient in MAM). A comparison to measurements of the upwelling itself is not possible due to the lack of such observation on multidecadal time scale. Therefore, I compare my results to other studies using reanalysis data, sediment cores or SST observations as upwelling indices. My results do agree with the findings of Narayan et al. (2010), who did not find a significant trend in upwelling-favourable wind of ERA40. My results, however, disagree with the positive trends in COADS (Comprehensive Ocean-Atmosphere Data Set) and NCEP/NCAR reanalysis. Nevertheless, the trends in the SST derived from HadISST mentioned by Narayan et al. (2010) strongly depend on the analysed period. The trends of upwelling shown by Narayan et al. (2010) based on sediment records are dominated by multidecadal variability rather by a long-term trend, although analysing only the last 30 years would probably lead to a positive trend. The long-term trend in the SLP may be more strongly burdened by uncertainties in the SLP data from NCEP/NCAR reanalysis in the Southern Hemisphere. For instance, Marshall (2003) found considerable deviations in the magnitude of SLP trends between those derived from the NCEP/NCAR reanalysis and those from station data in the Southern Hemisphere, although the sign of the trend seems to agree in both data sets. Since the STORM simulation was driven by the NCEP/NCAR reanalysis, this uncertainty is a strong caveat when estimating long-term upwelling trends. Unfortunately, it is difficult to ascertain which data set (reanalysis, station wind records) is closer to reality, as wind station records may also be strongly influenced by relocation of the stations and instrumental inhomogeneities. Nevertheless, the coarse resolution of NCEP/NCAR reanalysis has to be kept in mind when interpreting my results, not only when looking at the atmospheric variables (SLP and wind stress) but also for the output of the ocean model.

Another oceanic factor that may influence the upwelling is the meridional gradient of the sea surface height (SSH) (Colas et al., 2008). I calculate this gradient in the STORM simulation, defined as SSH in the box $10°$ N–$10°$ S, $50°$ W–$30°$ E minus SSH in the box $30°$ S–$40°$ S, $50°$ W–$30°$ E. This gradient is negatively correlated with the Benguela upwelling. The correlation with North Benguela upwelling is significant with a coefficient of -0.42. The correlation with South Benguela upwelling is not significant with a coefficient of -0.17. This gradient has a positive but not significant long-term trend in the STORM simulation in both seasons JJA and DJF. Therefore, although the sign of the trend of the SSH gradient opposes a positive trend in upwelling by an onshore transport in North Benguela and thus could theoretically contribute to mask the long-term trend in upwelling caused by anthropogenic forcing in this region, its magnitude seems to be too small. In addition, it does not appear related to upwelling in South Benguela.

The SLP mechanisms later augmented by Bakun et al. (2010) involve small-scale dynamics of humidity transport, which may not be properly represented in the coarse resolution atmospheric model used to generate the NCEP/NCAR reanalysis. Unfortunately, no long instrumental SLP records spanning this region are available, so this must remain an open question for the moment. Another possibility is that, although the effect of the external forcing on the SLP field as envisaged by Bakun (1990) may be correct, the amplitude of internally generated wind variability at decadal and multidecadal time scales blurs the long-term signal. Finally on interannual time scales, as also proposed by Bakun et al. (2010), the influence of other large-scale climate modes, such as ENSO, on BUS upwelling may mask the forcing by anthropogenic greenhouse gases. My correlation analysis sheds some light on this last question, as explained below.

The statistically significant negative correlation between ENSO and upwelling in South Benguela during the DJF has been reported by previous studies. Rouault et al. (2010) stated that El Niño leads to reduced upwelling whereas La Niña enhances upwelling. The same study argues that the upwelling-favourable winds are more pronounced during La Niña and weaker during El Niño, which explains the SST anomaly in the BUS during ENSO events. The connection between extreme SSTs (in the False Bay, South Africa) and ENSO is also supported by the study by Deutsch et al. (2011) and Dufois and Rouault (2012). The former authors also found significant correlations between El Niño and the first principal component of austral summer, autumn, and partly spring SST (strongest with a 4-month lag, which is contained in the seasonal resolution of my analysis).

The spectral analysis emphasises the connection between the upwelling and ENSO in DJF. The source of the other time scales in the spectrum (2.5 and 3.3 years) could be due to ENSO too.

The link between upwelling in South Benguela and ENSO has been invoked to explain the parent lack of a long-term trend in BUS upwelling. Earlier studies, for instance Vecchi et al. (2006), indicated a weakening of the trade winds across the tropical Pacific (i.e. a tendency towards El Niño state) as a response to anthropogenic greenhouse gas forcing. A trend towards more intense or more frequent El Niño phases would thus tend to weaken Benguelan upwelling, counteracting the direct effect on upwelling of the anthropogenic forcing. However, more recent studies of the response of ENSO to anthropogenic greenhouse gas forcing recognised much larger uncertainties in the predictions of the future evolution of ENSO (Vecchi and Wittenberg, 2010), although one recent multimodel study has found that the frequency of extreme El Niño events may increase as a result of anthropogenic greenhouse gas forcing (Cai et al., 2014), at least in the first 40 years of the 21st century (Kim et al., 2014). In the observations analysed here, the trend in the ENSO index since 1950 is weak and not significant, so that it is unclear how the long-term trend in ENSO could contribute to robust weakening of upwelling counteracting the greenhouse gas forcing in the past decades. My analysis rather shows that the climate modes ENSO

and the AAO could at most have influenced upwelling in South Benguela and to a lesser extend North Benguela. The observed long-term trend in the indices of these two climate modes could explain almost 100 % of the upwelling trend in DJF in South Benguela in the STORM simulation, but this contribution stems almost entirely from the AAO. In North Benguela, the influence of ENSO and the AAO is very weak and the evolution of the simulated upwelling there cannot be described well by a linear steady trend (Fig. 2.8) associated with the observed evolution of greenhouse gas forcing.

2.7 Conclusion

The large-scale atmospheric drivers of the Benguela upwelling system, as simulated in a global high-resolution ocean simulation (STORM), driven by a prescribed atmosphere in the last 6 decades, have been described in this chapter. The major results are summarised as follows.

- The BUS is better described by two subsystems, North Benguela and South Benguela, as their mean seasonality, their time evolution, and correlations with atmospheric drivers and large-scale climate modes differ.

- As general characteristic for upwelling-favourable atmospheric conditions in both subsystems are an intensified subtropical high, strong and southerly wind/wind stress along the coast, and a SLP contrast between land and ocean.

- There is some evidence of the influence of ENSO and the AAO on upwelling in South Benguela. The El Niño phase in the tropical Pacific tends to weakly hinder upwelling, whereas a stronger AAO tends to reinforce upwelling in this region. In North Benguela, there is no clear influence of these climate modes.

- The long-term trends of the simulated upwelling over approximately the last 50 years do not clearly support the hypothesis put forward by Bakun (1990) that anthropogenic greenhouse gas forcing should lead to more vigorous upwelling. The analysis of the trend of the SLP gradient between land and ocean as suggested by Bakun (1990) does not support an influence of the sea-land SLP contrast on the long-term behaviour of upwelling. The estimated influence of the trends of the large-scale climate modes on Benguela upwelling do not indicate that these climate modes may have disturbed the hypothesised connection between anthropogenic greenhouse forcing and upwelling in this region in the last decades.

- The atmospheric forcing and thus the model results are dependent on the uncertainties inherent in the NCEP/NCAR reanalysis data set. The influence of the atmospheric resolution on the long-term trends in the atmospheric fluxes

needs to be reassessed when higher-resolution data covering the past decades become available.

CHAPTER 3

GENUS-MOM simulation for the Benguela upwelling system

3.1 Introduction

As described in the previous chapter, understanding the atmospheric drivers of the Benguela upwelling system is of major importance when looking at its present variability and its past and future changes. Here, a statistical analysis of a regional ocean-only simulation is presented. In addition to the global ocean-only simulation STORM, analysed in the previous chapter, the analysis of a regional simulation could support the idea that the results do not depend on the simulation used for the analysis. Furthermore, this regional simulation not only contains a physical model but also a biogeochemical submodel, which is of major importance for the dynamics of an upwelling system.

This regional simulation was conducted at the Leibniz-Institut für Ostseeforschung Warnemünde (IOW) with the GENUS-MOM model (Schmidt and Eggert, 2012), which consists of the Modular Ocean Model version 4.0 (MOM-4, developed at NOAA's Geophysical Fluid Dynamics Laboratory) augmented with a regional 3-dimensional ecosystem model. The model was run for the Benguela upwelling system within the GENUS project to be able to compare the in-situ data measured in field excursions with research vessels and to have a continuous data set which could not be provided by measurements. The simulation is driven by the output of a simulation with the regional atmospheric climate model REMO (Haensler et al., 2011), in turn driven at their boundaries by the ERA-Interim meteorological reanalysis. The model REMO provided the atmospheric forcing for GENUS-MOM with the exception of

the near-surface wind field, which was taken from the QuikSCAT data set (Schmidt and Eggert, 2012). The GENUS-MOM domain covers the region between 10° W–18° E and 6.63° N–34° S with a horizontal resolution of 7 km, covering the period between July 1999 and May 2012 (due to the preference for the QuikSCAT wind forcing). This simulation is considerably shorter as the STORM simulation (with a length of 13 years compared to 61 years), has a similar horizontal resolution (7 km compared to 10 km), and covers only the southeastern part of the Atlantic compared to the global STORM simulation. In the final part of this chapter, the results of the analysis of the STORM and the GENUS-MOM simulation will be compared.

The atmospheric variables were obtained from National Centers for Environmental Prediction (NCEP)/ National Center of Atmospheric Research (NCAR) reanalysis 1 and from ERA-Interim reanalysis (Dee et al., 2011). Furthermore, the observational gridded sea surface temperature data set HadISST1 (Rayner et al., 2003) is used in this analysis. These data sets were described in more detail in the previous chapter. For comparison reasons, the analysis of the impact of wind on upwelling is repeated with QuikSCAT winds.

Similarly to the STORM simulation (see chapter 2) in which the upwelling index was derived from the vertical mass transport, in this case it is derived from the vertical water velocity. For the GENUS-MOM simulation it is extracted (at 50 m depth) between 8–18° E and 15–34° S, divided in two regions with the border at Lüderitz (28° S) (Fig. 1.3). Seasonal averages are calculated as follows: December–February (DJF), March–May (MAM), June–August (JJA), and September–November (SON). The upwelling index is correlated with the atmospheric variables as well as with the following climate indices: The Multivariate El Niño-Southern Oscillation (ENSO) Index (MEI; Wolter and Timlin, 1993), the Antarctic Oscillation (AAO; Marshall, 2003), the tropical Atlantic (ATL-3, 20° W–0° E, 3° N–3° S; Rodríguez-Fonseca et al., 2009), and the St. Helena Island Climate Index (HIX; Feistel et al., 2003).

For the linear correlations between the indices, a two-sided significance level of p=0.05 is adopted. The p-value of the correlation and of the trend significance indicates the significance of the correlation under the usual assumption of serially uncorrelated and normally distributed regression residuals. When these conditions are not met in reality, this significance level will be too liberal, flagging correlations or trends as statistically significant although they should not be considered as such. In these cases, where the conditions of normal and independent distributions of the residuals are clearly not met, I will apply a more sophisticated statistical test.

If no explicitly stated, all correlations have been calculated with long-term detrended series.
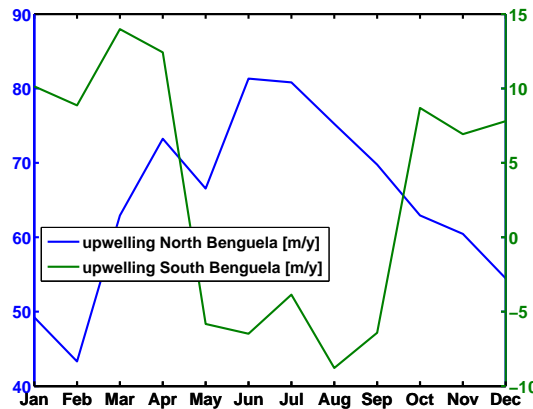
Figure 3.1: Annual cycle of the upwelling indices of the GENUS-MOM simulation derived from the simulated vertical velocity at 50 m in North and South Benguela in the period 1999–2012.

3.2   Upwelling index

The annual cycle of the upwelling index in North and South Benguela is displayed in figure 3.1.

The upwelling index in South and North Benguela display clear differences. Whereas in the north, upwelling shows a broad maximum in JJA, it tends to be stronger in DJF in South Benguela. Both cycles agree with the upwelling modelled in the STORM simulation (chapter 2) and with the observations.

The time evolution of upwelling through the period of the GENUS-MOM simulation is displayed in Fig 3.2. The interannual variations of the seasonal indices seem more coherent in North Benguela than in South Benguela. Furthermore, upwelling in all four seasons describe a decline in the last 4 years in North Benguela. A trend analysis could not be conducted due to the short time span of the data set. The visible trend could also be due to decadal variations.

3.3   Correlations with large-scale climate fields

The correlations of the upwelling index and the sea surface temperature (SST) are shown in figure 3.3. These correlations display a strong distinction between North and South Benguela. In North Benguela, negative correlations occur over the whole region in DJF and over a large fraction of the upwelling region in JJA. South Benguela upwelling is mainly positively correlated with the SST field in DJF, but for JJA the correlation pattern looks very similar to the one for North Benguela.

The relationship between the upwelling and atmospheric forcing are calculated, too. The correlation patterns between the upwelling indices and wind stress for DJF and JJA are displayed in figure 3.4. The correlations for North Benguela in DJF are low and patchy while the pattern of the correlation for upwelling in JJA shows
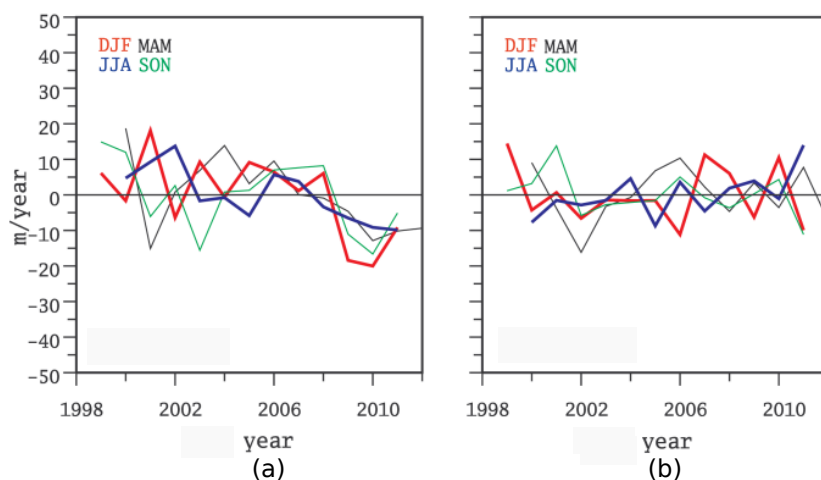
Figure 3.2: Time evolution of the seasonal upwelling indices in North Benguela (a) and South Benguela (b) derived from the vertical velocity of the GENUS-MOM simulation in the period 1999–2012.
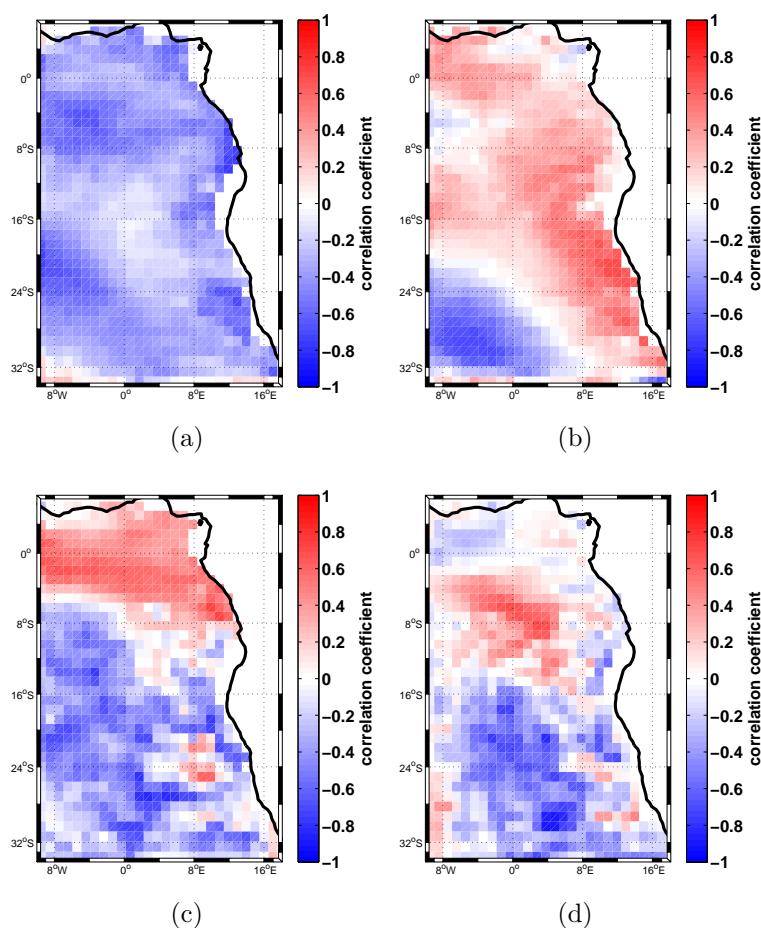
Figure 3.3: Correlation patterns between upwelling indices derived from the vertical velocity and the sea surface temperature field of the GENUS-MOM simulation in austral summer (DJF (North Benguela (a), South Benguela (b)), and in austral winter (JJA (North Benguela (c) and South Benguela (d)) in the period 1999–2012.

upwelling-favourable conditions at the coast north of 20° S. The correlation patterns of the upwelling in South Benguela look similar for both seasons with strong positive correlations around the southern tip of the African continent. This explains why the correlation pattern with the SST shows only positive values at the coast in DJF. The upwelling-favourable wind stress is south of the model domain and offshore of the west coast. Furthermore, for the upwelling in North Benguela the upwelling-favourable wind stress occurs more locally and more nearshore which is supported by the correlation pattern of the SST.

Compared to the correlation patterns derived from the STORM simulation described in the previous chapter, the correlations between wind stress and upwelling in North Benguela derived from the GENUS-MOM simulation are more locally and seasonally restricted. A reason for this could be the atmospheric forcing of the GENUS-MOM model. The STORM simulation has been driven by NCEP/NCAR reanalysis which is used here for the present analysis, too. However, the GENUS-MOM simulation has been forced by the REMO regional atmospheric model (which is driven at its boundaries by ERA-Interim reanalysis) and by the QuikSCAT winds. Therefore, the same correlations are calculated using the QuikSCAT wind data (wind instead of wind stress) (Fig. 3.5).

The obtained correlation patterns look quite different compared to the ones derived from NCEP/NCAR reanalysis, indicating that part of the differences detected between both ocean simulations may be traced back to the different atmospheric forcings used to drive the models.

The correlation between North Benguela upwelling and the wind field in DJF shows southerly wind offshore the whole coast but no correlation directly at the coast. The wind is upwelling-unfavourable in JJA. The wind pattern correlated with the upwelling in South Benguela in DJF agrees well with the pattern when correlating NCEP/NCAR reanalysis. For JJA the wind is upwelling-favourable only over North Benguela.

Thus, it seems that the connection between wind/wind stress and upwelling in North Benguela in the GENUS-MOM simulation depend on the data set used to represent the atmospheric forcing. Upwelling in North Benguela, in the mature upwelling season (JJA) seems to be driven by NCEP/NCAR reanalysis wind stress in the northern part of its coast, whereas the correlation pattern shows upwelling-unfavourable conditions when using QuikSCAT wind. South Benguela upwelling in DJF (the season when it is strongest) is clearly related to the wind/wind stress around South Africa for both forcing data sets. QuikSCAT and NCEP/NCAR reanalysis winds are correlated with 0.99 (for the zonal component) and 0.97 (for the meridional component). Figure 3.6 shows that the results derived from the different data sets differ only in North Benguela but that they are very similar in South Benguela. This supports the similar correlation pattern for upwelling in South Benguela in DJF and the different correlation patterns for upwelling in North Benguela.
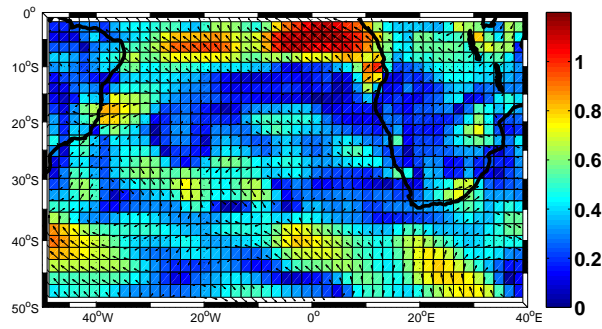
(a)
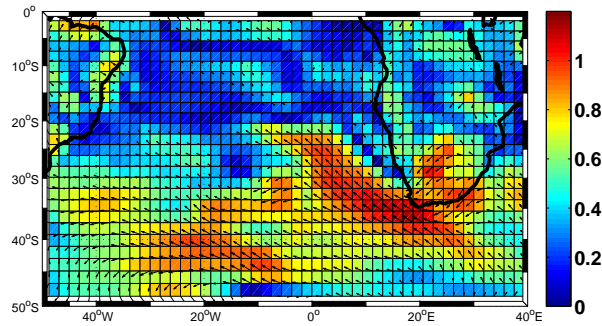
(b)
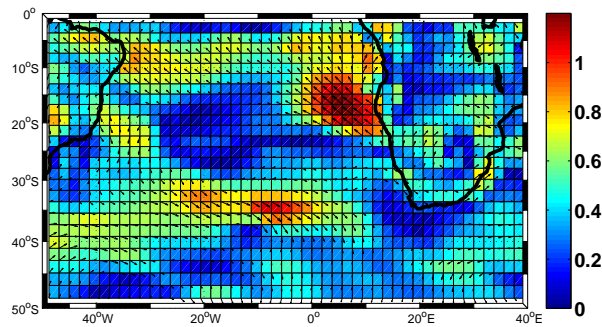
(c)
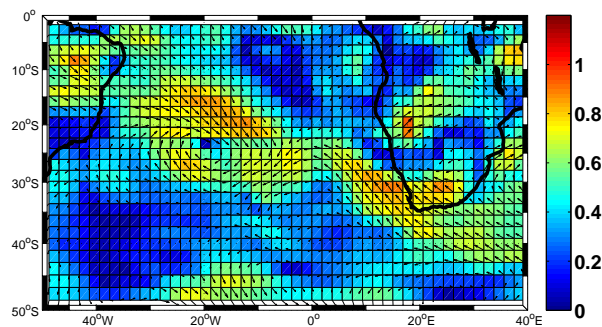
(d)

Figure 3.4: Correlation patterns between upwelling indices derived from the vertical velocity of the GENUS-MOM simulation and the wind stress field of NCEP/NCAR reanalysis in austral summer (DJF (North Benguela (a), South Benguela (b)), and in austral winter (JJA (North Benguela (c) and South Benguela (d)) in the period 1999–2012. The zonal and meridional components of the arrows represent the correlation with the corresponding component of the wind stress. The colours code the square root of the sum of these zonal and meridional correlations squared.
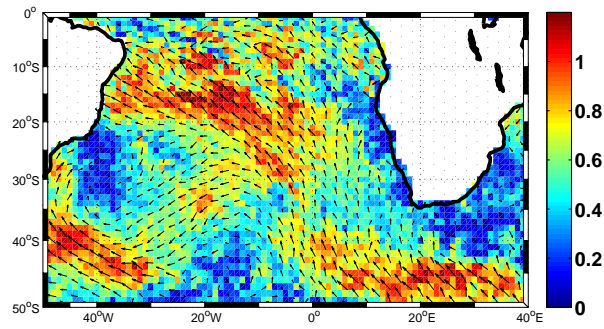
(a)
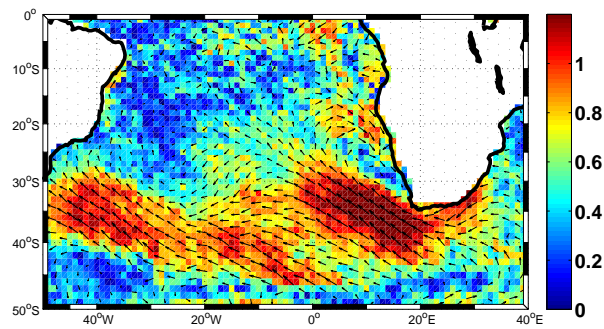
(b)
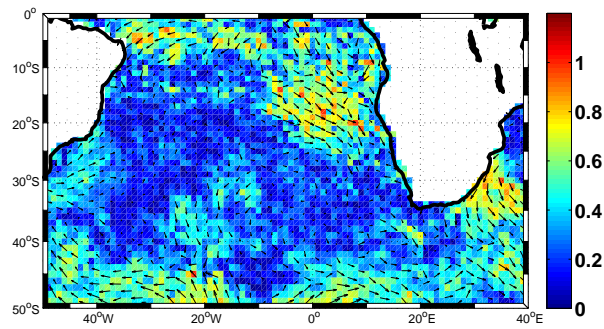
(c)
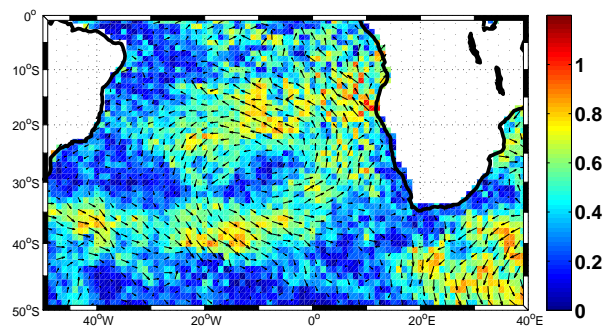
(d)

Figure 3.5: Correlation patterns between upwelling indices derived from the vertical ve-
locity of the GENUS-MOM simulation and the wind field of QuikSCAT in austral sum-
mer (DJF (North Benguela (a), South Benguela (b)), and in austral winter (JJA (North
Benguela (c) and South Benguela (d)) in the period 1999–2009. The zonal and meridional
components of the arrows represent the correlation with the corresponding component of
the wind stress. The colours code the square root of the sum of these zonal and meridional
correlations squared.
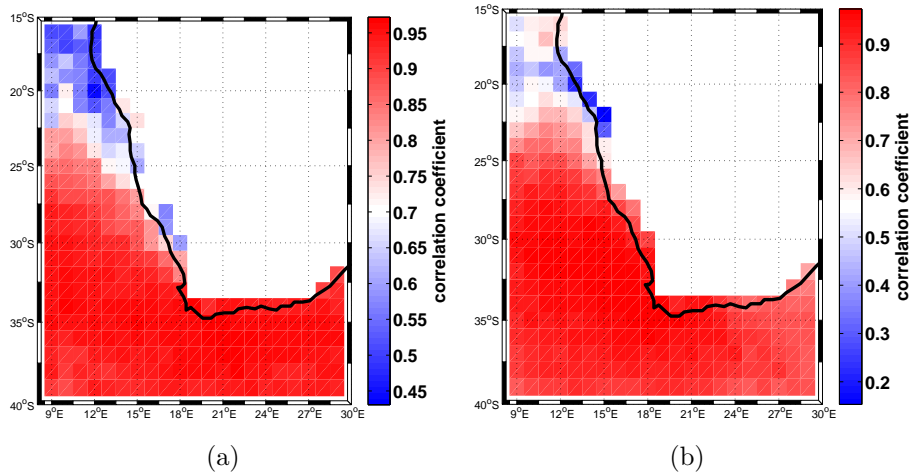
Figure 3.6: Correlation patterns between zonal wind (a) and meridional wind (b) of NCEP/NCAR reanalysis and QuikSCAT in the period 1999-2009.

As described in the previous chapter, Bakun (1990) hypothesised a long-term intensification of coastal upwelling driven by the increasing greenhouse gas concentration in the atmosphere. Because the GENUS-MOM simulation is too short to detect long term trends, only the correlation between upwelling and the sea level pressure (SLP) gradient is analysed here. The SLP gradient is calculated as described in the previous chapter. The correlations with the upwelling index are significant only for North Benguela in DJF with ERA-Interim reanalysis (0.68). Nevertheless, the correlation with upwelling in North Benguela are all positive, indicating an intensification of upwelling due to a positive SLP gradient. For the upwelling in South Benguela, the signal is lower and less clear. This could be due to the location of the continental atmospheric low pressure cell, favouring upwelling more in the northern part of Benguela than in the south.

3.4   Correlations with climate modes

To identify other possible drivers of the upwelling in Benguela, the upwelling indices are correlated here with indices of large-scale climate modes. The upwelling of GENUS-MOM depicts significant correlations between North Benguela upwelling and HIX in JJA and SON (positive) and with the AAO in JJA (positive). South Benguela upwelling is significantly correlated with ENSO in DJF (negative) and with the AAO in MAM and SON (positive) (Tab. 3.1). The significant and positive correlations between upwelling in North Benguela and HIX also support the results of the analysis of the SLP gradient.

Table 3.1: Correlation coefficients of the upwelling indices derived from the vertical velocity of the GENUS-MOM simulation of North Benguela and South Benguela with ENSO, AAO, ATL-3 of HadISST, ATL-3 of STORM, and HIX, significant correlations are highlighted by **

	ENSO	AAO	ATL-3 (HadISST)	ATL-3 (STORM)	HIX
North Benguela:					
MAM	−0.14	+0.28	−0.29	−0.10	−0.08
JJA	+0.21	+0.48**	+0.42	+0.47	+0.77**
SON	−0.20	+0.70	−0.21	−0.16	+0.61**
DJF	−0.11	+0.34	−0.12	−0.52	+0.19
South Benguela:					
MAM	−0.44	+0.59**	+0.14	−0.46	−0.11
JJA	+0.39	−0.02	−0.13	+0.12	+0.22
SON	−0.11	+0.65**	−0.05	−0.28	+0.11
DJF	−0.73**	+0.47	+0.35	−0.31	−0.19

3.5 Comparing the results of the STORM and the GENUS-MOM simulation

The large-scale atmospheric influence on the upwelling in Benguela has been analysed with the STORM simulation (in the previous chapter) and with the GENUS-MOM simulation (in this chapter). Both simulations produce a similar annual cycle of the upwelling. They show an upwelling maximum in JJA for North Benguela and in DJF for South Benguela. This also agrees with observations (Veitch et al., 2010). The correlation pattern of upwelling with SST for North Benguela is similar in both simulations. North Benguela upwelling is negatively correlated with the SST of the whole south east Atlantic in DJF and in the upwelling region in JJA. This supports the weaker seasonality in the North Benguela region. Here, upwelling takes place throughout the year (Veitch et al., 2010). In contrast, in South Benguela upwelling displays opposite correlation patterns with SST in the two simulations, with STORM showing negative correlations in both seasons at the south coast of southern Africa and only in DJF along the west coast. The pattern of the GENUS-MOM simulation is opposite. In JJA, the correlation between upwelling and SST is negative in the upwelling regions and in DJF the SST is positively correlated with the upwelling close to the coast. Because of the regional limitation of the GENUS-MOM simulation, the relationship between upwelling and SST at the southern tip of the continent and the south coast cannot be investigated.

Not only the connection of upwelling to SST, but also to wind or wind stress differ between the two simulations. This difference is not due to the different atmospheric forcing that is used in each simulation. With NCEP/NCAR reanalysis as

well as with QuikSCAT, the correlations of the wind stress with the upwelling of GENUS-MOM show different patterns than the ones derived from STORM, especially for North Benguela. The correlation pattern for upwelling in North Benguela derived from the GENUS-MOM simulation is upwelling-favourable only for JJA with wind stress of NCEP/NCAR reanalysis and not at all with QuikSCAT winds. Whereas the STORM simulation provides a pattern with upwelling-favourable wind stress off North Benguela in both seasons, stronger in JJA than in DJF. For upwelling in South Benguela, the correlation shows upwelling-favourable wind and wind stress along the South African coast, for both STORM and GENUS-MOM. It seems that despite the coarser resolution of the NCEP/NCAR reanalysis compared to QuikSCAT, NCEP/NCAR is suitable as atmospheric driver of upwelling in the Benguela region.

It has been found that the influence of the SLP gradient on the upwelling in North Benguela is stronger than on the upwelling in South Benguela, and both simulations capture the influence of the SLP gradient similarly. However, there is only one significant correlation between upwelling and the SLP gradient with the GENUS-MOM simulation, whereas there are numerous significant correlations with the STORM simulation. This may depend on the longer time period covered by the STORM simulation, because the significance of a correlation depends not only on the connection of the data sets but also on their length.

The results of the analysis of the impact of climate modes on the upwelling in Benguela are also similar for both simulations. ENSO has an influence on the upwelling in South Benguela in austral summer. A positive AAO phase tends to strengthen the whole Benguelan upwelling. The HIX exerts an influence on the upwelling in North Benguela. When analysing the STORM simulation, the tropical Atlantic and the AMM additionally have a significant influence in one season.

To summarise, the annual cycle and the impact of climate modes agree in the two simulations. The correlation pattern when correlating with SST and wind stress differ in some cases.

3.6   Conclusion

In this chapter, the large-scale atmospheric drivers of the Benguela upwelling system, as simulated in a regional high-resolution ocean simulations driven by a prescribed atmosphere of the last 13 years, have been described.

The GENUS-MOM simulation captures the different seasonality of the two subsystems, North Benguela and South Benguela. The general drivers of the upwelling are the SLP gradient (especially for North Benguela) and alongshore southerly winds. HIX, ENSO, and AAO additionally influence the upwelling.

The analysis of the drivers of the Benguela upwelling system has been conducted with two high-resolution ocean-only simulation, with the STORM simulation in the

previous chapter, with the GENUS-MOM simulation in this chapter. The two simulations generally agree on the drivers of the Benguela upwelling system. The seasonal cycle and the impact of the SLP gradient between ocean and land are similar. Furthermore, the influence of ENSO, AAO, and HIX on the upwelling has been detected in both simulations. However, the analysis of the correlation between upwelling in South Benguela and the SST field as well as the correlation between the wind/wind stress and the upwelling provide distinct results. These discrepancies could be due to the open boundary of the GENUS-MOM simulation south of South Benguela which could lead to possible difficulties in simulating the impact of the Agulhas Current and its eddies influencing this region. In addition, the atmospheric forcing of the GENUS-MOM simulation is not derived from one consistent data set but from a combination of the regional atmospheric model REMO and QuikSCAT winds. This may be responsible for the differences in the statistical link between the wind on the simulated upwelling. Nevertheless, analysing the regional GENUS-MOM simulation in addition to the global STORM simulation allows to identify the main drivers of the Benguelan upwelling and illustrate the complexity of this upwelling system.

<div style="text-align: right">

CHAPTER 4

</div>

Extrema of the North Benguela upwelling system

4.1   Introduction

In this chapter, I analyse the large-scale circulation that give rise to seasons with extrema of upwelling in the North Benguela upwelling system. Understanding the extremes, the phenomena driving the extremes, is essential to understand the dynamics of the upwelling system and its sensitivity to atmospheric and oceanic variability. Extreme events of upwelling in North Benguela are of major importance to the local fisheries, and thus for the economy of the adjacent countries Angola, Namibia, and South Africa. Strong changes in the upwelling intensity influence the nutrient content as well as the temperature and oxygen concentration of the water masses in the Benguela region. Very weak upwelling leads to low primary production first and less energy flowing throw the trophic chain later (Bakun and Weeks, 2004). On the other hand, very strong upwelling leads to very strong offshore transport of zooplankton so that the population cannot grow, leading to enhanced phytoplankton growth over the shelf and subsequent export of organic matter (Bakun and Weeks, 2004). Thus, predicting these extremes would be of help for fisheries management of the adjacent countries of the Benguela upwelling system.

In present understanding, the upwelling strength is modulated by several factors. The El Niño-Southern Oscillation (ENSO) is one of them as described in chapter 2 and chapter 3. An El Niño state leads to weak upwelling conditions and a La Niña state leads to enhanced upwelling (Rouault et al., 2010). ENSO is used for seasonal prediction in other areas due to its strong impact on the tropical and subtropical

climate, so that theoretically ENSO seasonal predictions could be used to predict upwelling in Benguela a few seasons in advance. As we will see later, the situation is more complex.

Another phenomenon that influences the Benguela upwelling, especially the upwelling in North Benguela, is the occurrence of Benguela Niños (Shannon et al., 1986). As again described in chapter 2, Benguela Niños are types of Atlantic Niños, the Atlantic counterpart of the Pacific ENSO. Atlantic Niños develop in the tropics due to changes in the winds at the Equator (McCartney, 1982) and occur on average every ten years (Shannon and O'Toole, 2003). With these two main phenomena in mind, I analyse in this chapter the influence of the atmospheric and oceanic conditions of the South Atlantic and the tropics of the Atlantic and Pacific Ocean on upwelling extremes in North Benguela.

Understanding and eventually predicting seasonal extremes is still in an early phase of development (Doblas-Reyes et al., 2013). In general, climate models used for seasonal prediction are initialized to situate the model close to the best knowledge of the real atmospheric and oceanic states, a step that involves very computing-intensive processes of data-assimilation. Since the knowledge of these initial conditions is always limited, a level of uncertainty is unavoidable. This uncertainty usually grows as the simulation proceeds further in time, so that the reliability of the simulated trajectory is usually lost after a few days, compared to the real trajectory of the atmosphere-ocean system. However, an ensemble of simulations may still contain statistical information about the seasonal distribution of certain climate variables, which can still be very useful for predictive applications. For instance, although it will not be possible to predict the weather months ahead, it might become possible to predict anomalies of seasonal mean precipitation, temperature, or the likelihood of extreme events.

Unfortunately, the status of present climate models make this type of predictions still very difficult. In the extra-tropical realm, the skill of seasonal predictions is still very low. Even in the Tropics, where coupled atmosphere-ocean modes like ENSO display a typical evolution over several months, it has proven difficult to successfully predict the occurrence of events. Statistical and dynamical prediction models for ENSO prediction have a comparable skill (Barnston et al., 1999). Recently, dynamical models attain skills that are sometimes better than statistical models (Barnston et al., 2012).

Here, I explore another possible way of seasonal prediction of only certain aspects of the regional climate, such as seasonal mean upwelling, concentrating on extreme upwelling seasons, seasons with extreme intensity of upwelling. I will work in the context of 'perfect model set-up'. This means that I assume that a climate model is a perfect representation of reality and try to assess to what extent a statistical analysis may prove useful to predict whether or not the main upwelling season in a particular year will exhibit extremely intense or extremely weak upwelling in North Benguela. The advantage of this approach is that, within this virtual set-up, the

data set is complete, with no gaps, and very large, allowing for a detailed statistical analysis. However, in the real world data are indeed incomplete, they include measurements errors, and the observation records are shorter. Therefore, in the real world, the prediction skill will very likely be lower than in the model world. Nevertheless, this type of studies are useful because they set an upper limit to the prediction skill that can be potentially obtained in the real world.

4.2   Data and methods

The model data used in this chapter is the ocean model MPI-OM (Jungclaus et al., 2013) of the Max Planck Institute Earth System Model (MPI-ESM) (Giorgetta et al., 2013). Here I analyse the low-resolution version (MPI-ESM-P) for the past1000 simulations covering the period 850–1850. It has a horizontal resolution of T63 (1.9 degrees) with 47 levels for the atmosphere, a horizontal resolution of 1 degree with 40 levels for the ocean, and a prescribed land cover and vegetation (Giorgetta et al., 2013).

Furthermore, two other simulations are used in this analysis to test the findings achieved with the MPI-ESM model. First, I use the Parallel Ocean Program version 2 (POP2), the ocean component of the coupled Earth System Model Community Climate System Model (CCSM4) (Gent et al., 2011). It covers as well the period 850–1850 and has a resolution 1 degree and 60 levels (Danabasoglu et al., 2012). Its atmospheric part is the Community Atmosphere version 4 (CAM4) in 1 degree horizontal resolution. Second, the STORM simulation a high-resolution version of the model MPI-OM (Marsland et al., 2003) is analysed for comparison. The STORM simulation is driven by the global NCEP/NCAR global meteorological reanalysis (von Storch et al., 2012; Li and von Storch, 2013). It has a horizontal resolution of 0.1 degrees and 80 levels and covers the period 1950–2010.

In addition, the pre-industrial control runs (PI) of the MPI-ESM (1155 years (1850–3005)) and of the CCSM4 (500 years (800–1300)) are used to analyse the drivers of upwelling extremes without external climate impacts.

To define the extreme upwelling years, the 90th and 10th percentile of upwelling in the main upwelling season are calculated in each simulation separately and the extremes are defined as those years when upwelling values are outside this range, values higher than 90% or lower than 10% of all upwelling values in the main upwelling season. For the MPI-ESM and CCSM4 past1000 simulations this means that the extreme weak and extreme strong upwelling years comprise 100 years each, whereas in the STORM simulation there are only 6 years defined as extreme strong and extreme weak upwelling years. For the pre-industrial runs (PI runs), each group of extremes comprise 115 years (MPI-ESM) and 50 years (CCSM4), respectively. In the following analysis, the pattern of anomalies are the seasonal mean of the analysed season of all extreme weak or extreme strong upwelling years minus the

seasonal mean of the analysed season of all years.

For MPI-ESM and CCSM4 the main upwelling season in North Benguela (8–30° E, 15–28° S) is September–November (SON), for STORM it is June–August (JJA). The seasonal cycle of the three simulations agree well with previous studies indicating that the strongest upwelling takes place in austral winter to spring (Veitch et al., 2010; Muller et al., 2014). As we have seen in figure 2.6, strongest upwelling in North Benguela takes place between July and October. If we want to identify which one of the standard seasons (JJA or SON) is the one with highest upwelling, it turns out that both could be defined as the main upwelling season, since the mean difference is small.

As upwelling index I use here the modelled vertical mass transport at 52 m depth (MPI-ESM, STORM) and 55 m depth (CCSM4) (close to the bottom of the mixed layer).

In the following, the results of the analysis of the extreme events with the MPI-OM are presented first.

4.3   Wind stress and SST of extreme upwelling years
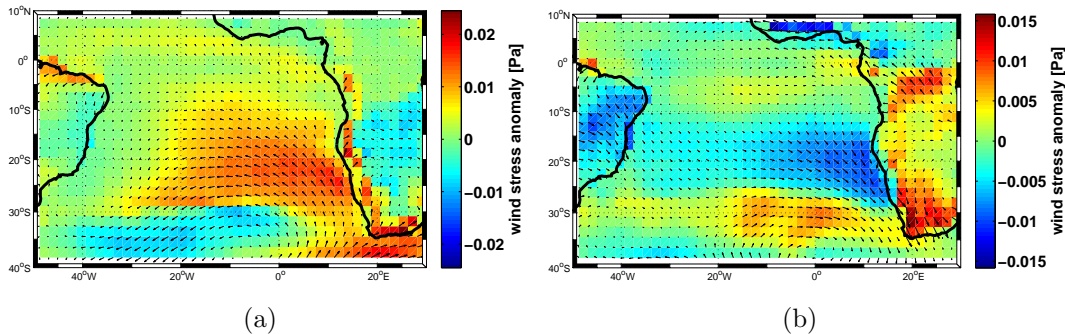
Figure 4.1: Wind stress anomalies of the 100 strongest upwelling years in North Benguela simultaneous (SON) (a) and of the previous season (JJA) (b) derived from the MPI-ESM past1000 simulation. Note the different scale.

In years of extreme upwelling in SON, the wind stress pattern looks quite similar to the climatology. When examining the anomalies, however, the differences with the climatological mean values become evident: the wind stress anomaly shows positive values off southwest Africa (Fig. 4.1a). Thus, stronger than usual upwelling takes place simultaneously with stronger than usual wind stress over the upwelling region. Interestingly, the wind stress pattern of the preceding season (JJA) in the years with strong SON upwelling is opposite (upwelling-unfavourable) (Fig. 4.1b), indicating that upwelling in the preceding season JJA tends to be weaker than normal. The sea surface temperature (SST) anomalies also support this, with negative
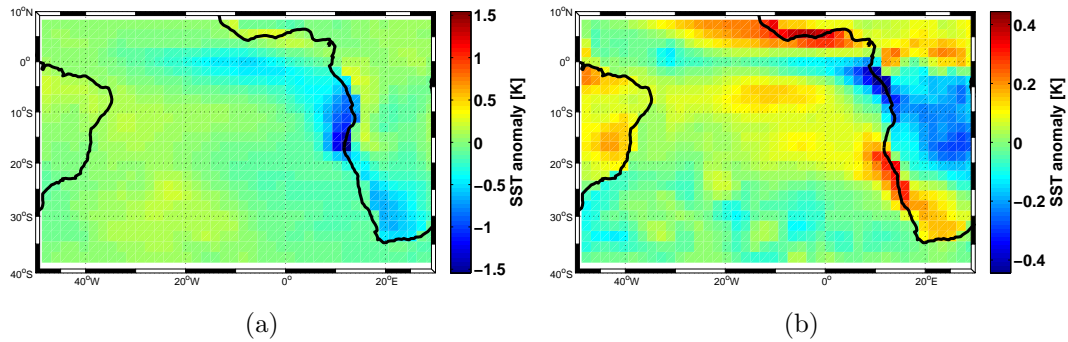
Figure 4.2: Sea surface temperature anomalies of the 100 strongest upwelling years in North Benguela simultaneous (SON) (a) and of the previous season (JJA) (b) derived from the MPI-ESM past1000 simulation. Note the different scale.

SST anomalies in northern North Benguela in SON and SST anomalies displaying a dipole structure with positive anomalies off the southwest African coast and negative ones at the coast between 0 and $10°$ S in the previous season (Fig. 4.2).

In the 100 years with weakest upwelling in North Benguela, the mean wind stress pattern shows the opposite situation. In the upwelling season, wind stress anomalies are negative, whereas in the season before the weak upwelling, the upwelling-favourable winds are stronger than average. Because both extremes behave in the opposite way, in the following I focus on the 90th percentile with strongest upwelling.

Subdividing the 90th percentile into the following parts 90 %–92 %, 92 %–98 %, 98 %–100 %, the wind stress anomalies in SON show an intensification with stronger extremes of upwelling (not shown).

The anomalous annual cycles of upwelling, wind stress, and SST (relative to the climatological annual cycle) for years with strong and weak upwelling seasons are shown in figure (Fig. 4.3). These annual cycles support my previous findings with positive upwelling anomalies, positive wind stress anomalies, and negative SST anomalies in SON of strong upwelling events and opposite anomalies in JJA prior to these events. The wind stress in JJA in strong upwelling years is significantly different from the wind stress in weak upwelling years. However, upwelling itself and the SST are not significantly different in both extreme cases. This may indicate that the signal in/over the South Atlantic might be of atmospheric origin and the ocean is reacting to anomalous atmospheric conditions. In the main upwelling season itself (SON), all three variables differ significantly between years with strong and weak upwelling. Note that the model bias is not relevant in this calculation, since for all three variables only deviations from the model climatological mean are considered.

4.4 Sea surface temperature as forecast index

Since I have found that the SST displays a clear pattern of anomalies in JJA before extreme upwelling in SON, I attempted to set up a statistical model based on SST
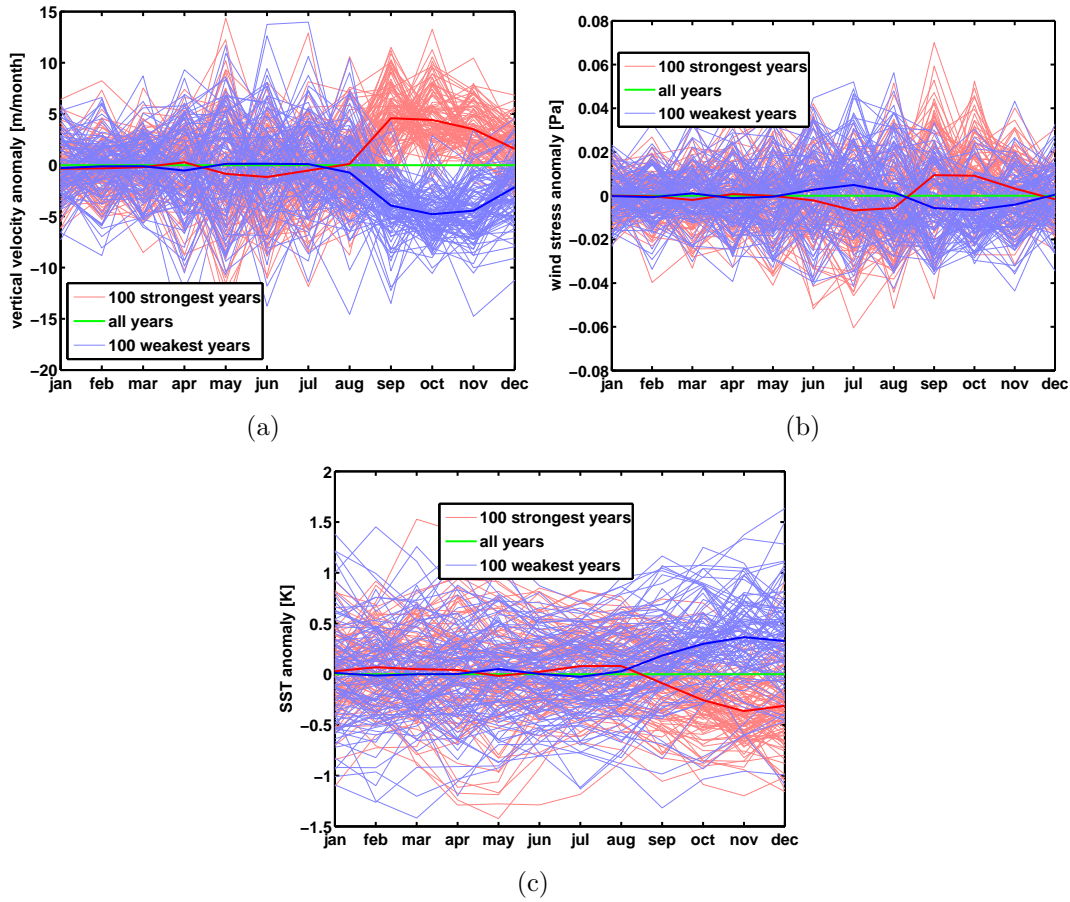
Figure 4.3: Anomaly of the annual cycle of years of extreme upwelling in SON relative to the climatological mean annual cycle, of upwelling (a), meridional wind stress (b) and sea surface temperature (c), derived from the MPI-ESM simulation. Meridional wind stress (over the ocean) and SST of 8–30° E, 15–40° S, upwelling of North Benguela (8–30° E, 15–28° S).

in JJA that may predict extreme upwelling in SON. I define an index by choosing the regions of 15–25° S, 8–25° E, which display positive SSTs in years with extreme upwelling, and the region 0–10° S, 5–15° E, which displays negative SSTs in years with extreme upwelling. The difference between SST in both regions is my predictor index. Thus, the 90th percentile of this index indicate events when the ocean in the Benguela upwelling system is warmer, equal or not much colder than the tropics. Simultaneously (in JJA), the upwelling pattern shows negative anomalies in the regions where SSTs are warm and vice versa. Also, the pattern of wind stress anomalies looks upwelling-unfavourable off southwest Africa. Thus, the index represents well the atmosphere-ocean interplay between SST, wind stress and upwelling itself. Unfortunately, when using this index of the SST conditions in the season before to forecast strong upwelling and wind stress anomalies in the main upwelling season, the wind stress and upwelling do not show a clear or strong signal.

Deriving the index by using only the positive SST anomaly off southwest Africa, the

wind stress anomaly in the following season does show upwelling-favourable con-
ditions, but the upwelling pattern does not depict a clear signal. Using only the
negative SST anomaly off the tropical coast as index, the wind stress anomaly in
the following season is upwelling-unfavourable, but the upwelling pattern shows no
signal with the exception of positive anomalies near the northern border of Namibia.
To sum it up, the SST in JJA in the South Atlantic does not seem to be suitable to
predict the upwelling in SON, either when using the anomaly differences between
tropics and Benguela, or when using only one of them. Thus, the signal causing
the change of wind stress from JJA to SON does not have its origin in the SST of
the South Atlantic. In the following I explore teleconnections that may explain the
potential seasonal predictability of Benguelan upwelling in the climate simulations.

4.5 Influence of the tropics on extreme Benguela upwelling

4.5.1 El Niño-Southern Oscillation

One strong driver of the tropical variability is the El Niño-Southern Oscillation
(ENSO), the dominant mode of climate variability on Earth. It is therefore reason-
able to explore the influence of ENSO on extreme upwelling in Benguela. Several
previous studies already have suggested an influence of ENSO on upwelling in this
region, although my analysis of the STORM simulation in chapter 2 indicated that
this influence is only noticeable in South Benguela and not very strong at interan-
nual time scales. Looking at the SST in the El Niño region in the equatorial Pacific,
it does show positive anomalies in the season December–February (DJF, the main
ENSO season) before the extreme upwelling in SON (Fig. 4.4). Nevertheless, the
anomalies are quite weak, at least too weak to call it an El Niño state.

(a)   (b)
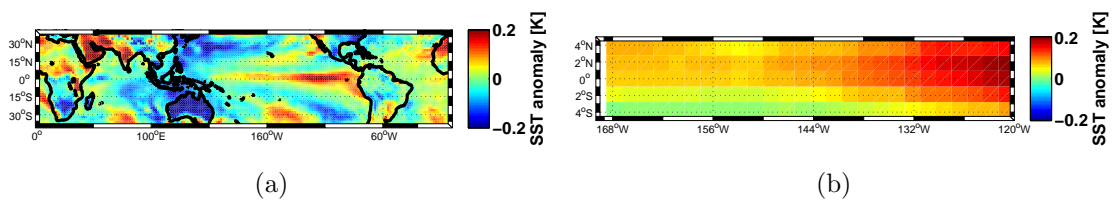
Figure 4.4: Tropical sea surface temperature anomaly (a) and sea surface temperature
anomaly in the Niño3.4 region (b) in austral summer (DJF) before the strong upwelling
events in North Benguela, derived from the MPI-ESM simulation.

To obtain a closer look, I display the mean pattern of monthly SST anomalies during the year before an extreme upwelling season in North Benguela. Figure 4.5 shows the temporal evolution of the SST anomaly in the tropical Pacific as well as in the tropical Atlantic. In the tropical Pacific, a positive SST anomaly is intensifying during the year before strong upwelling in North Benguela, whereas in the tropical Atlantic no signal occurs until the month of June before the upwelling season. In the further course of events, a positive SST anomaly develops north of the equator and a negative one south of the equator in the Atlantic, both spreading poleward in the following months.
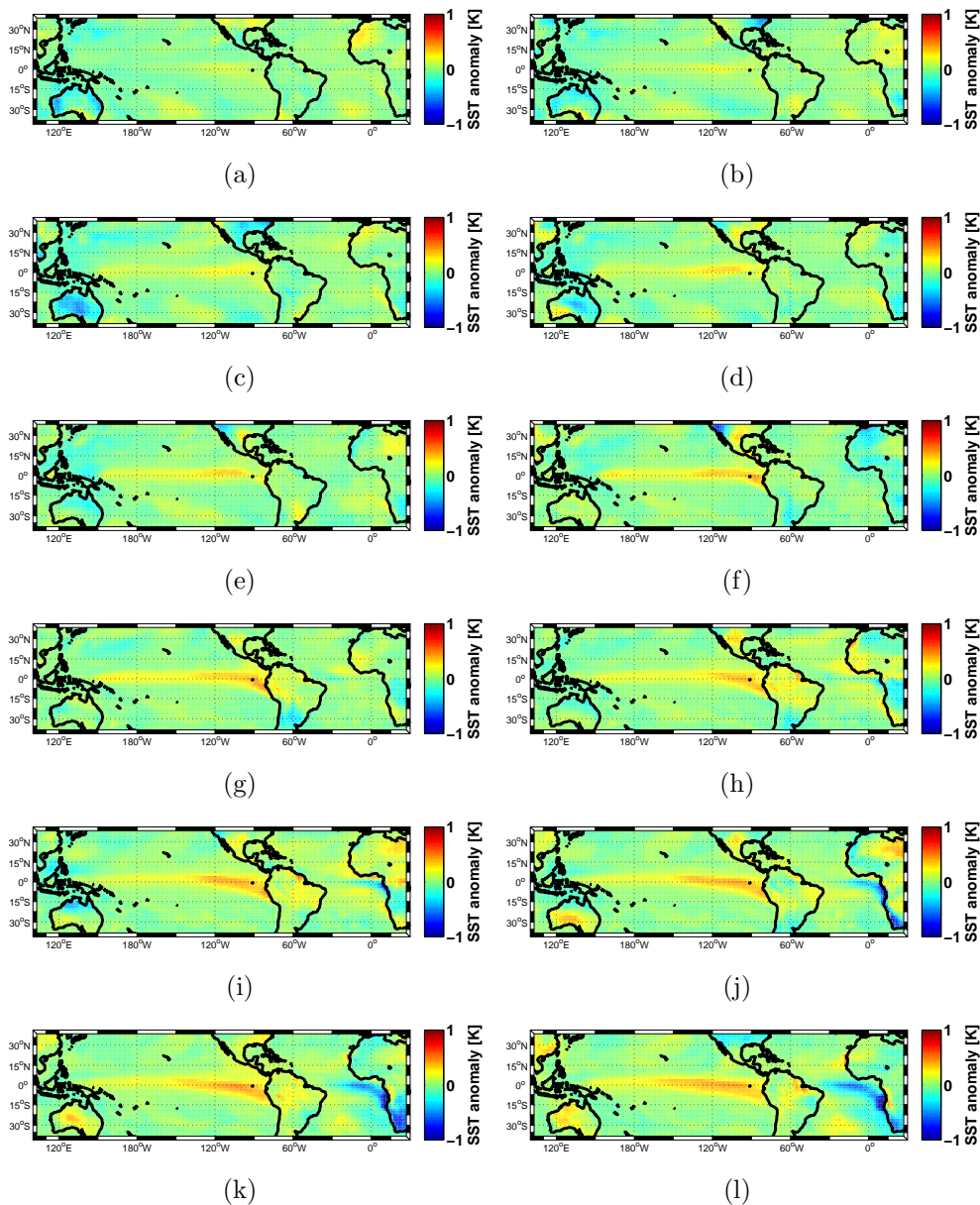
Figure 4.5: Sea surface temperature anomaly in the 12 months before and during extreme upwelling in North Benguela, starting in December (a) before and ending in November (l) during the strong upwelling events in SON, derived from the MPI-ESM simulation.

4.5.2 Sea surface height

As we have seen in the previous section, there seems to be a signal in the tropics travelling southward to the Benguela System in the months prior to an extreme upwelling season. This travelling signal could be due to coastal Kelvin waves. Kelvin waves occur when easterlies at the equator are weak (Rouault et al., 2007). They move eastward along the equator and poleward as coastal Kelvin waves when reaching the eastern boundary of the Atlantic (Rouault et al., 2007). If these waves reach the North Benguela, they lead to anomalous conditions in North Benguela, generically called Benguela Niño. Due to these Kelvin waves, the SST, sea surface height (SSH), and the stratification display positive anomalies (Rouault et al., 2007).

The SSH anomaly pattern in the simulation agrees well with the anomaly pattern of the SST, indicating higher sea levels with warmer temperatures (Fig. 4.6). Negative anomalies in SSH develop in June before positive extremes of upwelling at the Equator. These anomalies move eastward to the west coast of Africa and spread southward reaching North Benguela. Thus, the anomalously low SSH during strong upwelling has its origin in the tropical Atlantic and could constitute a Benguela equivalent of La Niña. The season before (JJA) is characterised by anomalously high SSH. Nevertheless, Benguela Niños generally develop in late summer and last for around half year (Shannon et al., 1986), whereas the signal found here in SST and SSH starts to develop later, in June.
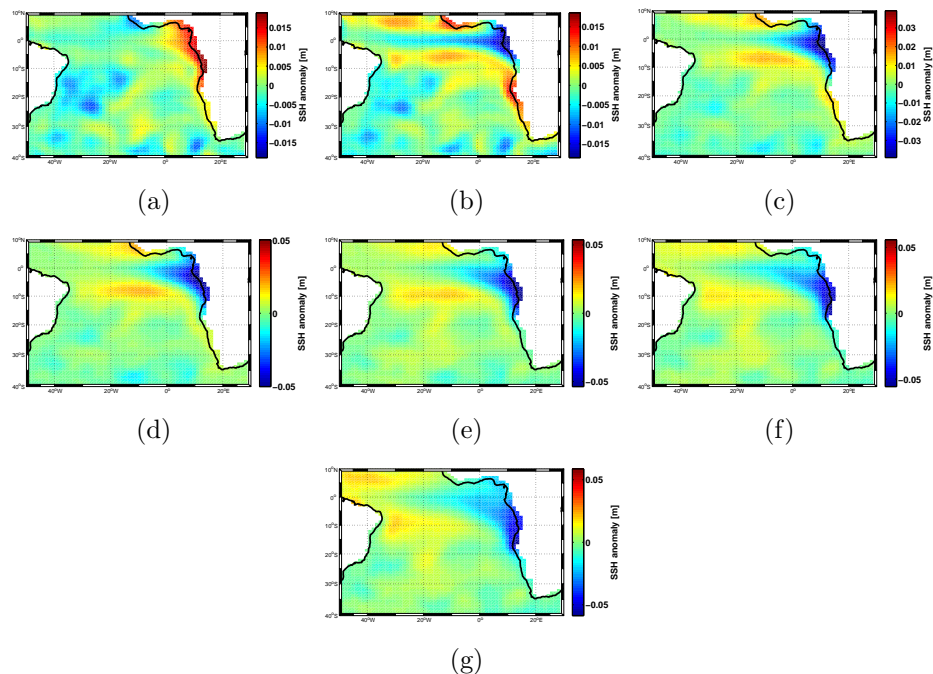
Figure 4.6: Sea surface height anomaly of the 7 months before and during extreme upwelling in North Benguela, starting in May (a) before and ending in November (g) during the strong upwelling events in SON, derived from the MPI-ESM simulation. Note the different scale.

4.5.3   Outgoing longwave radiation, precipitation, and sea level pressure

In addition to Pacific and Atlantic Niños, the location and strength of the Inter Tropical Convergence Zone (ITCZ) could impact the upwelling strength. The outgoing longwave radiation (OLR) can be used as index for the position and intensity of the ITCZ. The planetary emission of OLR is strong when the emission temperatures are high. This occurs when the emission is originated at the surface or in the lower atmospheric layers and it is not absorbed by higher level clouds. Thus, high OLR is indicative of clear skies and, in the tropics, of weak convection. In contrast, with strong convective activity, the emission of OLR is originated at the cloud tops, which are much colder than the surface. Therefore, low OLR is indicative of convective activity and precipitation. In reality, OLR is measured by satellites, but climate models also calculate their modelled OLR according to these physical considerations.

From June onwards before an intense upwelling until November, the end of the upwelling season, the OLR has a positive anomaly in the tropics at the west coast of Africa (Fig. 4.7a–f). This could indicate a weaker than usual ITCZ in years of stronger than usual upwelling. The anomaly of precipitation in the seasons before and during strong upwelling confirms the weaker ITCZ, with negative values over the same region (5° N–5° S, 5° W–10° E (Fig. 4.7g–l)). Stronger than usual OLR indicates a weaker ITCZ with less convective precipitation. This would induce weaker trade winds and thus weaker upwelling and warmer SST over Benguela. The tropical influence could therefore explain the weaker wind stress and warmer SST in JJA, the season before the intense upwelling, but it does not explain the sudden intensification of wind stress and thus the strong upwelling in SON.

The precipitation anomaly in the tropics in JJA is correlated with -0.37 with the upwelling in North Benguela in SON. Selecting the 200 extreme years (strongest and weakest) to calculate this correlation leads to an even stronger connection of precipitation in JJA and upwelling in SON (-0.59) (Fig. 4.8). Nevertheless, the wind stress (SON) in years of extremely low tropical precipitation (JJA) is upwelling-unfavourable (Fig. 4.9a). A low correlation of tropical precipitation in JJA and wind stress over Benguela in SON supports this. This is indicative of the missing impact of precipitation (convection) on wind stress. In years of extreme tropical precipitation in JJA, upwelling and precipitation are highly correlated (-0.63). The tropical precipitation in JJA is also strongly correlated with the wind stress over Benguela in JJA (0.58) but not with the wind stress in SON. Therefore, the tropical convective activity in this region has neither an impact on upwelling in SON in years of weak tropical precipitation.

Thus, the precipitation seems to impact the upwelling in the following upwelling season, but not the wind stress. To explain this discrepancy between the connection of tropical precipitation to upwelling but not to wind stress, I take a look at the
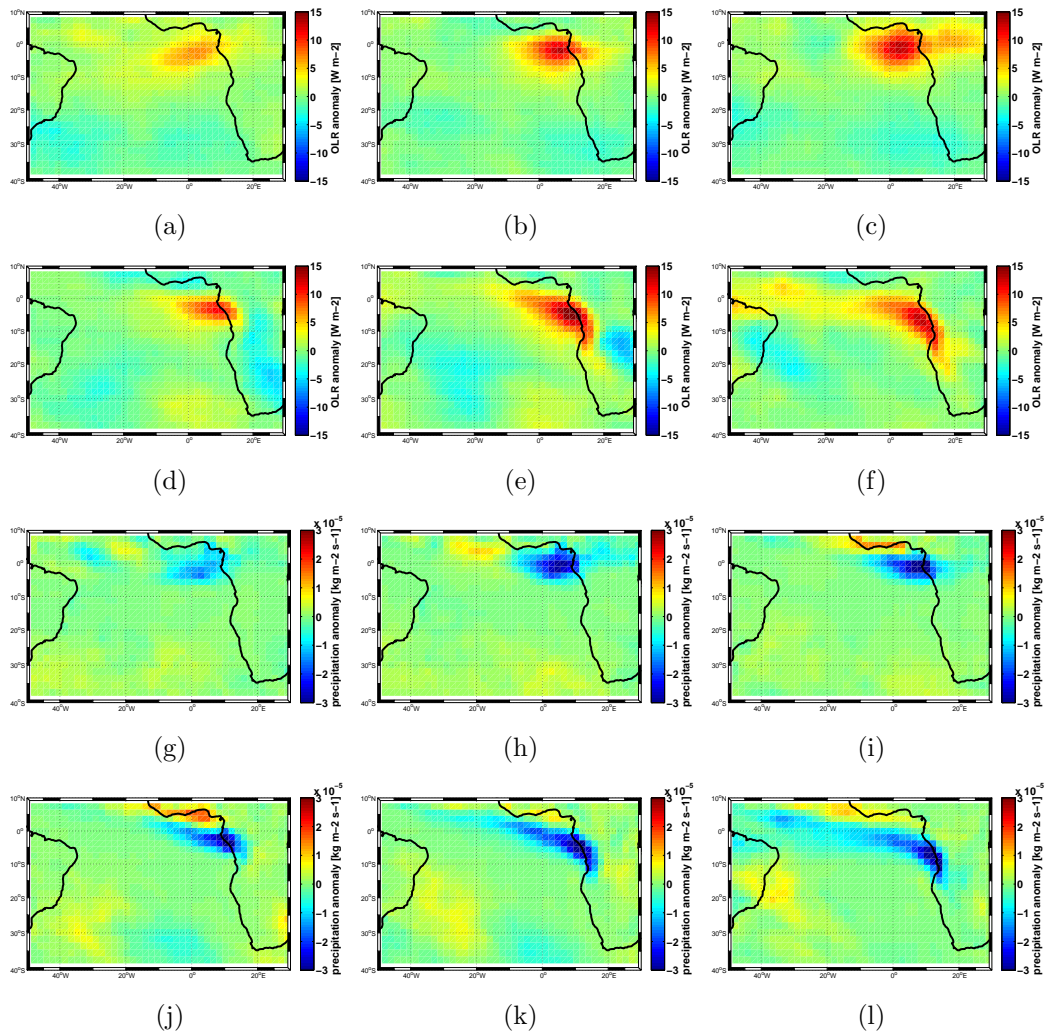
Figure 4.7: Outgoing longwave radiation anomaly (a–f) and precipitation anomaly (g–l) of the 100 strongest upwelling years in North Benguela (SON) in June to November, derived from the MPI-ESM simulation.

sea level pressure (SLP). The SLP anomaly pattern of the South Atlantic in JJA in the years with strong upwelling shows a weaker than usual subtropical high and a slightly intensified continental low (not shown). In SON, it shows an intensified subtropical high and weakened continental low (not shown). However, the SLP anomaly in SON in years of weak precipitation in JJA supports the pattern of wind stress, with a lower than usual subtropical high. Stronger than usual SLP occurs only north of it, directly over North Benguela and in the tropics, where the precipitation anomaly is located (Fig. 4.9c). Thus, the tropics may explain the weaker than usual SLP and wind stress in JJA before strong upwelling (Fig. 4.9b, d) but not the shift to upwelling-favourable conditions.
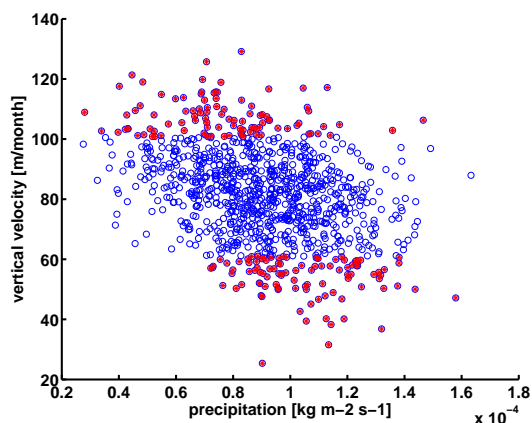
Figure 4.8: Scatterplot of precipitation in JJA over the tropics (5° N–5° S, 5° W–10° E) and upwelling in SON in North Benguela, derived from the MPI-ESM simulation. Blue circles indicate all years, red dots years of extreme upwelling intensity in North Benguela.
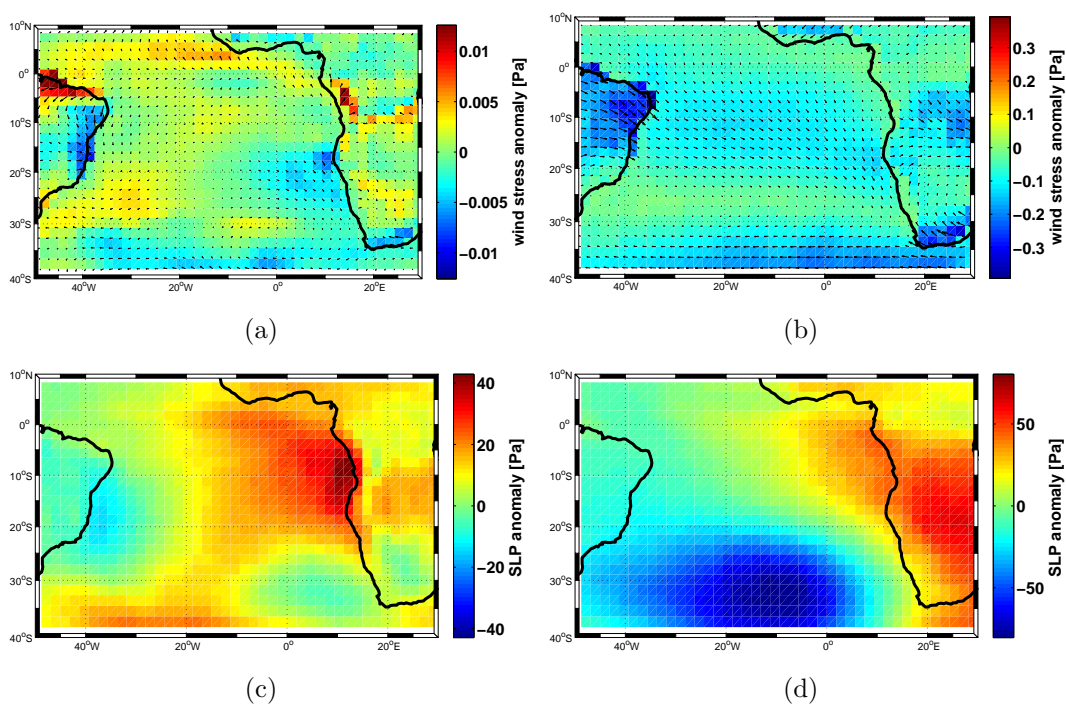
Figure 4.9: Wind stress in SON (a) and JJA (b) and sea level pressure in SON (c) and JJA (d) of the weakest 100 precipitation JJA season in the tropics (5° N–5° S, 5° W–10° E), derived from the MPI-ESM simulation. Note the different scale.

4.6   Comparing the results of the MPI-ESM to the results of STORM

In the STORM simulation, the analysis of the climate anomalies linked to years when the upwelling is stronger than the 90th percentile does not show strong wind stress anomalies in the upwelling region, neither simultaneously nor in the previous season. The SST anomalies are in both seasons very similar, with negative anomalies in North Benguela and positive ones north of 15° S. Thus, the STORM simulation does not support my findings in the MPI-ESM simulation of reversing wind stress and SST conditions in the season during and before the extreme event in upwelling. This could be due to the much shorter time period covered by the STORM simulation compared to the MPI-ESM, 60 years versus 1000 years, and accordingly to a low number, only 6, of years with extreme upwelling above the 90th percentile in the STORM simulation.

Another possible reason for the discrepancy between the two simulations could be the atmospheric forcing of the STORM simulation. STORM is forced by NCEP/NCAR reanalysis (for further details see chapter 2), whereas, the MPI-ESM simulation is a coupled ocean-atmosphere simulation. In the STORM simulation, any possible feedback of the ocean is not communicated back to the atmosphere, since the atmospheric forcing is prescribed and independent of the ocean response to the atmospheric forcing.

Finally, another reason, which we should always bear in mind, is that the MPI-ESM simulation is not realistic enough in the simulation of extreme upwelling seasons.

4.7   Comparing the results of the MPI-ESM to the results of the CCSM4

To test the robustness of the results obtained with MPI-ESM, I also analyse a similar simulation with the Earth System Model CCSM4. The CCSM4 coupled Earth System Model provides in some sense similar results as the MPI-ESM, but there are also striking differences. The clear similarity is provided by the wind stress and SST patterns in the upwelling season and in the previous season. Looking at the years within the 90th and 10th percentiles of upwelling in North Benguela in SON, SST and wind stress display upwelling-unfavourable pattern in North Benguela in the season before strong upwelling seasons and upwelling-favourable before weak upwelling seasons. The SST field in the season before shows even stronger anomalies than the pattern found in the MPI-ESM simulation. However, the positive anomalies in the CCSM4 simulation also extend into in the tropics, whereas in the MPI-ESM simulation the SST anomalies are negative there. Thus, there is not a SST dipole-like pattern as it was found in the MPI-ESM simulation, but rather a

homogeneous positive anomaly pattern.

This contrasting signal in the tropics is supported by the analysis of the SST in the El Niño region. Here, a strong upwelling season in SON is preceded by a negative SST anomaly in the eastern tropical Pacific in the previous DJF season. The temporal evolution of the anomalies in the eastern tropical Pacific as well as in the Benguela region shows slightly negative anomalies in the eastern tropical Pacific one year before the intense upwelling, becoming stronger every month. The anomaly in Benguela is initially slightly stronger than normal, becoming more intense, and turn to negative SST anomalies, as it should, only in October and November of the upwelling season.

The monthly anomalies through the annual cycle are very similar in both coupled Earth System Model simulations. The wind stress and upwelling itself in JJA are significantly different in years of strong and weak upwelling, whereas the SST is not. In SON, all three variables differ significantly between strong and weak years. Thus, the upwelling in JJA differs more strongly in the CCSM4 simulation between the two extremes than in the MPI-ESM simulation.

The SSH anomalies reflect the SST signal, with anomalies of the same sign. As in the SSH anomaly pattern of the MPI-ESM simulation, the SSH pattern in the CCSM4 simulation also indicates that the negative anomaly of the extreme upwelling season develops in the tropics, expands latitudinally around the Equator and spreads southwards along the west coast of Africa. This supports the hypothesis that the mechanism could have its origin in the tropics and impacts the Benguela region via coastal Kelvin waves. However, the negative SSH is much more locally restricted to the equator and the coastline of Africa compared to the more widespread signal in the MPI-ESM. Furthermore, the negative anomalies develop only in the upwelling season itself, and are not already present in the previous season as it is the case in the MPI-ESM.

The anomalies of precipitation and OLR derived from the CCSM4 are weak and indicate no strong influence of the tropical convective activity on extreme upwelling in North Benguela in this simulation.

4.8   Pre-industrial simulation

In the previous analysis, in which the large-scale patterns accompanying extreme upwelling were identified, I had not taken into account the role of the variable external forcing. For instance, SST may be strongly influenced by sudden increases or decreases of the external forcing due to volcanic eruptions or changes in solar irradiance. This influence may confound the link between these climate patterns and upwelling.

In this section, I present a similar analysis in long control simulations, conducted with external forcing that does not undergo any changes over time (other than the

annual and daily cycles). The pre-industrial control simulations have been produced with the same models MPI-ESM and CCSM4 as the past millennium simulations. The number of extreme years, as stated in section 4.2, is different in each simulation. The correlation pattern of upwelling in SON and the SLP field derived using all years of the simulations, or only the years with extreme upwelling (strong and weak), (Fig. 4.10a, b) shows the strong connection between the subtropical high over the South Atlantic and upwelling in North Benguela. This connection is even stronger when looking only at the extreme events (weak and intense upwelling). The pressure field

(a)

(b)

(c)

(d)
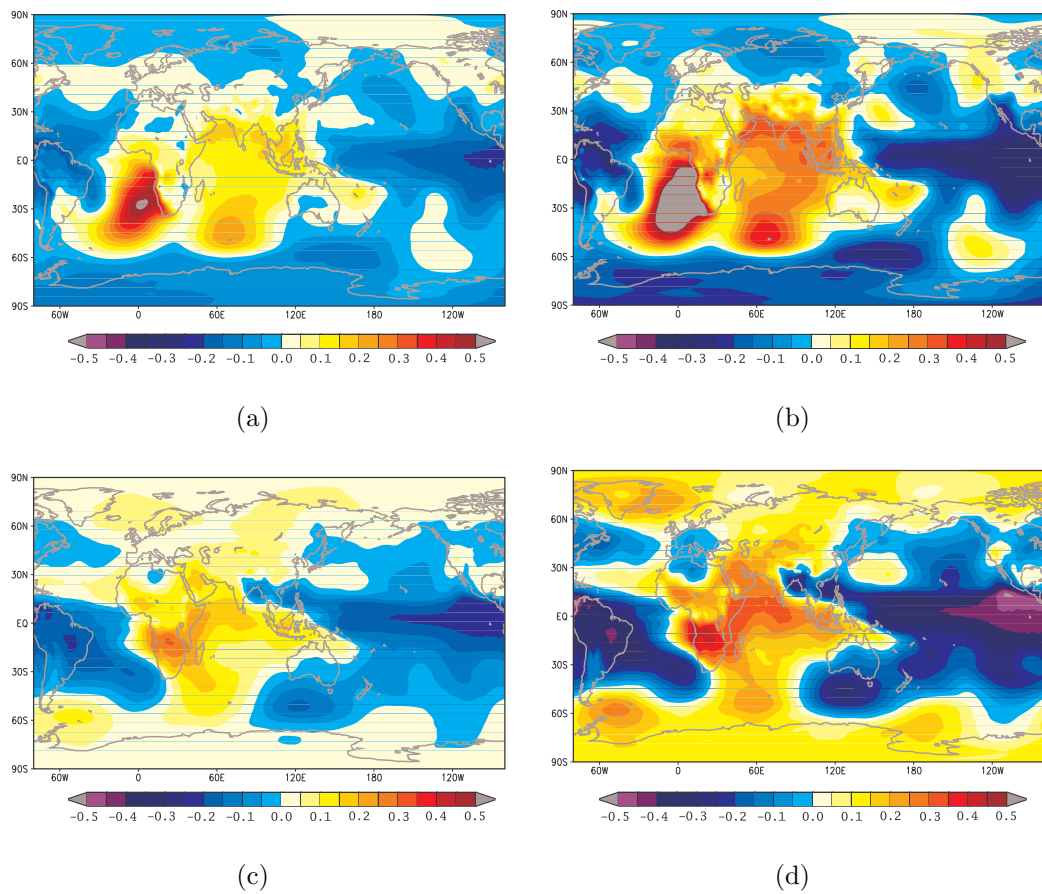
Figure 4.10: Correlation patterns between upwelling in SON and sea level pressure in SON calculated using all years (a) and using only extreme years (b) and sea level pressure in JJA of all years (c) and of extreme years (d), derived from the MPI-ESM simulation. The colours code the correlation coefficient.

of the South Atlantic subtropical high in JJA is negatively correlated with the upwelling in SON, with, again, stronger values for the extreme events (Fig. 4.10c, d). Thus, the shift from less upwelling-favourable conditions to strong upwelling conditions in SON takes place on average in all years, though this signal is much more clear in years with extreme upwelling. These correlation patterns indicate that the connection between SLP and upwelling is the same in extreme and non-extreme years, but that this signal strongly intensifies when looking only at the years of

extreme upwelling.

In figure 4.10d, two regions of strong SLP anomalies can be identified, one over the eastern equatorial Pacific and South America (120–70° W, 20° N–10° S) and one over the tropical Africa (10–40° E, 30–0° S). The sign of this anomalies is opposite. According to these regions, a SLP-index has been calculated (SLP anomalies in tropical Africa minus SLP anomalies in tropical South America). Figure 4.11 shows the connection of this index to the upwelling in North Benguela. In years of extreme upwelling, the SLP difference between Africa and South America is high and upwelling is extremely strong. The SLP difference is low when upwelling is extremely weak. Furthermore, in years of especially strong SLP differences between the two regions, upwelling is mostly strong, and vice versa. This shows the link of this SLP-regions on upwelling in North Benguela.

(a)   (b)
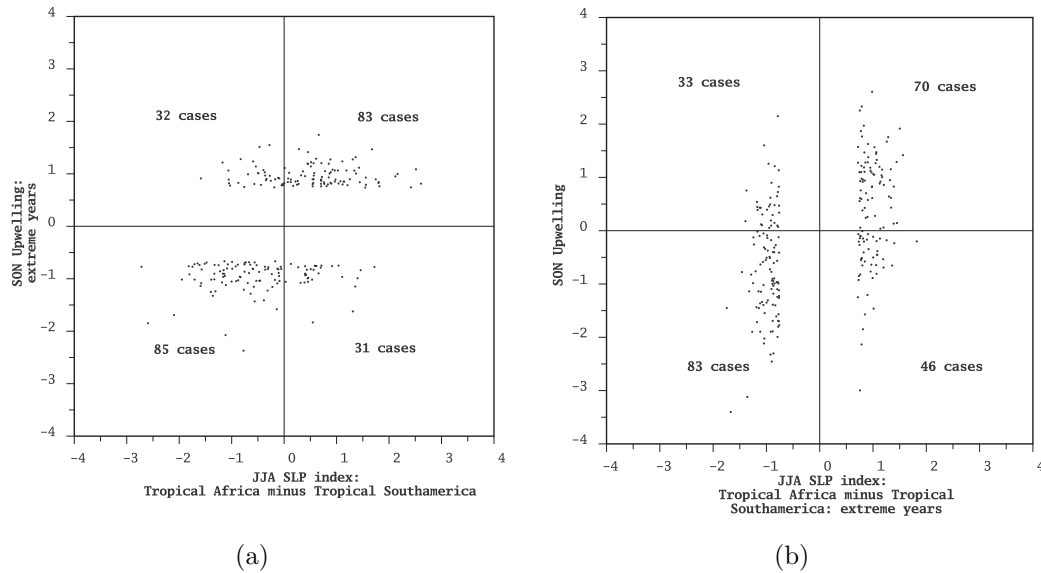
Figure 4.11: Scatter plot of sea level pressure index (tropical Africa minus tropical South America) in JJA of all years and upwelling in SON of extreme years (a) and JJA sea level pressure index of extreme years with upwelling in SON of all years (b), derived from the MPI-ESM simulation.

The correlations between upwelling and SST agree with the signal identified for the SLP. SSTs in SON in the South Atlantic are correlated negatively with upwelling, and SSTs in JJA are correlated positively with upwelling in SON (Fig. 4.12). Again, these correlations are intensified when the analysis is restricted to extreme years. Therefore, only the results for the extreme years are presented hereafter.

The correlation pattern with SST additionally shows a link of the SSTs in the equatorial Pacific, as we have seen in the previous section about the tropical influence on upwelling (section 4.5.1).

To get an insight into how these large-scale tropical SLP and SST anomalies may be linked to the upwelling, I correlate the 200 hPa zonal wind and the near-surface zonal wind (u-components) to upwelling in North Benguela. Changes in SST may lead

to changes in the atmospheric circulation, the Walker Circulation. These changes can be seen in the correlation pattern between upwelling and zonal wind. The zonal
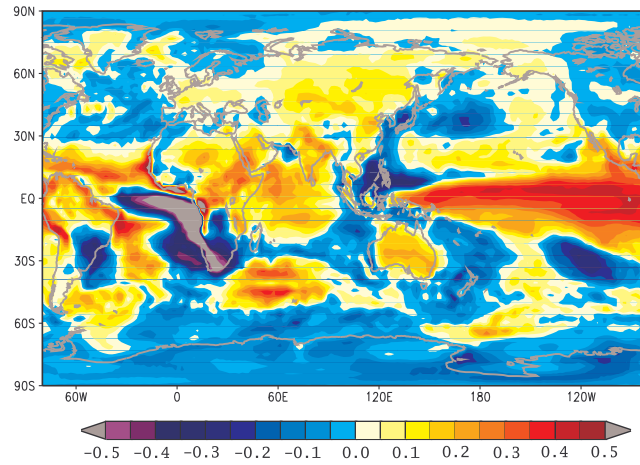
(a)
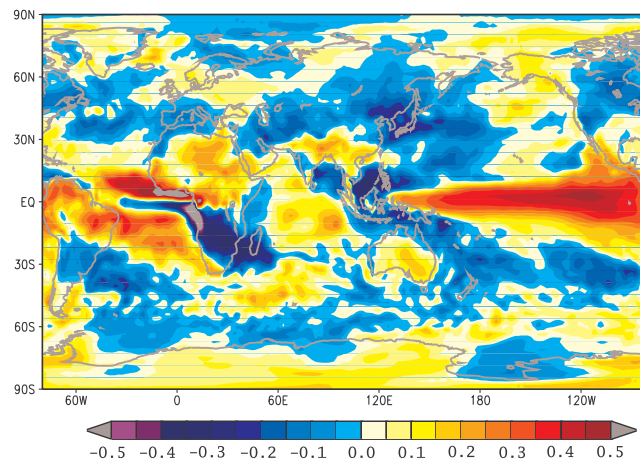
(b)

Figure 4.12: Correlation patterns between extreme upwelling in SON and sea surface temperature in SON (a) and in JJA (b), derived from the MPI-ESM simulation. The colours code the correlation coefficient.

wind is by definition positive when directed from West to East. Areas with positive zonal wind anomalies (eastward) that are accompanied at their eastward side by areas of negative anomalies (westward) indicate a convergence of the zonal wind. This convergence must be associated with ascending air if they occur at the surface or with descending air near the tropopause at 200 hPa height. Similarly, areas with negative zonal wind anomalies (westward) that are accompanied at their eastward side by areas of positive wind anomalies (eastward), are associated with zonal wind divergence. These areas indicate descending air if they occur at the surface, or ascending air if the happen near the tropopause.
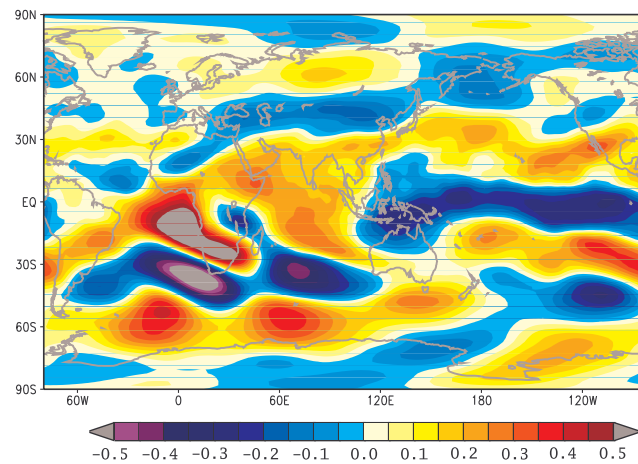
(a)
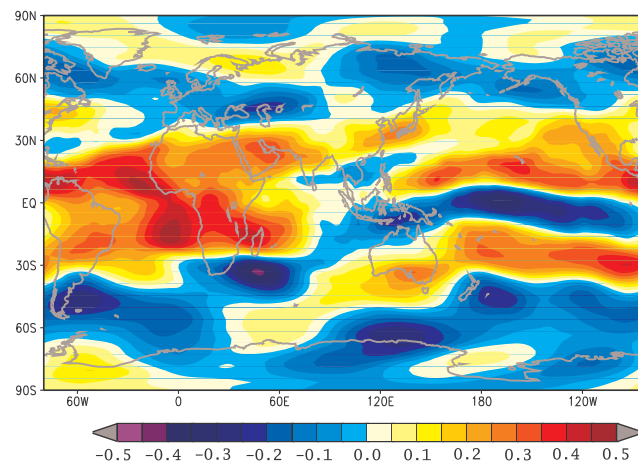
(b)

Figure 4.13: Correlation patterns between extreme upwelling in SON and 200 hPa zonal wind in SON (a) and in JJA (b), derived from the MPI-ESM simulation. The colours code the correlation coefficient.

In figure 4.13 and figure 4.14 one can see that winds in SON indicate a descending branch of the Walker Circulation over tropical Africa and Indonesia and an ascending branch over tropical South America. This agrees with the low pressure over the tropical South America, with the lower precipitation and with the high pressure over the tropical Africa. In the season previous to strong upwelling (JJA), the descending branch over the tropical Africa and Indonesia is diminished or displaced. Nevertheless, the SST and zonal winds near the surface and the tropopause of the equatorial Pacific and the tropical South America show the same pattern in JJA and SON when correlated with upwelling in SON. Thus, ENSO or rather ENSO-like mechanisms is indeed correlated to upwelling. This connection is intensified during years of extreme upwelling. Therefore, a seasonal prediction of the strength of the

upwelling in North Benguela in SON could be estimated by the ENSO-like intensity the previous season in this simulation. (Note, however, that ENSO fully develops in DJF, and not in JJA. This is the reason why I write ENSO-like).
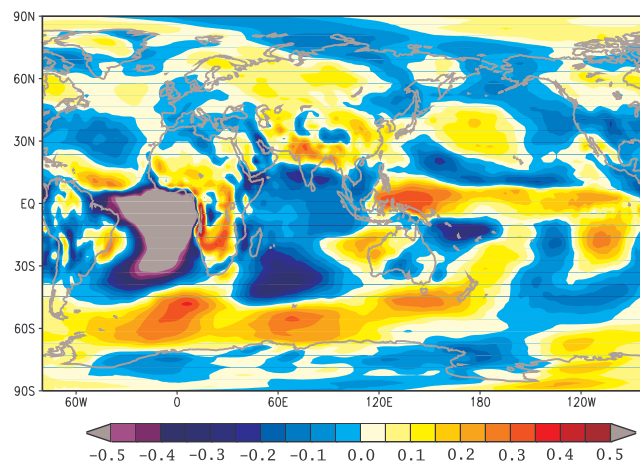
(a)
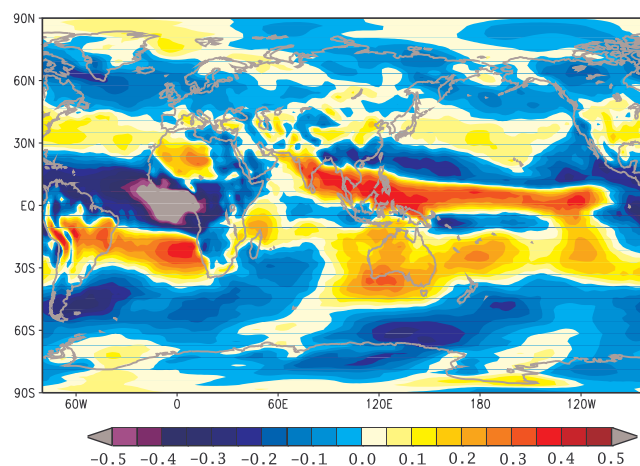
(b)

Figure 4.14: Correlation patterns between extreme upwelling in SON and 10 m zonal wind in SON (a) and in JJA (b), derived from the MPI-ESM simulation. The colours code the correlation coefficient.

Somewhat surprisingly, the comparison between the two Earth System Models reveals contradicting results regarding the impact of the tropical Pacific and Indian Ocean on Benguela upwelling. This can be clearly seen in figure 4.15 and figure 4.16. The correlation patterns in the CCSM4 in the South Atlantic is very similar to the one derived from the MPI-ESM, for both variables SLP and SST. In contrast, the correlations to SST in the equatorial Pacific is opposite in both models. This leads to differences in the Walker Circulation and compromises the predictability based on the ENSO-like patterns intensity, too. Since both models yield opposite results,
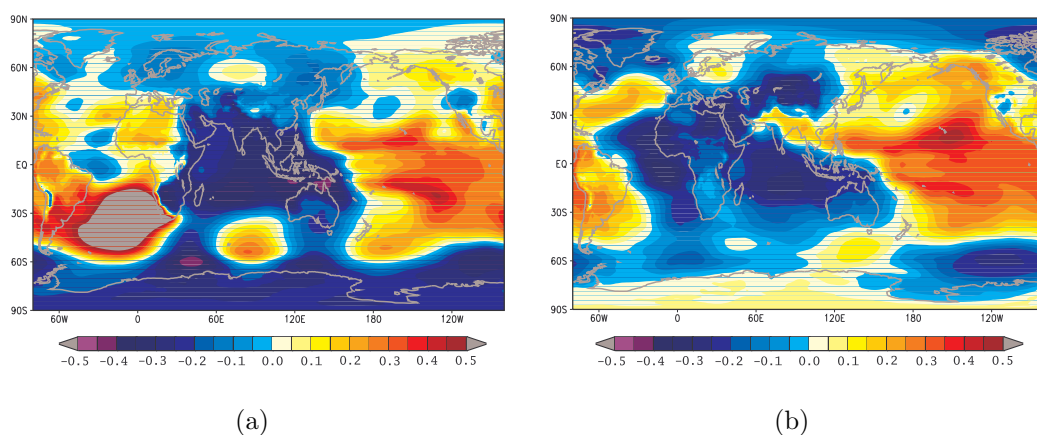
Figure 4.15: Correlation patterns between extreme upwelling in SON and sea level pressure in SON (a) and in JJA (b), derived from the CCSM4 simulation. The colours code the correlation coefficient.
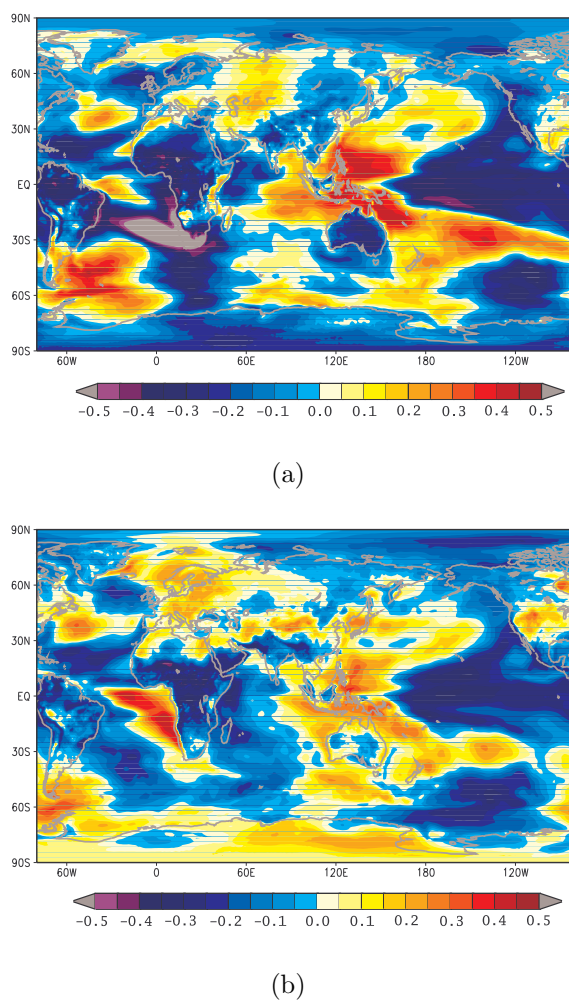
Figure 4.16: Correlation patterns between extreme upwelling in SON and sea surface temperature in SON (a) and in JJA (b), derived from the CCSM4 simulation. The colours code the correlation coefficient.
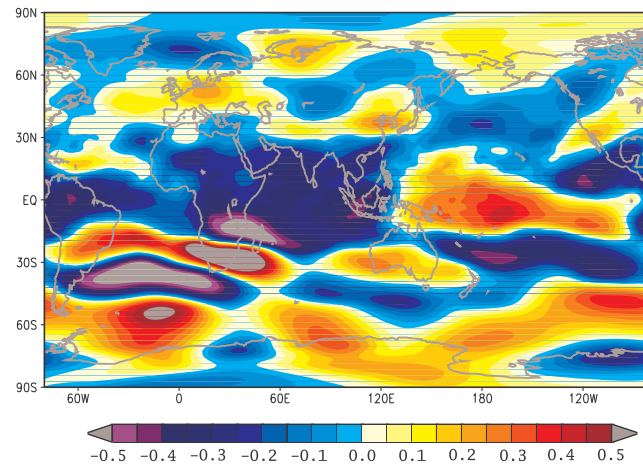
(a)
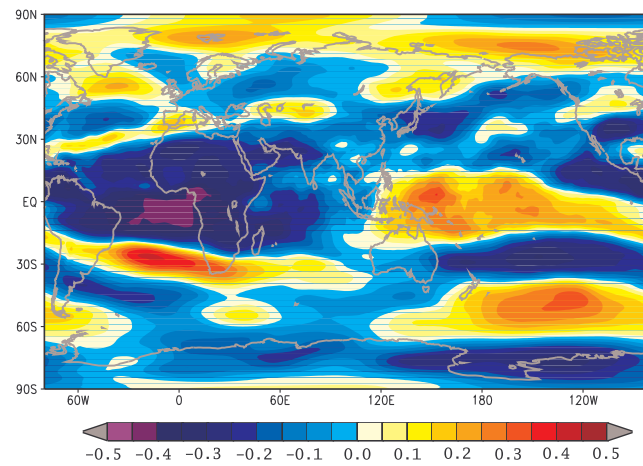
(b)

Figure 4.17: Correlation patterns between extreme upwelling in SON and 200 hPa zonal wind in SON (a) and in JJA (b), derived from the CCSM4 simulation. The colours code the correlation coefficient.

before a statistical seasonal prediction scheme can be envisaged, the realism of both models have to be evaluated. Nevertheless, both simulations do indicate the presence of potential seasonal predictability of extreme upwelling.

The differences between both models are made more explicit by looking in more detail at the correlation patterns between upwelling and the zonal wind. Figure 4.17 and figure 4.18 show the zonal wind pattern correlated to upwelling. We have seen that in the MPI-ESM simulation, strong upwelling is linked to strong westward zonal winds at the surface over the South Atlantic (Fig. 4.14) – these zonal winds obviously cause strong upwelling. At 200 hPa height, the zonal wind are strong and directed eastward over North Benguela and the tropical South Atlantic. This means that over the region of upwelling and the tropical South Atlantic there is an anom-
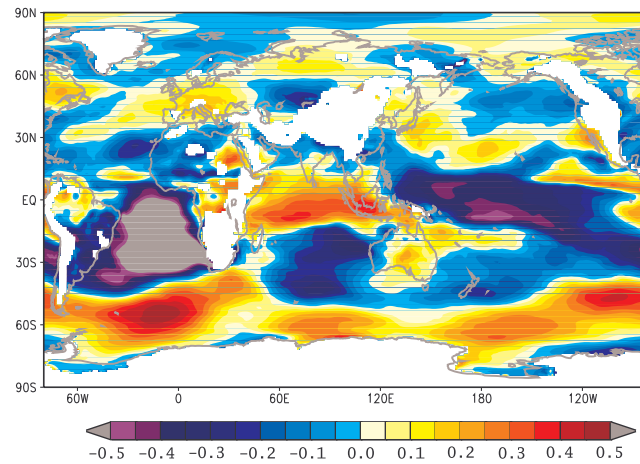
(a)
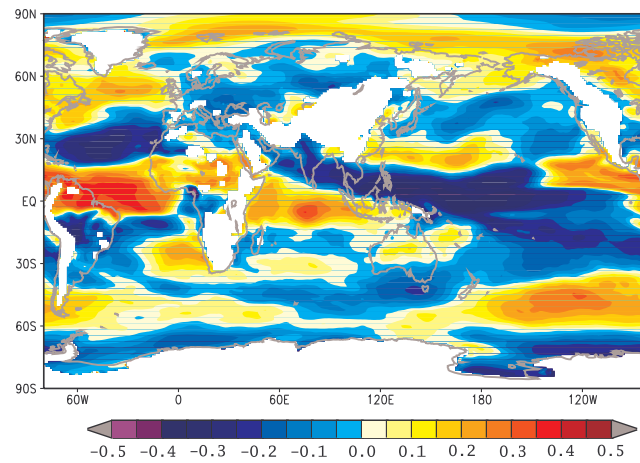
(b)

Figure 4.18: Correlation patterns between extreme upwelling in SON and 10 m zonal of wind in SON (a) and in JJA (b), derived from the CCSM4 simulation. The colours code the correlation coefficient.

alous strong wind shear going from the surface up to the upper atmospheric layers. In the CCSM4 simulation, the surface zonal winds causing strong upwelling (westwards) occur with anomalies of the zonal winds at 200 hPa height that are directed eastward only over North Benguela. This means that in the CCSM4 simulation we do not see such a strong widespread anomalous wind shear in years with extreme upwelling as in the MPI-ESM simulation. We see already here that although in both simulations the surface winds conductive for strong upwelling are realistically directed (westward off the Benguela coast), the simultaneous circulation in the upper troposphere over southwestern Africa and the tropical South Atlantic is different. A possible explanation could lie in the representation of topography in southwestern Africa. Since the spatial resolution of the MPI-ESM model is coarser than the

CCSM4 (about 1.9 versus 1 degree), the link between the atmospheric circulation at the surface and in the upper troposphere may be also different in both models.

In terms of large scale patterns of surface winds, except for the tropical Africa in SON where the pattern is similar to the one derived from the MPI-ESM, the patterns display opposite signs for the tropical Africa, the tropical South America, Indonesia, and remarkably over the Indian Ocean.

Thus, instead of an El Niño-like pattern in the equatorial Pacific to forecast extreme events, La Niña-like conditions seem to be indicative for extreme upwelling in North Benguela. The branches of the Walker Circulation are zonally shifted comparing to the patterns obtained from the MPI-ESM simulation. The ascending branch is located over Indonesia, whereas in the MPI-ESM simulation it is located at the west coast of South America. Over the Indian Ocean, surface zonal winds in SON seasons with extreme upwelling are directed westward in the MPI-ESM simulations and eastward in the CCSM4 simulation. In the MPI-ESM simulation, the descending air over Indonesia seems to be driving the large-scale tropical circulation in the Indian Ocean up to the South Atlantic in years with extreme upwelling, whereas in the CCSM4 simulation it is the descending air over South Africa itself that is driving the extreme upwelling in Benguela.

Since the large-scale zonal wind patterns that are linked with strong Benguela upwelling are already different in both simulation in the upwelling season, they are also different in the previous season.

Thus, in both models, the pattern of zonal winds at 200 hPa height that are conductive to strong upwelling in SON are already broadly present in the previous season. Unfortunately, the sign of these large-scale patterns of zonal wind at 200 hPa height are opposite in both simulations.

4.9   Discussion and conclusion

Extreme seasons of upwelling in North Benguela seem to be preceded by anomalous conditions of opposite sign in the previous season in the two simulations with Earth System Models, MPI-ESM and CCSM4. This seems not to be an artefact of a model simulation because I have found similar results for two Earth System Model simulations. However, no precursors of strong upwelling anomalies could be found in the shorter STORM ocean-only simulation. The discrepancy regarding the results of the STORM simulations could be due to the much shorter time period covered by this simulation compared to the millennium scale simulations of the Earth System Models.

In the MPI-ESM, the near-surface easterly winds over the equatorial Atlantic are strengthened in JJA. This wind anomaly causes low SSH and low SST. In addition, the signal of higher OLR and less precipitation starts to develop in and over the tropical South Atlantic and propagate along the African coast southward by Kelvin

waves, indicating an Atlantic La Niña. The stronger OLR and lower precipitation in the tropics could be due to a weaker ITCZ. A weaker ITCZ would lead to reduced trade winds over Benguela and thus weaker upwelling and warmer SST. This could explain the upwelling-unfavourable wind stress and the dipole structure of SSTs in JJA.

Regarding the large-scale teleconnections to the tropical belt, both models behave differently. The tropical Pacific seems to play a crucial role for the extreme upwelling in Benguela in both simulations. In the years with extreme upwelling in SON, anomalous SSTs develop in the region and the Walker Circulation changes. In the MPI-ESM, the warmer SSTs in the Eastern Pacific lead to convection, ascending air and thus a lower SLP there. This ascending branch is closed over Indonesia, where we have a descending branch that causes divergence near the surface. The westward zonal winds anomalies at the surface extend all the way to tropical Africa and North Benguela, causing strong upwelling there. The zonal winds at 200 hPa height display the opposite to those at the surface. The discrepancy between the results obtained with the MPI-ESM model and the CCSM4 model regarding the tropics cannot be completely explained so far, although my analysis sheds some light as to why both models behave differently.

In summary, I have identified, in each simulation with the models MPI-ESM and CCSM4, the large-scale precursors that are statistically linked to extreme upwelling SON season in each model. Both models agree that upwelling in the prior season JJA tend to have the opposite sign, weaker when SON upwelling is stronger and vice versa. However, although both modes indicate that the tropical Pacific is potentially a useful predictor of extreme upwelling in Benguela, the precursor patterns in both simulations are very different, and generally display opposite signs. This model difference hinders the identification of the mechanism that link large-scale climate patterns to extreme strong and extreme weak upwelling.

CHAPTER 5

Imprint of external climate forcing on coastal upwelling systems in past and future climate

5.1 Introduction

Eastern Boundary Upwelling Systems (EBUSs) are highly productive coastal ocean areas where nutrient rich, cold water upwells by the action of favourable winds. The link between external climate forcing, such as greenhouse gases and solar activity, and coastal upwelling has primarily been framed by the theoretical considerations put forward by Bakun (1990). Surface temperature over land should warm faster than over the oceans under increased radiative forcing, leading to an intensification of the subtropical continental lows and the oceanic highs and a strengthening of the upwelling-favourable winds (Bakun, 1990). Some observations over the 20th century (Narayan et al., 2010) and simulations of the 21st century (Wang et al., 2015) have been interpreted as indicative of upwelling intensification due to stronger external climate forcing. Also, coastal sediment records covering the past millennium and indicative of upwelling (McGregor et al., 2007) have been interpreted as a response to past variations in the external climate forcing, mainly solar irradiance and volcanism. However, the empirical evidence for a long-term intensification of coastal upwelling over the 20th century is not clear-cut. A meta-data analysis has found a significant intensification of wind stress in only three of the four major coastal

upwelling systems (California, Benguela, and Humboldt but not Canary) (Sydeman et al., 2014). Previous studies have detected increasing upwelling intensity over the past century (Di Lorenzo et al., 2005; Gutierrez et al., 2011; Santos et al., 2012), but others have not (Rykaczewski and Dunne, 2010; Pardo et al., 2011). A possible cause may lie on insufficient data homogeneity in long-term wind station records and in meteorological reanalysis, which may blur the identification of long-term trends (Sydeman et al., 2014). Also, other long-term records of upwelling intensity are indirect, and sometimes even based on wind records themselves (Bakun et al., 2010). The direct evidence for upwelling intensification is, therefore, still not conclusive. For instance, the Benguela upwelling system does not exhibit a long-term intensification in the recent decades (Bakun et al., 2010). This has been explained by the counteracting influence of El Niño-Southern Oscillation (ENSO) on humidity in the Peru and Benguela EBUSs regions, which would also influence the regional radiative forcing and modulate the land-ocean thermal contrast (Bakun et al., 2010). According to this explanation, the upwelling trend due to stronger external radiative forcing would be biased by a changing frequency of ENSO events in the recent past. The effect of increasing greenhouse gas concentrations on upwelling regimes in future scenarios has been investigated by Wang et al. (2015). They analysed the simulated trend of upwelling in several simulations included in the Climate Model Intercomparison Project (CMIP5) (Taylor et al., 2012) driven by the Representative Concentration Pathways (rcp) 8.5 scenario, a scenario with an increase of the globally averaged external radiative forcing of 8.5 Wm^{-2} by the year 2100. They found that in most of the EBUSs, models tend to simulate an intensified upwelling and longer upwelling seasons under climate change.

Due to the lack of direct observations, sediment cores are used as proxy for upwelling (McGregor et al., 2007). Though, not the upwelling itself is derived from the sediment cores, but rather indirectly indicated on the basis of the water temperatures, assuming that cooler temperatures are indicative of stronger upwelling. This assumption could lead to a missinterpretation because temperature changes could have other origins than upwelling, for instance due to variations in the external forcing.

The verification of Bakun's hypothesis in the recent past is critical to establish its validity for the future. Even if Bakun's hypothesis is correct, it is not clear whether past variations in external forcing have been strong enough to drive upwelling intensity beyond the range of variations caused by internal chaotic climate variability. Hence, an apparent agreement between the predicted and observed trend could just occur by chance. The analysis of the recently available ensemble of climate simulations with CMIP5 models over the recent past can shed light on this question. If the upwelling is mainly externally driven, all simulations should show approximately the same time evolution of upwelling.

A recent paper by Small et al. (2015) investigated the relevance of model resolution for the question of the warm bias that global climate models usually display in the

eastern ocean basins (Richter, 2015). This bias may be related to the simulated upwelling intensity. Their analysis indicate that a high atmospheric horizontal resolution is of larger importance than the horizontal resolution of the ocean model. The most realistic wind stress curl and upwelling was simulated with a high resolution nested regional atmospheric model coupled with an eddy-resolving ocean model, resulting in more intense values of wind stress and shifted towards the coast. Restoring the SST of Benguela further reduce the typical warm bias in these upwelling regions because the model improvement also impacts the shortwave radiation.

5.2   Data and methods

I analyse here ensembles comprising three simulations of two different Earth System Models, the MPI-ESM and the Community Earth System Model - Community Atmosphere Model version 5 (CESM-CAM5).

The simulations with the MPI-ESM, a model developed by the Max Planck Institute for Meteorology in Hamburg (Giorgetta et al., 2013), cover the periods 900–1850 (past1000), 1850–2005 (historical), and 2006–2100 (future). For the future, I analyse here three scenarios with different strength in greenhouse gas forcing, rcp2.6, rcp4.5, and rcp8.5, where the numbers indicate the anthropogenic radiative forcing in Wm^{-2} reached by the year 2100 (Fig. 5.1). The climate model MPI-ESM participated in the CMIP5 project (Giorgetta et al., 2013), contributing three simulations to the historical ensemble, three simulations to the future ensemble and one simulation for the past1000 period. These data can be downloaded from the CMIP5 web site (http://cmip-pcmdi.llnl.gov/cmip5/). Two additional past1000 simulations were later conducted with the MPI-ESM and were kindly provided by the Max Planck Institute for Meteorology.

The simulations in each ensemble were driven by almost identical external forcing (only the width of the probability distribution of the volcanic aerosol size slightly differs in the last two past1000 simulations). The forcings (Schmidt et al., 2011) prescribed in the past1000 and historical simulations include the orbital forcing, variability in solar irradiance (Vieira et al., 2011), seasonally varying natural tropospheric aerosols, stratospheric aerosols from volcano eruptions (Crowley et al., 2008), and five well-mixed greenhouse gases: CO_2, CH_4, N_2O CFC-11, and CFC-12, as well as O_3, anthropogenic sulphate aerosols, and changes due to anthropogenic land use (Pongratz et al., 2009). In the scenario simulations, only changes in anthropogenic forcing were prescribed according to the Representative Concentration Pathways (rcp) scenarios.

Within each ensemble of simulations (past1000, historical, and future), the simulations differ in their initial state. Thus, a coherent evolution of upwelling in all simulations with an ensemble would suggest a quantifiable influence of the external forcing, whereas a lack of correlation among the simulations would clearly indicate
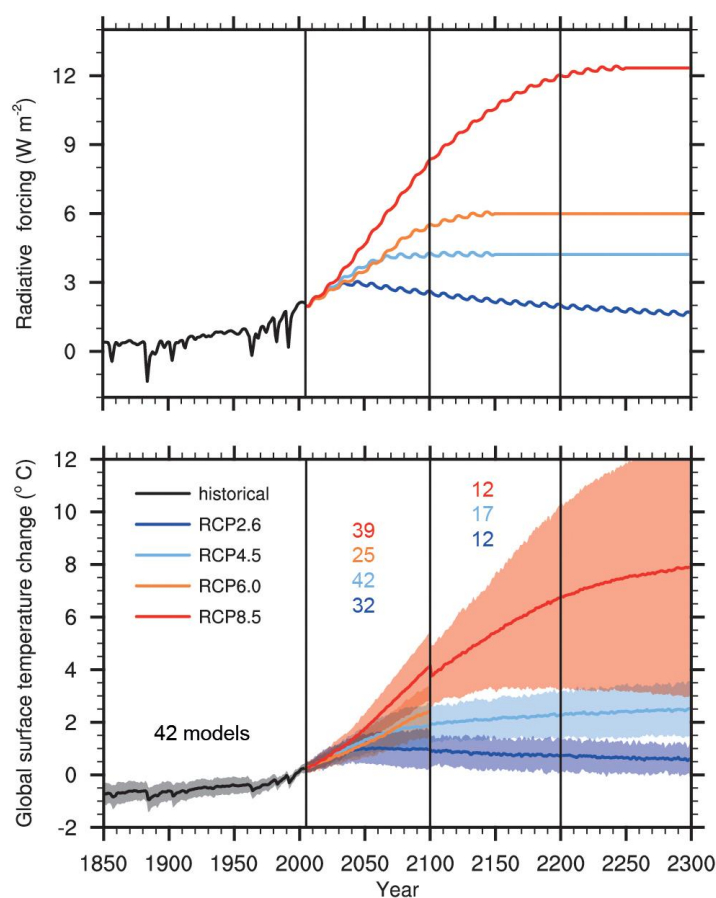
Figure 5.1: Global mean radiative forcing for the Representative Concentration Pathways (rcp) scenarios (Model for the Assessment of Greenhouse-gas Induced Climate Change (MAGICC)) (upper panel). Multi-model mean (solid line) and spectra of all models (shaded) time series of global annual mean surface air temperature anomalies (relative to 1986–2005) from CMIP5 simulations (lower panel). The numbers indicate how many model are available for the corresponding time period and scenario. Source: Stocker et al. (2013).

a preponderance of internal dynamics.

To test the sensitivity of my results with respect to the choice of model, I also analyse simulations with the CESM-CAM5 model. These simulations were conducted after the CMIP5 project was closed. The CESM-CAM5 ensemble comprises a large amount of simulations with different configurations of the external forcing and different initial conditions. Here, I analyse simulations driven by all external forcings, natural and anthropogenic (denoted as 'all-forcings' in the CESM-CAM5 Last Millennium ensemble project (Otto-Bliesner et al., 2015) (https://www2.cesm.ucar.edu/models/experiments/LME). The CESM-CAM5 covers the period 850 to 2005 with a horizontal resolution of the ocean of 1 degree (Otto-Bliesner et al., 2015). These simulations were driven by the same set of external forcings as used in the MPI-ESM simulations. Unfortunately, no future

simulations with this model are publicly available (Kay et al., 2015).

The horizontal resolution of the atmospheric model of the MPI-ESM is about 1.9 degrees (spatially varying) with 95 levels for the historical period and 47 levels for the past1000 and future period, whereas the ocean model resolution is approximately 1 degrees (past1000 and future) and 0.4 degrees (historical), including 40 ocean layers. These resolutions are similar to the resolution of the CMIP5 models used by Wang et al. (2015). Although ocean processes of spatial scales of a few kilometres are only imperfectly resolved, this resolution should be fine enough to realistically represent the basic relationship between upwelling dynamics and the large-scale wind forcing, including the shoreline-parallel winds and the wind stress curl.

Upwelling intensity in each of the four upwelling regions is defined by the vertical mass transport (wmo) at the ocean model layer at 52 m (MPI-ESM) and the vertical velocity (wvel) at 50 m (CESM-CAM5) (close to the modelled mixed layer depth), and averaged over each of the upwelling regions: Benguela (8–30° E, 15–28° S), Peru (80–70° W, 20–10° S), California (130–110° W, 20–50° N), and Morocco (20–10° W, 20–34° N). Upwelling indices are here defined as the seasonal means over the main upwelling season in each region. In the MPI-ESM past1000 and historical simulations, the main upwelling season in Benguela is September–November and June–August in all other upwelling regions. In the future simulations, the main upwelling season in Benguela is also June–August. In the CESM-CAM5 simulations, the main upwelling season is September–November in Benguela and Peru and June–August in California and Morocco.

If it is not explicitly stated, all correlations have been calculated with long-term detrended series.

Here, I show results from three of the available simulations from the CESM-CAM5 ensemble, as three simulations already confirm the results obtained with the MPI-ESM model. These two models used here are the only ones that provided an ensemble of simulations with basically the same forcing and with different initial conditions, thus being suitable to detect the possible imprint of external forcing.

After assessing the realism of the connection between atmospheric drivers and simulated upwelling, I further evaluate whether the upwelling intensity in these regions displays any imprint of the external climate forcing. To estimate the ratio of forced variability to total variability I build a simple model of the variations of a climate record that decomposes its variability into a sum of a forced component, proportional to the external climate forcing, and an internal component caused by the non-linear interactions within the climate system:

$$y = y^f(t) + y^i(t) \tag{5.1}$$

The same model can be applied to describe climate records simulated in two climate simulations driven by the same forcing and started with different and random initial

conditions:

$$y_1(t) = y^f(t) + y_1^i(t)$$
$$y_2(t) = y^f(t) + y_2^i(t)$$

(5.2)

where the forced components are by construction equal in both simulations and the internal components are uncorrelated in time. The ratio between the variance of y^f and the variance of y_1, equal to the variance of y_2, can be shown to be equal to the correlation between y_1 and y_2

$$r = <y_1, y_2> / <y_1, y_1> = <y^f, y^f> / <y_1, y_1>$$

(5.3)

where $<x, y> = \sum_t x(t)y(t)$

5.3 Representations of upwelling and its drivers in the model

The patterns of long-term mean sea surface temperature (SST) (June–August, main upwelling season in three of the four regions) display depressed values in the areas of upwelling relative to the zonal SST mean at the same latitude, although the fine spatial structure appears smoothed due to the model resolution (Fig. 5.2a). The shape of the modelled seasonal cycle of upwelling generally agrees with what is known from observations (Fig. 5.2b, c), with upwelling being more intense in the boreal warm half-year. The mean upwelling is, however, about a factor two more intense in the lower resolution past1000 simulations, indicating that ocean model resolution is important to simulate the correct mean upwelling intensity, which may be relevant for the SST bias in the EBUSs simulated by many climate models (Wang et al., 2014).

The link between each upwelling index and wind stress, calculated as the patterns of correlations between the index and wind stress in each model grid-cell (not shown), is also very realistic, displaying in each case a characteristic alongshore wind stress that favours Ekman transport, the main mechanism causing coastal upwelling (Tomczak and Godfrey, 2003). The correlation patterns between each upwelling index and the sea level pressure (SLP) realistically show regions with negative correlations over land and positive correlations off-shore (Fig. 5.3), indicating that the across-coastline SLP gradient is conductive for alongshore wind stress through the geostrophic relation.
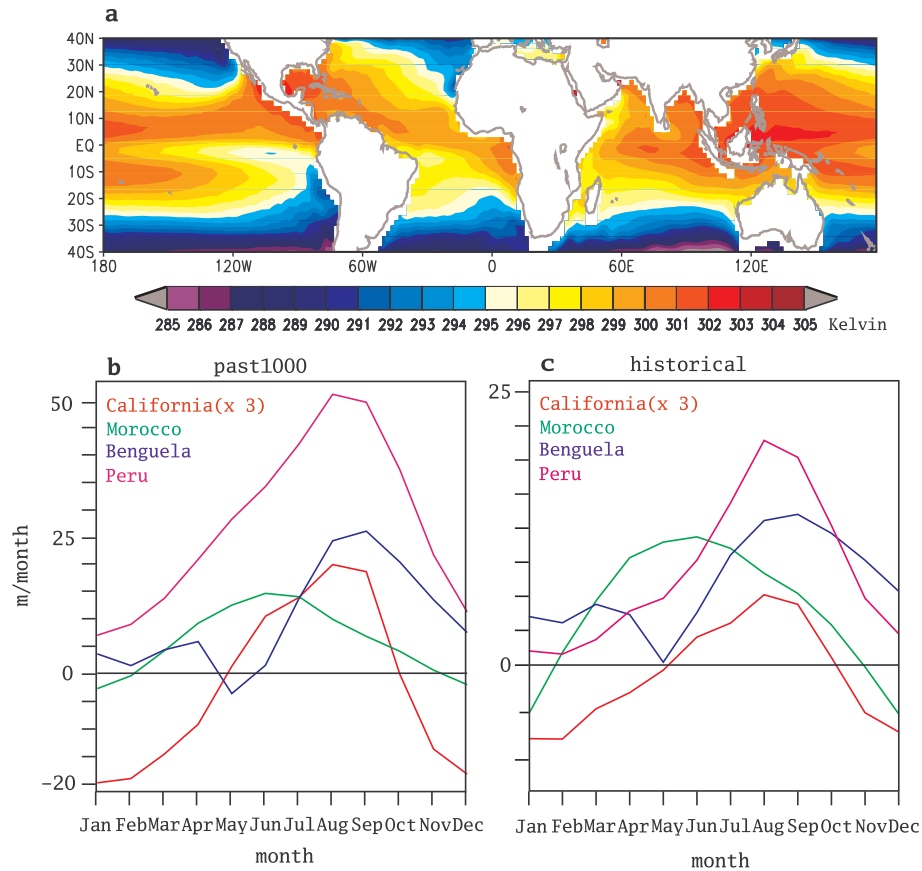
Figure 5.2: Mean sea surface temperature in June–August simulated by one past1000 simulation with the MPI-ESM Earth System Model in the tropics and subtropics (a). Monthly mean vertical velocity at 52 m depth in four main coastal upwelling regions simulated in one past1000 (900–1850) (b) and one historical (1850–2005) simulation (c) of the MPI-ESM. The values for California have been re-scaled for better visibility. Note the different y-axis scale for each simulation.

5.4 Imprint of external forcing on coastal up- welling

5.4.1 Past1000 and historical simulations

In the last millennium, the climate changed driven by the external climate forcing. The main external climate drivers over this period were volcanic forcing, solar variability, greenhouse gases, and land-use changes (Hegerl et al., 2006) and at millennium time-scale the slowly varying orbital configuration of the Earth (Laskar et al., 2004). These forcings had an effect on the global mean surface temperatures, both in climate simulations driven by these forcings as in proxy-based climate reconstructions (Fernández-Donado et al., 2013). There was a period of relatively high
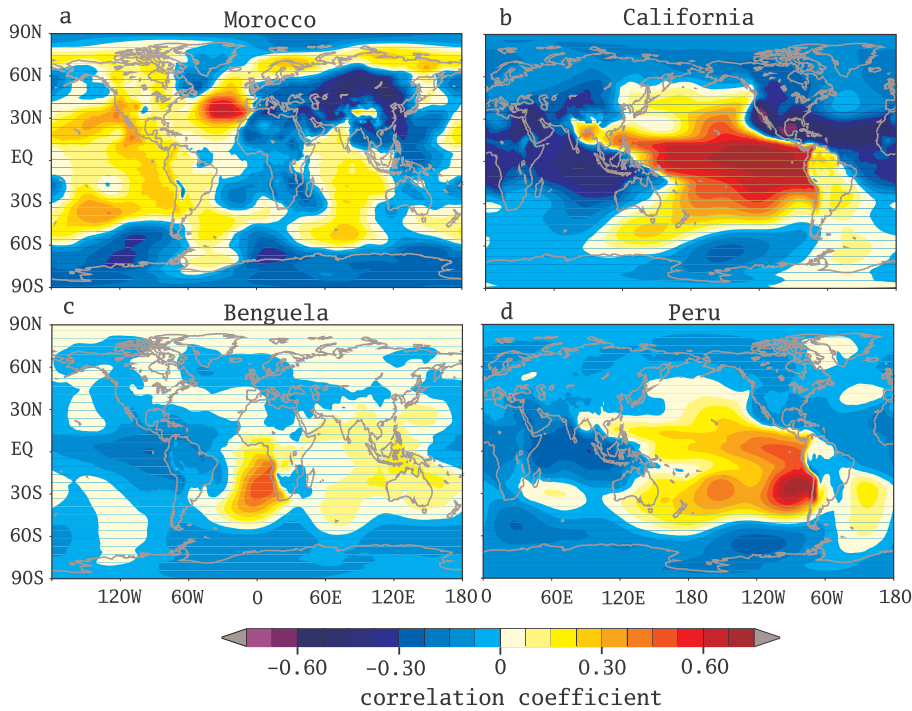
Figure 5.3: Correlation patterns between the seasonal (June–August, except for Benguela September–November) upwelling index in each Eastern Boundary Upwelling System and the simultaneous seasonal mean sea level pressure field simulated in one of the past1000 simulations (900–1850) with the Earth System Model MPI-ESM.

temperatures, the Medieval Warm Period with its maximum at around 1000–1300 A.D. These high temperatures were caused by high solar and low volcanic activity. The Medieval Warm Period was followed by the Little Ice Age, a period of low temperatures caused by low solar and high volcanic activity. After the Little Ice Age, global mean temperatures rose mainly as result of higher concentration of greenhouse gases (Fernández-Donado et al., 2013).

For both ensembles of simulation of the past, the decadally smoothed time series of regional upwelling extracted from each of the three simulations display different time evolutions (Fig. 5.4) and do not show a centennial evolution comparable to the global mean temperatures or the global mean external forcing as just described. The correlations between these series for each region are correspondingly low (Tab. 5.1, Fig. 5.5) and mostly statistically not significant. These correlations remain low and non-significant for stronger low-pass time filtering up to 50 years (Fig. 5.6a). This indicates that the upwelling variance shared by all simulations, which could only be due to the common external forcing, is also small. These simulations, therefore, do not support any significant imprint of the external forcing on upwelling in any of the EBUSs up to multidecadal time scales over the past millennium.
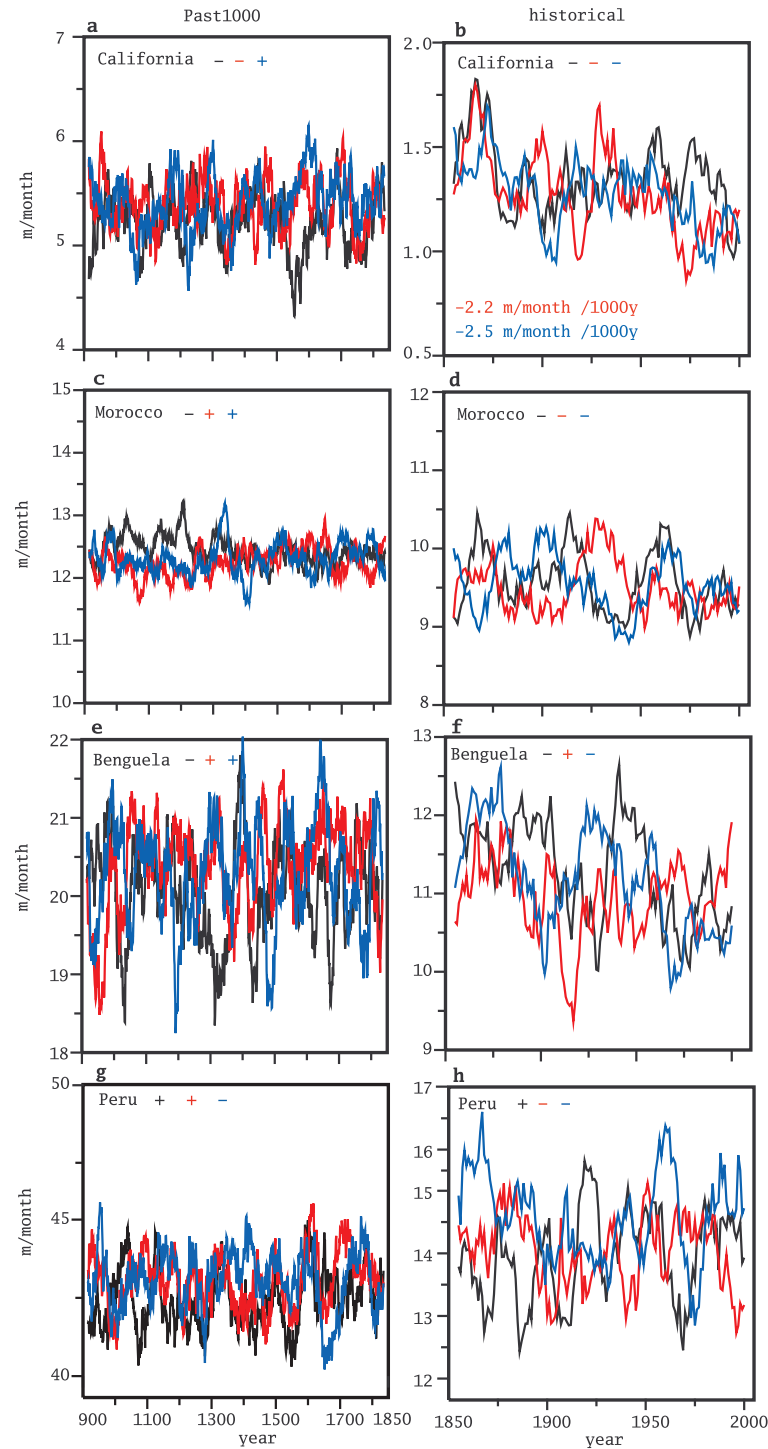
Figure 5.4: Time series of the simulated upwelling indices in each upwelling region simulated in two ensembles of climate simulations (three members each), denoted past1000 (900–1850) and historical (1850–2005), with the MPI-ESM model. The plus and minus signs in each panel indicate the sign of the long-term trend, their value being included whenever statistically significant. The series have been low-pass filtered with a 30-year filter for past1000 and a 10-year filter for the historical ensemble.

Table 5.1: Correlation coefficients of the simulations of the upwelling indices of all up-
welling regions for the past1000 and historical simulations with the MPI-ESM model with
30-year and 10-year filter, respectively.

	California	Morocco	Benguela	Peru
past1000:				
r1−r2	+0.07	−0.11	+0.05	+0.22
r1−r3	−0.04	+0.16	+0.04	−0.004
r2−r3	+0.14	−0.14	+0.06	+0.23
historical:				
r1−r2	+0.15	−0.14	−0.10	−0.18
r1−r3	+0.30	+0.14	−0.19	−0.09
r2−r3	−0.12	−0.38	+0.06	−0.03
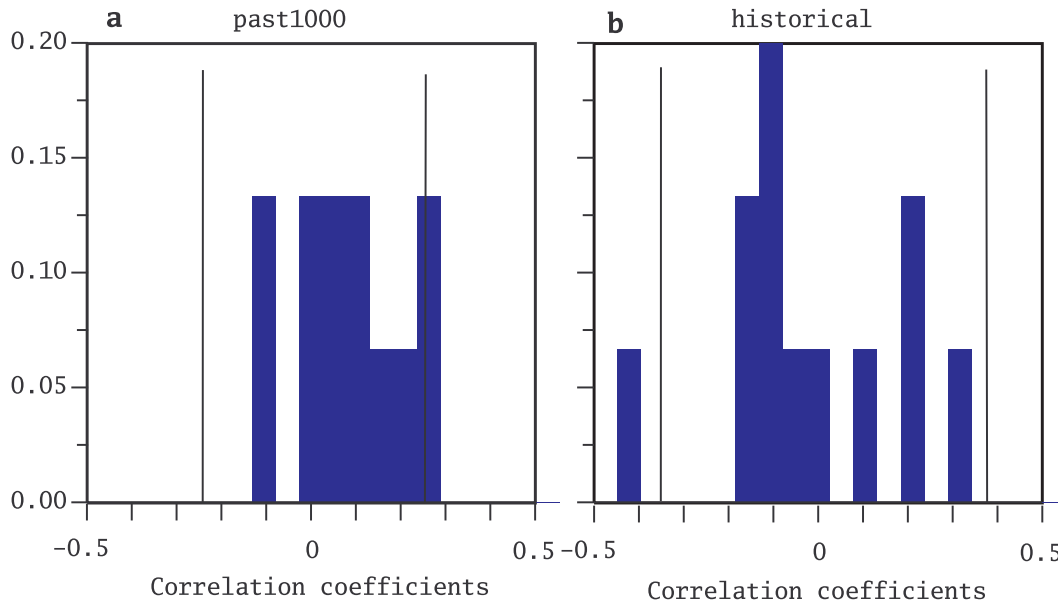
Figure 5.5: Frequency histogram in bins of 0.05 width showing the distribution of across-
ensemble correlations between the upwelling indices simulated in each upwelling region for
the ensembles past1000 (a) and historical (b) of the MPI-ESM, after low-pass filtering with
a 30-year (past1000 simulation) and a 10-year (historical simulation) filter, respectively.
The vertical black lines indicate the 5 %–95 % significance bounds taking the time filtering
into account.

This finding supports previous studies derived from observed records, that identified a strong influence of the Pacific North American pattern on California upwelling. The Pacific North America pattern is a well-known mode of internal climate variability, probably linked to the dynamics of the Tropical and mid-latitude Pacific Ocean (Macias et al., 2012).

At centennial time scales, the externally forced climate variability is a large portion of the total climate variability, as the random internal decadal variability is filtered out. Additionally, the increase in the external climate forcing over the past 150 years is stronger than the variations in the forcing prescribed in the past1000 simulations. For instance, the amplitude of decadal variations of the preindustrial external forcing is of the order of 0.3 Wm^{-2} (Schmidt et al., 2011), whereas the increase in the external forcing over the past 250 years is 1.6 Wm^{-2} (Myhre et al., 2013).

Thus, the long-term influence of the external forcing – the strongest being anthropogenic greenhouse gases in the historical simulations – could be more easily detected in the form of common long-term upwelling trends. However, the simulated trends are small, mostly statistically not significant, and generally display opposite signs in the different simulations (Fig. 5.4). The two exceptions here are California and Morocco in the historical simulations, in which all members exhibit a negative trend (opposite to the expected strengthening), of which only two trends of the California upwelling region are statistically significant. Analysing the imprint of external forcing on upwelling with the CESM-CAM5 confirms the results with the MPI-ESM. The simulated upwelling velocity in three simulations are weakly correlated with each other (Fig. 5.7) and the trends are either not coherent in the simulations or are not statistically significant.
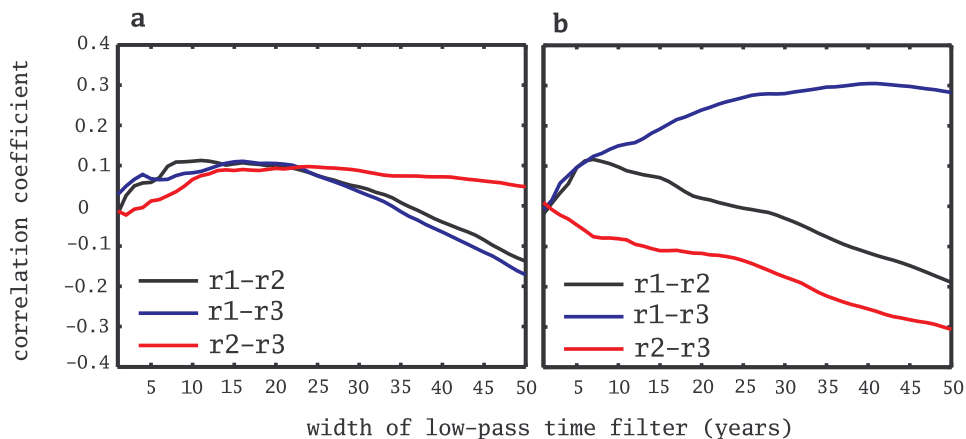
Figure 5.6: Correlations between the simulated upwelling indices in Benguela in three past1000 simulations with the MPI-ESM model after filtering the time series with low-pass filter of increasing period (a) and the same as (a) but for the time series of sea level pressure difference between land and ocean averaged over the areas most closely correlated with the simulated upwelling in this region (b).
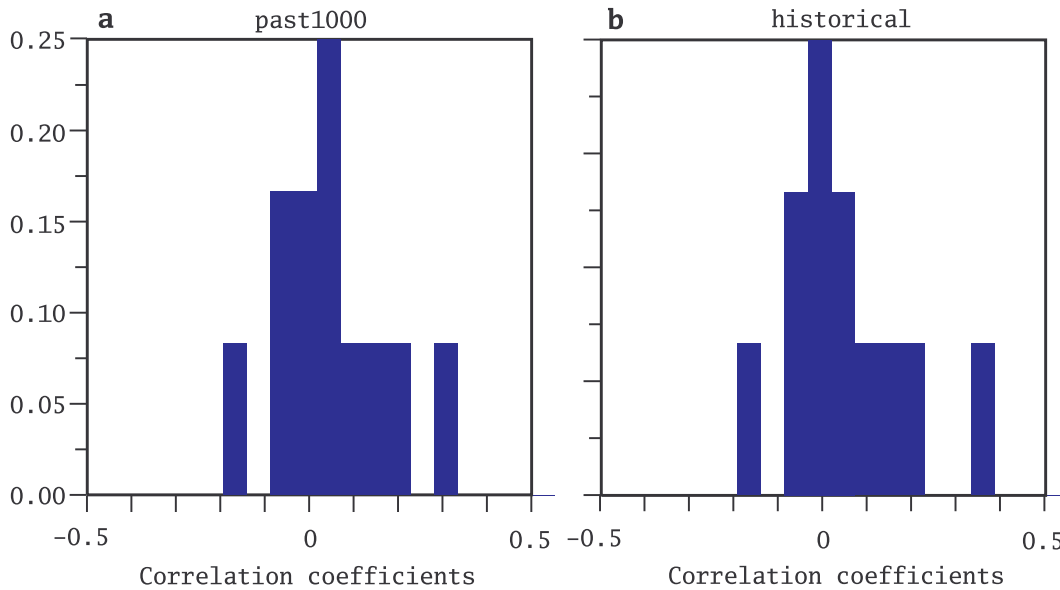
Figure 5.7: Frequency histogram in bins of 0.05 width showing the distribution of across-ensemble correlations between the upwelling indices simulated in each upwelling region for the ensembles past1000 (a) and historical (b) of the CESM-CAM5, after low-pass filtering with a 30-year (past1000 simulation) and a 10-year (historical simulation) filter, respectively.

5.4.2   Scenarios

Looking at the future development of the upwelling in the EBUSs, I analyse the future simulations conducted with the MPI-ESM model under three different emission scenarios. An effect of the external forcing should be reflected in consistent centennial trends in upwelling in all members of each ensemble. Consistent significant trends in all three simulations of an ensemble only occur in the rcp8.5 scenario, the one with the strongest external forcing (Tab. 5.2, Fig. 5.8). The trends are negative in California and Morocco and positive only in Benguela. In Peru no significant trends can been seen. This support my results obtained for the past millennium, indicating that the external forcing has not been intense enough in the past to force the upwelling significantly. Furthermore, the expected positive trend only occurs in one of the four regions, underlining the local differences among the EBUSs. These results do not fully support the ones obtained by Wang et al. (2015). They analysed the trend for another period (1950 to 2099) and only the rcp8.5 scenario. They concluded that a clear connection between external forcing and upwelling could be found. However, when analysing the trends simulated in other scenarios, it turns out that in the weaker greenhouse gas scenarios this link is weaker, and it cannot be easily identified. Differences between the northern hemisphere and southern hemisphere EBUSs could be caused by changes in the Hadley cell. As a consequence of global warming, the Hadley cell expands polewards (Lu et al., 2007). Due to

the larger fraction of land on the northern than on the southern hemisphere, the temperature differences between the equator and the subtropics will decrease on the northern hemisphere leading to a weakening of the Hadley cell and thus to weaker trades (Ma and Xie, 2013). In the southern hemisphere this effect will be smaller due to a weaker warming of mid and high latitudes (Ma and Xie, 2013).

Table 5.2: Sign of trends of the upwelling time series of all upwelling regions for the past1000, the historical, and the scenarios (rcp2.6, rcp4.5, rcp8.5) simulations with the MPI-ESM model, significant correlations are highlighted by **

	California	Morocco	Benguela	Peru
past1000:				
r1	−	−	−	+
r2	−	+	+	+
r3	+	+	+	−
historical:				
r1	−	−	−	+
r2	−**	−	+	−
r3	−**	−	−	−
rcp2.6:				
r1	−	−	−	−
r2	−	−	+	+
r3	−	−**	+	+
rcp4.5:				
r1	−	−**	−	−
r2	−	−	+	−
r3	−**	−**	+**	+
rcp8.5:				
r1	−**	−**	+**	+
r2	−**	−**	+**	−
r3	−**	−**	+**	−
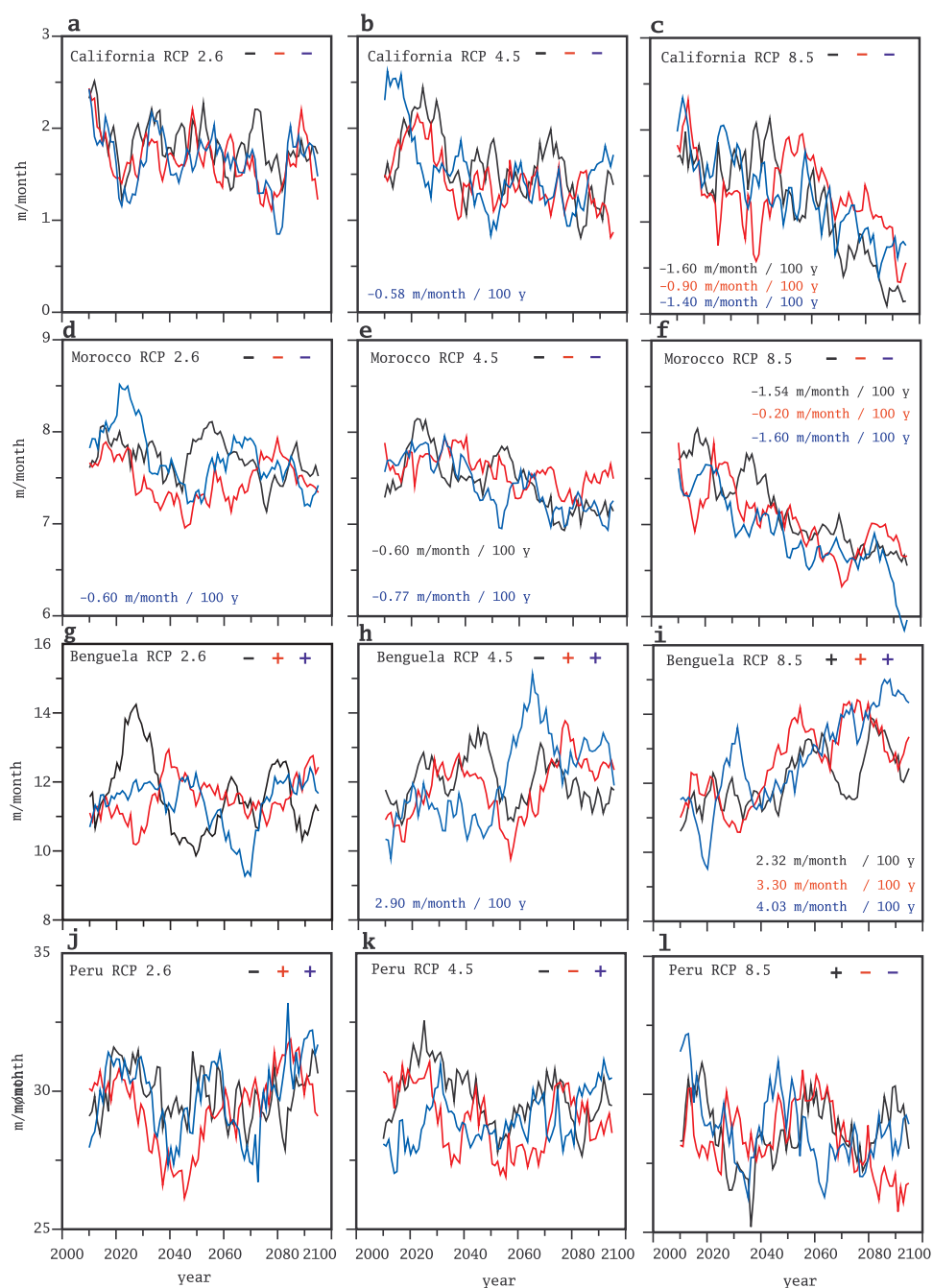
Figure 5.8: Time series of the simulated upwelling indices in each upwelling region simulated in three ensembles of climate simulations (three members each) for 2006–2100, rcp2.6, rcp4.5, and rcp8.5, with the MPI-ESM model. The plus and minus signs in each panel indicate the sign of the long-term trend, their value being included whenever statistically significant. The series have been low-pass filtered with a 10-year filter.

5.5 Imprint of external forcing on the drivers of upwelling

Upwelling in all four investigated regions is mainly driven by the wind stress curl that modulates upwelling in offshore regions and by the alongshore wind stress that drives the coastal upwelling. The latter is related to the SLP gradient between land and ocean (Tomczak and Godfrey, 2003; Mackas et al., 2006). I investigate whether the time evolution of this SLP gradient is consistent across the simulations and whether the lack of correlations between the upwelling indices across the ensemble may be due to a weak influence of the external forcing on wind stress and on the SLP gradient. The across-coastline SLP gradients in the simulations are calculated by subtracting the averaged air pressure over land from the averaged pressure over ocean in the regions identified as most closely correlated to the upwelling indices (Fig. 5.3).

As in the case of the upwelling indices, the correlations between the time series of wind stress and SLP gradients across the simulations in the ensemble are all low (Tab. 5.3, Tab. 5.4). These correlations also remain low regardless of the time

Table 5.3: Correlation coefficients of the simulations of the cross-coastline pressure gradient of all upwelling regions for the past1000 and historical simulations with the MPI-ESM model after 30-year and 10-year filter, respectively.

	California	Morocco	Benguela	Peru
past1000:				
r1−r2	+0.12	+0.04	−0.03	+0.11
r1−r3	+0.21	+0.21	+0.28	+0.25
r2−r3	+0.32	−0.30	−0.18	+0.36
historical:				
r1−r2	+0.09	+0.10	−0.25	+0.26
r1−r3	−0.27	+0.27	−0.20	+0.06
r2−r3	−0.13	−0.13	+0.13	−0.09

filtering (Fig. 5.6b). Regarding the longest time scales captured in the simulations, the long-term trends of the wind stress and of the SLP gradient within each ensemble have either inconsistent signs, or are not statistically significant, or are incompatible with the expected effect of the external forcing varying at centennial time scales. These expected trends are negative in past1000 due to the long-term orbital forcing and positive in historical due to the increase in greenhouse gas forcing. Therefore, even if the connection between the atmospheric drivers and upwelling were not totally realistic in the Earth System Model, the lack of common time evolution of wind stress or SLP across the simulations clearly shows that, from the atmospheric

perspective alone, the simulations do not support a discernible influence of the external forcing on the atmospheric drivers of upwelling over the last centuries. This implies that such an influence could not have been found even if the ocean model perfectly represented the real upwelling dynamics.

Table 5.4: Correlation coefficients of the simulations of alongshore wind stress of all upwelling regions for the past1000 and historical simulations with the MPI-ESM model after 30-year and 10-year filter, respectively.

	California	Morocco	Benguela	Peru
past1000:				
r1−r2	−0.02	−0.22	+0.001	+0.07
r1−r3	−0.05	+0.09	−0.13	+0.09
r2−r3	+0.27	−0.05	+0.22	+0.14
historical:				
r1−r2	+0.45	−0.01	−0.27	+0.19
r1−r3	−0.08	+0.09	−0.06	+0.04
r2−r3	+0.14	−0.02	−0.07	+0.23

5.6 Imprint of external forcing on stratification

Another possible mechanism by which the external climate forcing could influence upwelling involves the stratification of the water column. In periods with a stronger external forcing, the temperatures at the surface should warm more rapidly than in the deeper layers, increasing the stability of the water column, and hindering the mechanical effect of the alongshore wind stress (Hsueh and Kenney III, 1972). The amount of variability in the SST that can be attributed to the variations in the external forcing can also be estimated by the correlation between the grid-cell SST series simulated in each members of the simulation ensemble (Fig. 5.9). The correlation patterns indicate that the SST variability is more strongly driven by the external forcing in the tropical belt and tends to the weaker in the mid and high latitudes. This occurs despite the strongest response of high latitudes to external radiative forcing, known as the Arctic amplification. The reason is that at high latitudes the internal variability is also larger than at low latitudes. The ratio between both, external forcing signal and internal variability, which is encapsulated by the correlation patterns shown in figure 5.9, is therefore highest in the tropics, a feature which has been so far overlooked but that has been found in previous analysis of paleoclimate simulations (Tett et al., 2007). In the EBUSs, the correlations between the simulated SSTs are all positive, of the order of 0.2–0.3

after 10 year low-pass filtering. Therefore, the external forcing has some influence on the SST variability in these regions but most of the multi-decadal variability is internally generated.
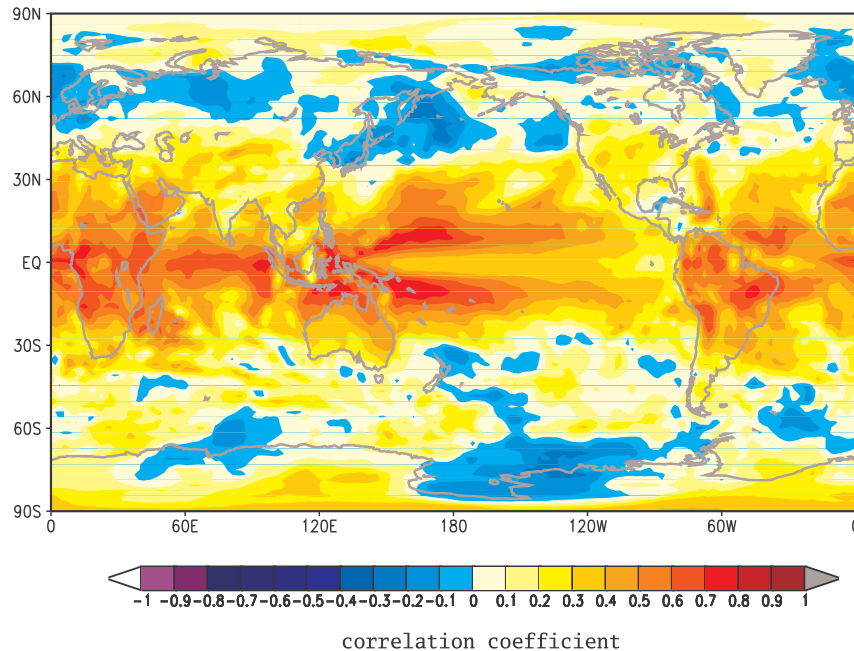
Figure 5.9: Correlation pattern between the global skin temperatures simulated in two past1000 simulations (900–1850) with the Earth System Model MPI-ESM in the June–August season after applying a 10-year low-pass filter.

5.7   Conclusion

The analysis of three simulation ensembles with the Earth System Model MPI-ESM over the past millennium and the future are in contrast with the hypothesis of a discernible influence of the external forcing on coastal upwelling intensity. Uncertainties still remain. For instance, the magnitude of the external forcing variations over the past millennium is still not well established (Schmidt et al., 2011), and larger variations than hitherto assumed may cause a tighter connection between forcing and upwelling. Over the past 150 years, however, the trends in external climate forcings are much more certain and over this period the historical simulations do not show any consistent sign of intensification or weakening.

For the future, the effect of external forcing on the EBUSs can be identified when greenhouse gas concentrations are assumed to follow the strongest scenario, rcp8.5, among the three Representative Concentration Paths analysed here. All three simulation in the ensemble display consistent trends, but these trends are not always

consistent with the expected intensification of upwelling, with some regions showing an intensification but others showing a weakening.

The definition of the upwelling index can be sensitive to the region over which the vertical velocities are averaged. Redefining the subregions of the Eastern Boundary Upwelling Systems (EBUSs) (Canary (18.5–10.5° W, 16.5–42.5° N), South Benguela (8–30° E, 28–40° S), Chile (80–70° W, 20–40.5° S)) does not change the main results of this study. The correlation between the three simulations remains low for upwelling. Significant trends with the same sign in all three simulations do not occur, neither in the simulations of past periods nor in the future simulations.

My results generally agree with the ones obtained by Wang et al. (2015) on the influence of a strongly increased future greenhouse gas forcing on upwelling intensity in the EBUSs. However, my results indicated that the conclusion obtained from the analysis of only the rcp8.5 scenario cannot be extended to weaker scenarios of future greenhouse gas forcing nor to the trends observed over the 20th century not the evolution of upwelling over the past millennium. The same can be said on the study of Rykaczewski et al. (2015) where again only the upwelling in the EBUSs in the rcp8.5 scenario is analysed. They found significant positive trends in the upwelling-favourable winds in the Canary, Humboldt and Benguela systems and negative trends in the California system. These results agree partly with my findings, underline the differences between the upwelling regions, and indicate the complexity of the upwelling by the different results depending on the analysed model – but stress the impact of the external forcing on upwelling in the rcp8.5 scenario.

It has to be kept in mind that my results are based on the realism of the analysed Earth System Models. The relatively low model resolution of the atmosphere and of the ocean components could result in an unrealistic representation of the upwelling itself and/or its drivers. As stated by Small et al. (2015), especially the resolution of the atmospheric model has the strongest influence on the simulated coastal upwelling. Furthermore, the current global coupled climate models still display a strong SST bias in the EBUSs. The cause of this bias is not completely understood, it may be related to a deficient representation of coastal upwelling but it may have other causes, for instance related to biases in the climate clouds (Richter, 2015). This caveat, nevertheless, also affects the recent studies by Rykaczewski et al. (2015) and Wang et al. (2015), since they are also based on the CMIP5 models.

Analysing ensembles of simulation of the Earth System Model CESM-CAM5 over the past millennium supports the results of the MPI-ESM.

Thus, the circumstantial evidence linking the recent observed trends in EBUSs upwelling to external climate forcing is in conflict with state-of-the-art climate simulations.

CHAPTER 6

Conclusion and Outlook

The Benguela upwelling system is one of the four major upwelling regions in the world ocean (Eastern Boundary Upwelling Systems, EBUSs). It is located off Angola, Namibia, and South Africa. The focus of this thesis was to identify the large-scale atmospheric drivers of the upwelling in the Benguela upwelling system via statistical analysis of different climate simulations. In addition, the extrema of upwelling in the Benguela upwelling system were closely looked at and the trends over the recent past and possible future changes in upwelling due to anthropogenic climate change were investigated in all four EBUSs, too.

For these purposes, two ocean-only simulations (STORM and GENUS-MOM), two global coupled Earth System Models (MPI-ESM and two version of the Community Earth System Model CESM-CAM5 and CCSM4), and reanalysis data sets (NCEP/NCAR reanalysis I and ERA-Interim) were analysed. In this chapter, the main results of this analysis will be summarised by answering the research questions raised in the introduction. Finally, an outlook about further research objectives is included.

6.1   Conclusion

What are the atmospheric drivers of the Benguela upwelling system?
I addressed this question in chapter 2 (for the period 1950–2010) and chapter 3 (for the period 1999–2012). Upwelling in North and South Benguela (separated by the Lüderitz upwelling cell at 28° S) has different seasonality and variability. Upwelling in North Benguela is strongest in austral winter (June–August), upwelling in South Benguela is strongest in austral summer (December–February). Both upwelling

subregions are driven by the large-scale pressure fields (intensified subtropical high and continental low) and thus the southeasterly trades. However, the influence of the large-scale climate modes differ for both regions. Among the various climate modes analysed, the El Niño-Southern Oscillation (ENSO) and the Antarctic Oscillation (AAO) have an impact on the upwelling, which is more pronounced in South Benguela.

The decadal variability is temporally more coherent between the seasons in North Benguela than in South Benguela. This indicates a more persistent driving of the tropical upwelling region. Furthermore, North Benguela upwelling varies on longer time scales than the upwelling in the south. In addition, the spectral analysis reveals a red spectral background which is probably due to tropical dynamics. In contrast, the spectra of upwelling in South Benguela are more similar to the spectral of white noise, as it is typical for the midlatitudes.

The detected atmospheric drivers of the two subregions of the Benguela upwelling system are captured well by both high-resolution ocean-only simulations, the global STORM simulation and the regional GENUS-MOM simulation. Nevertheless, the analysis of these two simulations illustrates their differences with regard to the drivers of the upwelling. In general, the STORM simulation captures the atmosphere-ocean interaction more realistically, whereas the GENUS-MOM simulation seems to have some difficulties due to its open boundaries and possibly due to its atmospheric forcing.

Are there any multi-decadal trends in the Benguela upwelling?

When analysing the upwelling derived from the STORM simulation in chapter 2, I detect no clear trend over the last 60 years, neither for North Benguelan upwelling nor for upwelling in South Benguela. This result is in contrast to the well-known hypothesis of Bakun (1990). He hypothesised that due to an increase in greenhouse gas concentrations, the land would heat up more rapidly than the ocean, intensifying the air pressure contrast (the high over the ocean and the low over the land), and leading to stronger than usual trade winds in the EBUSs. Over the last 60 years, the upwelling does not show a linear trend and is better described by decadal variability. Furthermore, the analysis of the sea level pressure (SLP) gradient supports the idea of the effect of rising greenhouse gas concentrations not being detectable in the Benguela upwelling system over the last 60 years. Nevertheless, the SLP gradient has a significant impact on the strength of the upwelling in North and South Benguela at shorter time scales.

How do years of extreme upwelling in Benguela differ from the climatological mean with regard to their drivers and oceanic responses?

This question is answered in chapter 4. An extreme upwelling season is defined as the 90th or 10th percentile of all upwelling season (September–November). Here I used the past1000 simulation of the last millennium (850–1850) and the

pre-industrial control runs (1850–3005, 800–1300) of two Earth System Models (MPI-ESM, CCSM4). The analysis indicated that these extreme upwelling seasons are preceded by upwelling seasons of upwelling of opposite sign. If upwelling is stronger than usual, with stronger than usual trade winds and colder than usual sea surface temperature (SST) in the upwelling season, winds in the previous season tend to be weaker and SSTs warmer than usual. The same is true for seasons of extreme weak upwelling. These seasons are preceded by upwelling-favourable wind conditions. The mechanism behind that could involve changes in the Walker Circulation due to ENSO, which modulates the position of the high and low pressure systems and accordingly the direction and strength of the trade winds, the main driver of the North Benguela upwelling system.

However, the two models yield incompatible results about the large-scale influence of the state of the tropical Pacific in the season previous to the main upwelling season. Therefore, although both models indicate that seasonal prediction of extreme upwelling could be theoretically possible, it is not clear why they do not agree on the sign of SSTs in the tropical Pacific that are conductive to extreme Benguela upwelling.

How did upwelling in the Eastern Boundary Upwelling Systems change in the last thousand years and how sensitive it is to external forcing, especially anthropogenic forcing due to greenhouse gas concentrations?
This question is motivated by the hypothesis of Bakun (1990): changes in greenhouse gas concentrations would affect the upwelling strength. The question is answered in chapter 5. There, I analysed not only the Benguela upwelling system, but also the other three EBUSs (Peru, California, and Morocco) in two ensembles (each containing three ensemble members) of Earth System Model simulations (MPI-ESM, CESM-CAM5). Although, these simulations have a relatively low resolution (~1 degree), the annual cycle as well as the correlation between SLP and upwelling and wind stress and upwelling clearly suggests that these model simulations are able to capture the upwelling and its link to large-scale drivers. The same models have been used in other studies to investigate coastal upwelling. I analysed ensembles of simulations differing only in their initial conditions which allows me to identify whether its temporal variations are driven internally or externally (by greenhouse gas concentrations, orbital forcing, variability in solar irradiance, seasonally varying natural tropospheric aerosols, stratospheric aerosols from volcano eruptions, anthropogenic sulphate aerosols, and changes due to anthropogenic land use). I analysed two time periods of the past: the past1000 period (900–1850) and the historical period (1850–2005). Trends of the three ensemble members should be consistent and the time series of the upwelling of the ensemble members should be correlated if the variability is driven externally. I found trends with consistent signs in all three simulations only for California and Morocco for the last 150 years. However, these trends are of negative sign, whereas

a positive trend was expected based on the Bakun hypothesis and only the trends of two simulations for California are significant. Furthermore, the correlations of the upwelling time series of the three ensemble members are low. Thus, the variations and long-term trends in upwelling are driven internally over the last thousand years and also over the last 150 years when changes in the external forcing were relatively strong.

How might the upwelling in the Eastern Boundary Upwelling Systems change in the future under global climate change?
Future changes of upwelling due to climate change have been analysed in the same chapter (chapter 5). As for the past, trends are mostly insignificant and their signs are inconsistent within the three simulations for Representative Concentration Pathways (rcp) 2.6 and 4.5 (where the number indicate the amount of anthropogenic radiative forcing in Wm^{-2} reached by the year 2100). In contrast, under extreme climate change conditions (rcp8.5) trends are significantly negative in California and Morocco and significantly positive in North Benguela. Thus, only in the scenario with the strongest greenhouse gas increase, upwelling is changing significantly. However, the sign of the upwelling trend differs among the four upwelling regions indicating the importance of local driving factors and the complexity of the four EBUSs.

6.2   Outlook

This thesis sheds some light on the question how extreme events in the Benguela upwelling system are triggered and how they could be predicted some months in advance. The impact of the equatorial Pacific could be further investigated with regard to these extremes. The Walker Circulation, acting as an atmospheric bridge, seems to be modulated by the SST anomalies in the El Niño region and they also seem to modulate the position and strength of the subtropical oceanic high and thus the trade winds that drive the Benguela upwelling.

However, both analysed Earth System Model simulations disagree regarding the tropical/subtropical SST and SLP pattern connected to upwelling extremes. Analysing other simulations could answer this still open question of why their behaviour is contradicting. This would probably also lead to the answer on how to predict the extremes of the Benguela upwelling system. Furthermore, observational data sets could be used to investigate the predictability of extremes which occurred in the past based on SSTs of the equatorial Pacific. For that purpose, sediment cores could be analysed in addition to reanalysis data sets.

In a recent paper (Rykaczewski et al., 2015), the authors also analysed the trends in future upwelling in a set of models. Although they found an increase in the temperature contrast between land and ocean in the future, they did not find an increase

in the air pressure contrast as hypothesised by Bakun. The impact of anthropogenic climate change to increased SLP gradients and thus to increased trade wind could not be found in an ensemble of Earth System Models simulating the future climate. This supports my finding about the missing trend in upwelling in the past centuries. The reason why the link from air temperatures contrast to SLP does not seem to occur in models should be further investigated with regard to the four EBUSs.

One possible reason is the coarse atmospheric resolution in the Earth System Models. The analysis of the atmospheric drivers of the Benguela upwelling with the GENUS-MOM simulations highlighted that an adequate wind forcing is critical to realistically simulated upwelling in an ocean-only model. In the phase I of GENUS, the GENUS-MOM model was driven by the winds simulated by the regional atmosphere-only model REMO. This caused problems in the dynamics of the GENUS-MOM model so that the authors of the simulation decided to switch to QuikSCAT wind as forcing. QuikSCAT covers only 13 years so that decadal variability and trend cannot be analysed with the current GENUS-MOM simulation. Therefore, a new simulation with the regional atmosphere-only model CCLM (COSMO-CLM, Climate limited-area modelling) was run at the Helmholtz-Zentrum Geesthacht to provide an atmospheric forcing over a longer period than satellite data being available. This simulation covers 34 years (1979–2012) and has a very high spatial resolution – 0.07 degree a finer resolution as REMO (min 0.22 degree). It also uses the spectral nudging method, so that the global atmosphere data set (ERA-Interim) is not only driving the simulation at its boundaries but at large spatial scales inside of the model domain, too. A comparison between the trends and variability of the simulated wind stress in this high-resolution simulation and in other low resolution simulations could provide indications as to why the upwelling-favourable winds do not respond as expected to changing land-sea contrast.

A next step would be to drive the GENUS-MOM model with this CCLM atmospheric forcing do detect how fine the resolution of the wind forcing has to be for the upwelling dynamics as well as the added value of spectral nudging for upwelling.

Bibliography

Bakun, A. (1990). Global Climate Change and Intensification of Coastal Ocean Upwelling. *Science*, 247:198–201, doi:10.1126/science.247.4939.198.

Bakun, A., Field, D. B., Redondo-Rodriguez, A., and Weeks, S. J. (2010). Greenhouse gas, upwelling-favorable winds, and the future of coastal ocean upwelling ecosystems. *Global Change Biol.*, 16:1213–1228, doi:10.1111/j.1365-2486.2009.02094.x.

Bakun, A. and Nelson, C. S. (1991). The Seasonal Cycle of Wind-Stress Curl in Subtropical Eastern Boundary Current Regions. *J. Phys. Oceanogr.*, 21:1815–1834, doi:10.1175/1520-0485(1991)021¡1815:TSCOWS¿2.0.CO;2.

Bakun, A. and Weeks, S. J. (2004). Greenhouse gas builtup, sardines, submarine eruptions and the possibility of abrupt degradation of intense marine upwelling ecosystems. *Ecol. Lett.*, 7:1015–1023, doi:10.1111/j.1461-0248.2004.00665.x.

Barnston, A. G., Glantz, M. H., and He, X. (1999). Predictive Skill of Statistical and Dynamical Climate Models in SST Forecasts during the 1997-98 El Niño Episode and the 1998 La Niña Onset. *B. Am. Meteorol. Soc.*, 80(2):217–243, doi:10.1175/1520-0477(1999)080<0217:PSOSAD>2.0.CO;2.

Barnston, A. G., Tippett, M. K., L'Heureux, M. L., Li, S., and DeWitt, D. G. (2012). Skill of Real-Time Seasonal ENSO Model Predictions During 2002-11. *B. Am. Meteorol. Soc.*, 93:631–651, doi:10.1175/BAMS-D-11-00111.1.

Belmadani, A., Echevin, V., Codron, F., Takahashi, K., and Junquas, C. (2014). What dynamics drive future wind scenarios for coastal upwelling off Peru and Chile? *Clim. Dyn.*, 43:1893–1914, doi:10.1007/s00382-013-2015-2.

Blamey, L. K., Shannon, L. J., Bolton, J. J., Crawford, R. J. M., Dufois, F., Evers-King, H., Griffiths, C. L., Hutchings, L., Jarre, A., Rouault, M., Watermeyer, K. E., and Winker, H. (2015). Ecosystem changes in the southern Benguela and the underlying processes. *J. Mar. Syst.*, 144:9–29, doi:10.1016/j.jmarsys.2014.11.006.

Blanke, B., Speich, S., Bentamy, A., Roy, C., and Sow, B. (2005). Modelling the structure and variability of the southern Benguela upwelling using QuikSCAT wind forcing. *J. Geophys. Res.*, 110:C07018, doi:10.1029/2004JC002529.

Cai, W., Borlace, S., Lengaigne, M., Van Rensch, P., Collins, M., Vecchi, G., Timmermann, A., Santos, A., McPhaden, M. J., Wu, L., England, M. H., Wang, G., Guilyardi, E., and Jin, F.-F. (2014). Increasing frequency of extreme El Niño events due to greenhouse warming. *Nature Climate Change*, 4:111–116, doi:10.1038/NCLIMATE2100.

Casey (2010). *Oceanography from Space*, chapter The Past, Present, and Future of the AVHRR Pathfinder SST Program, pages 273–287. Springer Netherlands.

Chaigneau, A., Eldin, G., and Dewitte, B. (2009). Eddy activity in the four major upwelling systems from satellite altimetry (1992-2007). *Prog. Oceanogr.*, 83:117–123, doi:10.1016/j.pocean.2009.07.012.

Chavez, F. P. and Messié, M. (2009). A comparison of Eastern Boundary Upwelling Ecosystems. *Prog. Oceanogr.*, 83:80–96, doi:10.1016/j.pocean.2009.07.032.

Chelton, D. B., Schlax, M. G., Freilich, M. H., and Milliff, R. F. (2004). Satellite measurements reveal persistent small-scale features in ocean winds. *Science*, 303:978–983, doi:10.1126/science.1091901.

Chen, Z., Yan, X.-H., Jo, Y.-H., Jiang, L., and Jiang, Y. (2012). A study of Benguela upwelling system using different upwelling indices derived from remotely sensed data. *Cont. Shelf Res.*, 45:27–33, doi:10.1016/j.csr.2012.05.013.

Chiang, J. C. H. and Vimont, D. J. (2004). Analogous Pacific and Atlantic Meridional Modes of Tropical Atmosphere-Ocean Variability. *J. Climate*, 17:4143–4158, doi:10.1175/JCLI4953.1.

Colas, F., Capet, X., McWilliams, J. C., and Shchepetkin, A. (2008). 1997-1998 El Niño off Peru: A numerical study. *Prog. Oceanogr.*, 79:138–155, doi:10.1016/j.pocean.2008.10.015.

Colberg, F. and Reason, C. J. C. (2006). A model study of the Angola Benguela Frontal Zone: Sensitivity to atmospheric forcing. *Geophys. Res. Lett.*, 33:L19608, doi:10.1029/2006GL027463.

Crowley, T. J., Zielinski, G., Vinther, B., Udisti, R., Kreutz, K., Cole-Dai, J., and Castellano, E. (2008). Volcanism and the Little Ice Age. *PAGES News*, 16:22–23.

Danabasoglu, G., Bates, S. C., Briegleb, B. P., Jayne, S. R., Jochum, M., Large, W. G., Peacock, S., and Yeager, S. G. (2012). The CCSM4 Ocean Component. *J. Climate*, 25:1361–1389, doi:10.1175/JCLI-D-11-00091.1.

Dee, D. P., Uppala, S. M., Simmons, A. J., Berrisford, P., Poli, P., Kobayashi, S., Andrae, U., Balmaseda, M. A., Balsamo, G., Bauer, P., Bechtold, P., Beljaars, A. C. M., van de Berg, L., Bidlot, J., Bormann, N., Delsol, C., Dragani, R., Fuentes, M., Geer, A. J., Haimberger, L., Healy, S. B., Hersbach, H., Hólm, E. V., Isaksen, L., Kållberg, P., Köhler, M., Matricardi, M., McNally, A. P., Monge-Sanz, B. M., Morcrette, J.-J., Park, B.-K., Peubey, C., de Rosnay, P., Tavolato, C., Thépaut, J.-N., and Vitart, F. (2011). The ERA-Interim reanalysis: configuration and performance of the data assimilation system. *Q. J. Roy. Meteor. Soc.*, 137:553–597, doi:10.1002/qj.828.

Demarcq, H. (2009). Trends in primary production, sea surface temperature and wind in upwelling systems (1998-2007). *Prog. Oceanogr.*, 83:376–385, doi:10.1016/j.pocean.2009.07.022.

Deutsch, C., Brix, H., Ito, T., Frenzel, H., and Thompson, L. (2011). Climate-Forced Variability of Ocean Hypoxia. *Science*, 333:335–339, doi:10.1126/science.1202422.

Di Lorenzo, E., Miller, A. J., Schneider, N., and McWilliams, J. C. (2005). The Warming of the California Current System: Dynamics and Ecosystem Implications. *J. Phys. Oceanogr.*, 35:336–362, doi:10.1175/JPO-2690.1.

Doblas-Reyes, F. J., García-Serrano, J., Lienert, F., Pintó Biescas, A., and Rodrigues, L. R. L. (2013). Seasonal climate predictability and forecasting: status and prospects. *WIREs Clim. Change*, 4:245–268, doi:10.1002/wcc.217.

Dufois, F., Penven, P., Whittle, C. P., and Veitch, J. (2012). On the warm nearshore bias in Pathfinder monthly SST products over Eastern Boundary Upwelling Systems. *Ocean Model.*, 47:113–118, doi:10.1016/j.ocemod.2012.01.007.

Dufois, F. and Rouault, M. (2012). Sea surface temperature in False Bay (South Africa): Towards a better understanding of its seasonal and inter-annual variability. *Cont. Shelf Res.*, 43:24–35, doi:10.1016/j.csr.2012.04.009.

Ebisuzaki, W. (1997). A Method to Estimate the Statistical Significance of a Correlation When the Data Are serially Correlated. *J. Climate*, 10:2147–2153, doi:10.1175/1520-0442(1997)010<2147:AMTETS>2.0.CO;2.

Echevin, V., Goubanova, K., Belmadani, A., and Dewitte, B. (2012). Sensitivity of the Humboldt Current system to global warming: a downscaling experiment of the IPSL-SM4 model. *Climate Dyn.*, 38:761–774, doi:10.1007/s00382-011-1085-2.

Feistel, R., Hagen, E., and Grant, K. (2003). Climatic changes in the subtropical Southeast Atlantic: the St. Helena Island Climate Index (1893-1999). *Prog. Oceanogr.*, 59:321–337, doi:10.1016/j.pocean.2003.07.002.

Fennel, W., Junker, T., Schmidt, M., and Mohrholz, V. (2012). Response of the Benguela upwelling systems to spatial variations in the wind stress. *Coastl. Shelf Res.*, 45:65–77, doi:10.1016/j.csr.2012.06.004.

Fennel, W. and Lass, H. U. (2007). On the impact of wind curls on coastal currents. *J. Mar. Syst.*, 68:128–142, doi:10.1016/j.jmarsys.2006.11.004.

Fernández-Donado, L., González-Rouco, J. F., Raible, C. C., Ammann, C. M., Barriopedro, D., García-Bustamante, E., Jungclaus, J. H., Lorenz, S. J., Luterbacher, J., Phipps, S. J., Servonnat, J., Swingedouw, D., Tett, S. F. B., Wagner, S., P., Y., and Zorita, E. (2013). Large-scale temperature response to external forcing in simulations and reconstructions of the last millennium. *Clim. Past.*, 9:393–421, doi:10.5194/cp-9-393-2013.

Gent, P. R., Danabasoglu, G., Donner, L. J., Holland, M. M., Hunke, E. C., Jayne, S. R., Lawrence, D. M., Neale, R. B., Rasch, P. J., Vertensein, M., Worley, P. H., Yang, Z.-L., and Zhang, M. (2011). The Community Climate System Model Version 4. *J. Climate*, 24:4973–4991, doi:10.1175/2011JCLI4083.1.

Giorgetta, M. A., Jungclaus, J., Reick, C. H., Legutke, S., Bader, J., Böttinger, M., Brovkin, V., Crueger, T., Esch, M., Fieg, K., Dlushak, K., Gayler, V., Haak, H., Hollweg, H.-D., Ilyina, T., Kinne, S., Kornblueh, L., Matei, D., Mauritsen, T., Mikolajewiez, U., Mueller, W., Notz, D., Pithan, F., Raddatz, T., Rast, S., Redler, R., Roeckner, E., Schmidt, H., Schnur, R., Segschneider, J., Six, K. D., Stockhause, M., Timmreck, C., Wegner, J., Widmann, H., Wieners, K.-H., Claussen, M., Marotzke, J., and Stevens, B. (2013). Climate and carbon cycle changes from 1850 to 2100 in MPI-ESM simulations for the Coupled Model Intercomparison Project phase 5. *J. Adv. Model. Earth Syst.*, 5:572–597, doi:10.1002/jame.20038.

Gordon, S. L., Weiss, R. F., Smethie Jr, W. M., and Warner, M. J. (1992). Thermocline and intermediate water communication between the South Atlantic and Indian Ocean. *J. Geophys. Res.*, 97(C5):7223–7240, doi:10.1029/92JC00485.

Grodsky, S. A., Carton, J. A., and Nigam, S. (2012). Tropical Atlantic Biases in CCSM4. *J. Climate*, 25:3684–3701, doi:10.1175/JCLI-D-11-00315.1.

Gutierrez, D., Bouloubassi, I., Sifeddine, A., Purca, S., Goubanova, K., Graco, M., Field, D., Mejanelle, L., Velazco, F., Lorre, A., Salvattcci, R., Quispc, D., Vargas, G., Dewitte, B., and Ortlieb, L. (2011). Coastal cooling and increased productivity in the main upwelling zone off Peru since the mid-twentieth century. *Geophys. Res. Lett.*, 38:L07603, doi:10.1029/2010GL046324.

Haensler, A., Hagemann, S., and Jacob, D. (2011). Dynamical downscaling of ERA40 reanalysis data over southern Africa: added value in the simulation of the seasonal rainfall characteristics. *Int. J. Climatol.*, 31:2338–2349, doi:10.1002/joc.2242.

Hagen, E., Agenbag, J. J., and Feistel, R. (2005). The winter St. Helena climate index and extreme Benguela upwelling. *J. Mar. Syst.*, 57:219–230, doi:10.1016/j.jmarsys.2005.03.006.

Hagen, E., Feistel, R., Agenbag, J. J., and Ohde, T. (2001). Seasonal and interannual changes in Intense Benguela Upwelling (1982-1999). *Oceanol. Acta*, 24(6):557–568, doi:10.1016/s0399-1784(01)01173-2.

Ham, Y.-G., Kug, J.-S., and Park, J.-Y. (2013). Two distinct role of Atlantic SSTs in ENSO variability: North Tropical Atlantic SST and Atlantic Niño. *Geophys. Res. Lett.*, 40:4012–4017, doi:10.1002/grl.50729.

Hardman-Mountford, N. J., Richardson, A. J., Agenbag, J. J., Hagen, E., Nykjaer, L., Shillington, F. A., and Villacastin, C. (2003). Ocean climate of the South East Atlantic observed from satellite data and wind models. *Prog. Oceanogr.*, 59:181–221, doi:10.1016/j.pocean.2003.10.001.

Hartmann, D. L., Klein Tank, A. M. G., Rusticucci, M., Alexander, L. V., Brönnimann, S., Charabi, Y., Dentener, F. J., Dlugokencky, E. J., Easterling, D. R., Kaplan, A., Soden, B. J., Thorne, P. W., Wild, M., and Zhai, P. M. (2013). *Climate Change 2013: The Physical Science Basis. Contribution of Working Group I to the Fifth Assessment Report of the Intergovernmental Panel on Climate Change*, chapter Observations: Atmosphere and Surface, pages 159–254. Cambridge University Press, Cambridge, UK and New York, NY, USA.

Hegerl, G. C., Crowley, T. J., Hyde, W. T., and Frame, D. J. (2006). Climate sensitivity constrained by temperature reconstructions over the past seven centuries. *Nature*, 440:1029–1032, doi:10.1038/nature04679.

Hsueh, Y. and Kenney III, R. N. (1972). Steady Coastal Upwelling in a Continuously Stratified Ocean. *J. Phys. Oceanogr.*, 2:27–33, doi:10.1175/1520-0485(1972)002<0027:SCUIAC>2.0.CO;2.

Huang, H.-P., Robertson, A. W., and Kushnir, Y. (2005). Atlantic SST gradient and the influence of ENSO. *Geophys. Res. Lett.*, 32:L20706, doi:10.1029/2005GL023944.

Hutchings, L., van der Lingen, C. D., Shannon, L. J., Crawford, R. J. M., Verheye, H. M. S., Bartholomae, C. H., van der Plas, A. K., Louw, D., Kreiner, A., Ostrowski, M., Fidel, Q., Barlow, R. G., Lamont, T., Coetzee, J., Shillington, F., Veitch, J., Currie, J. C., and Monteiro, P. M. S. (2009). The Benguela Current: An ecosystem of four components. *Prog. Oceanogr.*, 83:15–32, doi:10.1016/j.pocean.2009.07.046.

Jenskins, G. M. and Watts, D. G. (1968). *Spectral Analysis and its Applications*. Holden-Day, San Francisco, USA.

Jones, J. M. and Widmann, M. (2004). Early peak in Antarctic oscillation Index. *Nature*, 432:290–291, doi:10.1038/432290b.

Jungclaus, J. H., Fischer, N., Haak, H., Lohmann, K., Marotzke, J., Matei, D., Mikolajewicz, U., Notz, D., and von Storch, J. S. (2013). Characteristics of the ocean simulations in MPIOM, the ocean component of the MPI-Earth system model. *J. Adv. Model. Earth Syst.*, 5:422–446, doi:10.1002/jame.20023.

Kalnay, E., Kanamitsu, M., Kistler, R., Collins, W., Deqaven, D., Gandln, L., Iredell, M., Saha, S., White, G., Woollen, J., Zhu, Y., Chelliah, M., Ebisuzaki, W., Higgins, W., Janowlak, J., Mo, K. C., Ropelewski, C., Wang, J., Leetmaa, A., Reynolds, R., Jenne, R., and Joseph, D. (1996). The NCEP/NCAR 40-year reanalysis project. *B. Am. Meteorol. Soc.*, 77:437–470, doi:10.1175/1520-0477(1996)077.

Kay, J. E., Deser, C., Phillips, A., Mai, A., Hannay, C., Strand, G., Arblaster, J. M., Bates, S. C., Danabasoglu, G., Edwards, J., Holland, M., Kushner, P., Lamarque, J.-F., Lawrence, D., Lindsay, K., Middleton, A., Munoz, E., Neale, R., Oleson, K., Polvani, L., and Vertenstein, M. (2015). The Community Earth System Model (CESM) Large Ensemble Project: A Community Resource for Studying Climate Change in the Presence of Internal Climate Variability. *B. Am. Meteorol. Soc.*, 96:1333–1349, doi:10.1175/BAMS-D-13-00255.1.

Kim, S. T., Cai, W., Jin, F.-F., and Yu, J.-Y. (2014). ENSO stability in coupled climate models and its association with mean state. *Clim. Dyn.*, 42:3313–3321, doi:10.1007/s00382-013-1833-6.

Labitzke, K. and van Loon, H. (1988). Associations between the 11-year solar cycle, the QBO and the atmosphere. Part I: the troposphere and stratosphere in the northern hemisphere in winter. *J. Atmos. Terr. Phys.*, 50(3):197–206, doi:10.1016/0021-9169(88)90068-2.

Lachkar, Z. and Gruber, N. (2012). A comparative study of biological production in eastern boundary upwelling systems using an artificial neural network. *Biogeoscience*, 9:293–308, doi:10.5194/bg-9-293-2012.

Laskar, J., Robutel, R., Joutel, F., Gastineau, M., Correia, A. C. M., and Levrard, B. (2004). A long-term numerical solution for the insolation quantities of the Earth. *Astron. Astrophys.*, 428:261–285, doi:10.1051/0004-6361:20041335.

Latif, M. and Grötzner, A. (2000). The equatorial Atlantic oscillation and its response to ENSO. *Clim. Dyn.*, 16:213–218, doi:10.1007/s003820050014.

Leduc, G., Herbert, C. T., Blanz, T., Martinez, P., and Schneider, R. (2010). Contrasting evolution of sea surface temperature in the Benguela upwelling system

under natural and anthropogenic climate forcings. *Geophys. Res. Lett.*, 37:L20705, doi:10.1029/2010GL044353.

Li, H. and von Storch, J.-S. (2013). On the Fluctuating Buoyancy Fluxes Simulated in a 1/10° OGCM. *J. Phys. Oceanogr.*, 43:1270–1287, doi:10.1175/JPO-D-12-080.1.

Lu, J., Vecchi, G. A., and Reichler, T. (2007). Expansion of the Hadley cell under global warming. *Geophys. Res. Lett.*, 34, doi:10.1029/2006GL028443.

Ma, J. and Xie, S.-P. (2013). Regional Patterns of Sea Surface Temperature Change: A Source of Uncertainty in Future Projections of Precipitation and Atmospheric Circulation. *J. Climate*, 26:2482–2501, doi:10.1175/JCLI-D-12-00283.1.

Macias, D., Landry, M. R., Gershunov, A., Miller, A. J., and Franks, P. J. S. (2012). Climatic Control of Upwelling Variability along the Western North-American Coast. *PLoS ONE*, 7:e30436, doi:10.1371/journal.pone.0030436.

Mackas, D. L., Strub, P. T., Thomas, A., and Montecino, V. (2006). *The Sea. The Global Coastal Ocean: Interdisciplinary Regional Studies and Syntheses*, chapter Eastern Ocean Boundaries Pan-Regional Overview, pages 21–59. Harvard Press.

Marshall, G. J. (2003). Trends in the Southern Annular Mode from Observations and Reanalyses. *J. Climate*, 16:4134–4143, doi:10.1175/1520-0442(2003)016<4134:TITSAM>2.0.CO;2.

Marsland, S. J., Haak, H., Jungclaus, J. H., Latif, M., and Röske, F. (2003). The Max-Planck-Institute global ocean/sea ice model with orthogonal curvilinear coordinates. *Ocean Model.*, 5:91–127, doi:10.1016/S1463-5003(02)00015-X.

McCabe, R. M., Hickey, B. M., Dever, E. P., and MacCready, P. (2015). Seasonal Cross-Shelf Flow Structure, Upwelling Relaxation, and the Alongshelf Pressure Gradient in the Northern California Current System. *J. Phys. Oceanogr.*, 45(1):209–227, doi:10.1175/JPO-D-14-0025.1.

McCartney, M. S. (1982). The subtropical recirculation of Mode Waters. *J. Mar. Res.*, 40:427–464.

McGregor, H. V., Dima, M., Fischer, H. W., and Mulitza, S. (2007). Rapid 20th-Century Increase in Coastal Upwelling off Northwest Africa. *Science*, 315:637–639, doi:10.1126/science.1134839.

Mohrholz, V., Batholomae, C. H., van der Plas, A. K., and Lass, H. U. (2008). The seasonal variability of the northern Benguela undercurrent and its relation to the oxygen budget on the shelf. *Cont. Shelf Res.*, 28:424–441, doi:10.1016/j.csr.2007.10.001.

Muller, A. A., Schmidt, M., Reason, C. J. C., Mohrholz, V., and Eggert, A. (2014). Computing transport flux budget along the shelf and across the shelf edge in the northern Benguela during summer (DJF) and winter (JJA). *J. Mar. Syst.*, 140:82–91, doi:10.1016/j.jmarsys.2014.02.007.

Myhre, G., Shindell, D., Bréon, F.-M., Collins, W., Fuglestvedt, J., Huang, J., Koch, D., Lamarque, J.-F., Lee, D., Mendoza, B., Nakajima, T., Robock, A., Stephens, G., T., T., and Zhang, H. (2013). *Climate Change 2013: The Physical Science Basis. Contribution of Working Group I to the Fifth Assessment Report of the Intergovernmental Panel on Climate Change*, chapter Anthropogenic and Natural Radiative Forcing, pages 659–740. Cambridge University Press, Cambridge, United Kingdom and New York, NY, USA.

Narayan, N., Paul, A., Mulitz, S., and Schulz, M. (2010). Trends in coastal upwelling intensity during the late 20th century. *Ocean Sci.*, 6:815–823, doi:10.5194/os-6-815-2010.

Nelson, G. and Hutchings, L. (1983). The Benguela Upwelling Area. *Prog. Oceanogr.*, 12:333–356, doi:10.1016/0079-6611(83)90013-7.

Otto-Bliesner, B. L., Brady, E. C., Fasullo, J., Jahn, A., Landrum, L., Stevenson, S., Rosenbloom, N., Mai, A., and Strand, G. (2015). Climate Variability and Change since 850 C.E.: An Ensemble Approach with the Community Earth System Model (CESM). *B. Am. Meteorol. Soc.*, in press, doi:10.1175/BAMS-D-14-00233.1.

Pardo, P. C., Parín, X. A., Gilcoto, M., Farina-Busto, L., and Pérez, F. F. (2011). Evolution of upwelling systems coupled to the long-term variability in sea surface temperature and Ekman transport. *Clim. Res.*, 48:231–246, doi:10.3354/cr00989.

Parrish, R. H., Bakun, A., Husby, D. M., and Nelson, C. S. (1983). *Proceedings of the Expert Consultation to Examine Changes in Abundance and Species Composition of Neritic Fish Resources*, volume Report 291, chapter Comparative climatology of selected environmental processes in relation to eastern boundary current pelagic fish reproduction, pages 731–777. Food and Agriculture Organization of the United Nations, Rome.

Pauly, D. and Christensen, V. (1995). Primary production required to sustain global fisheries. *Nature*, 374:255–257, doi:10.1038/374255a0.

Pongratz, J., Raddatz, T., Reick, C. H., Esch, M., and Claussen, M. (2009). Radiative forcing from anthropogenic land cover changes since A.D. 800. *Geophys. Res. Lett.*, 36:L02709, doi:10.1029/2008GL036394.

Rathmann, J. (2008). *Klima- und Zirkulationsvariabilität im südhemisphärischen Afrika seit Beginn des 20. Jahrhunderts*. PhD thesis, Universität Augsburg.

Rayner, N. A., Parker, D., Horton, E., Folland, C. K., Alexander, L., Rowell, D. P., Kent, E. C., and Kaplan, A. (2003). Global analyses of sea surface temperature, sea ice, and night marine air temperature since the late nineteenth century. *J. Geophys. Res.*, 108:4407, doi:10.1029/2002JD002670.

Richter, I. (2015). Climate model biases in the eastern tropical ocean: causes, impacts and ways forward. *WIREs Clim. Change*, 6:345–358, doi: 10.1002/wcc.338.

Richter, I., Behera, S., Masumoto, Y., Taguchi, B., Komori, N., and Yamagata, T. (2010). On the triggering of Benguela Niños: Remote equatorial versus local influences. *Geophy. Res. Lett.*, 37:L20604, doi:10.1029/2010GL044461.

Richter, I. and Xie, S.-P. (2008). On the origin of equatorial Atlantic biases in coupled general circulation models. *Clim. Dyn.*, 31:587–598, doi:10.1007/s00382-008-0364-z.

Risien, C. M. and Chelton, D. B. (2008). A Global Climatology of Surface Wind and Wind Stress Fields from Eight Years of QuikSCAT Scatterometer Data. *J. Phys. Oceanogr.*, 38:2379–2413, doi:10.1175/2008JPO3881.1.

Risien, C. M., Reason, C. J. C., and Shillington, F. A. (2004). Variability in satellite winds over the Benguela upwelling system during 1999-2000. *J. Geophys. Res.*, 109:C03010, doi:10.1029/2003JC001880.

Rodríguez-Fonseca, B., Polo, I., García-Serrano, J., Losada, T., Mohino, E., Mechoso, C. R., and Kucharski, F. (2009). Are Atlantic Niños enhancing Pacific ENSO events in recent decades? *Geophys. Res. Lett.*, 36:L20705, doi:10.1029/2009GL040048.

Rouault, M., Illig, S., Bartholomae, C., Reason, C. J. C., and Bentamy, A. (2007). Propagation and origin of warm anomalies in the Angola Benguela upwelling system in 2001. *J. Mar. Syst.*, 68:473–488, doi:10.1016/j.jmarsys.2006.11.010.

Rouault, M., Pohl, B., and Penven, P. (2010). Coastal oceanic climate change and variability from 1982 to 2009 around South Africa. *Afr. J. Mar. Sci.*, 32(2):237–246, doi:10.2989/1814232X.2010.501563.

Rykaczewski, R. and Dunne, J. P. (2010). Enhanced nutrient supply to the California Current Ecosystem with global warming and increased stratification in an earth system model. *Geophys. Res. Lett.*, 37:L21606, doi:10.1029/2010GL045019.

Rykaczewski, R. R. and Checkley, D. M. (2008). Influence of ocean winds on the pelagic ecosystem in upwelling regions. *Proc. Nat. Acad. Sci.*, 105(6):1965–1970, doi:10.1073/pnas.0711777105.

Rykaczewski, R. R., Dunne, J. P., Sydeman, W. J., García-Reyes, M., Black, B. A., and Bongrad, S. J. (2015). Poleward displacement of coastal upwelling-favourable winds in the ocean's eastern boundary currents through the 21st century. *Geophys. Res. Lett.*, 42:6424–6431, doi:10.1002/2015GL064694.

Santos, F., Gomez-Gesteira, M., deCastro, M., and Alvarez, I. (2012). Differences in coastal and oceanic SST trends due to the strengthening of coastal upwelling along the Benguela current systems. *Cont. Shelf Res.*, 34:79–86, doi:10.1016/j.csr.2011.12.004.

Schmidt, G. A., Jungclaus, J. H., Ammann, C. M., Bard, E., Braconnot, P., Crowley, T. J., Delaygue, G., Joos, F., Krivova, N. A., Muscheler, R., Otto-Bliesner, B. L., Pongratz, J., Shindell, D. T., Solanki, S. K., Steinhilber, F., and Vieira, L. E. A. (2011). Climate forcing reconstructions for use in PMIP simulations of the last millennium (v1.0). *Geosci. Model Dev.*, 4:33–45, doi:10.5194/gmd-4-33-2011.

Schmidt, M. and Eggert, A. (2012). Meereswissenschaftliche Berichte, Marine Science Reports: A regional 3D coupled ecosystem model of Benguela upwelling system. Technical Report 87, Leibniz-Institut für Ostseeforschung Warnemünde (IOW).

Serazin, G., Penduff, T., Gregorio, S., Barnier, B., Molines, J., and Terray, L. (2015). Intrinsic variability of sea-level from global 1/12° ocean simulations: spatio-temporal scales. *J. Climate*, 28:4279–4292, doi:10.1175/JCLI-D-14-00554.1.

Shannon, L. V. (1985). The Benguela Ecosystem Part I: Evolution of the Benguela, physical features and processes. *Oceanogr. Mar. Biol.: Annual Review*, 23:105–182.

Shannon, L. V., Boyd, A. J., Brundrit, G. B., and Taunton-Clark, J. (1986). On the existence of an El Niño-type Phenomenon in the Benguela System. *J. Mar. Res.*, 44:495–520, doi:10.1357/002224086788403105.

Shannon, L. V. and Nelson, G. (1996). *The South Atlantic: Present and Past Circulation*, chapter The Benguela: Large Scale Features and Processes and System Variability, pages 163–210. Springer-Verlag.

Shannon, L. V. and O'Toole, M. J. (2003). *Large Marine Ecosystems of the World: Trends in Exploitation*, chapter Sustainability of the Benguela: ex Africa semper aliquid novi, pages 227–253. Elsevier.

Small, R. J., Curchitser, E., Hedstrom, K., Kauffman, B., and Large, W. G. (2015). The Benguela Upwelling System: Quantifying the Sensitivity to Resolution and Coastal Wind Representation in a Global Climate Model. *J. Climate*, 28:9409–9432, doi:10.1175/JCLI-D-15-0192.1.

Smith, S. R., Legler, D. M., and Verzone, K. V. (2001). Quantifying Uncertainties in NCEP Reanalyses Using High-Quality Research Vessel Observations. *J. Climate*, 14:4062–4072, doi:10.1175/1520-0442(2001)014<4062:QUINRU>2.0.CO;2.

Stocker, T. F., Qin, D., Plattner, G.-K., Alexander, L. V., Allen, S. K., Bindoff, N. L., Bréon, F.-M., Church, J. A., Cubasch, U., Emori, S., Forster, P., Friedling-stein, P., Gillett, N., Gregory, J. M., Hartmann, D. L., Jansen, E., Kirtman, B., Knutti, R., Krishna Kumar, K., Lemke, P., Marotzke, J., Masson-Delmotte, V., Meehl, G. A., Mokhov, I. I., Piao, S., Ramaswamy, V., Randall, D., Rhein, M., Rojas, M., Sabine, C., Shindell, D., Talley, L. D., Vaughan, D. G., and Xie, S.-P. (2013). *Climate Change 2013: The Physical Science Basis. Contribution of Working Group I to the Fifth Assessment Report of the Intergovernmental Panel on Climate Change*, chapter Technical Summary, pages 33–115. Cambridge University Press, Cambridge, United Kingdom and New York, NY, USA.

Sydeman, W. J., García-Reyes, M., Schoeman, D. S., Rykaczewski, R. R., Thompson, S. A., Black, B. A., and Bograd, S. J. (2014). Climate change and wind intensification in coastal upwelling ecosystems. *Science*, 345:77–80, doi:10.1126/science.1251635.

Taylor, K. E., Stouffer, R. J., and Meehl, G. (2012). An overview of CMIP5 and the experiment design. *B. Am. Meteorol. Soc.*, 93:485–498, doi:10.1175/BAMS-D-11-00094.1.

Tett, S. F. B., Betts, R., Crowley, T. J., Gregory, J., Johns, T. C., Jones, A., Osborn, T. J., Öström, E., D.J., R., and Woodage, M. J. (2007). The impact of natural and anthropogenic forcings on climate and hydrology since 1550. *Clim. Dyn.*, 28:3–34, doi:10.1175/BAMS-D-13-00255.1.

Tim, N., Zorita, E., and Hünicke, B. (2015). Decadal variability and trends of the Benguela Upwelling System as simulated in a high ocean-only simulation. *Ocean Sci.*, 11:483–502, doi:10.5194/os-11-483-2015.

Tomczak, M. and Godfrey, J. S. (2003). *Regional Oceanography: An Introduction.* Number ISBN: 8170353068. Daya Publishing House, Delhi, 2nd edition.

Vecchi, G. A., Soden, B. J., Wittenberg, A. T., Held, I. M., Leetmaa, A., and Harrison, M. J. (2006). Weakening of tropical Pacific atmospheric circulation due to anthropogenic forcing. *Nature*, 441:73–76, doi:10.1038/nature04744.

Vecchi, G. A. and Wittenberg, A. T. (2010). El Niño and our future climate: where do we stand? *WIREs Clim. Change*, 1:260–270, doi:10.1002/wcc.33.

Veitch, J., Penven, P., and Shillington, F. (2010). Modeling Equilibrium Dynamics of Benguela Current System. *J. Phys. Oceanogr.*, 40:1942–1964, doi:10.1175/2010JPO4382.1.

Vieira, L. E. A., Solanki, S. K., Krivova, N. A., and Usoskin, I. (2011). Evolution of solar irradiance during the Holocene. *Astron. Astrophys.*, ArXiv:1103.4958v2, 531, doi:10.1051/0004-6361/201015843.

von Storch, J.-S., Eden, C., Fast, I., Haak, H., Hernández-Deckers, D., Maier-Reimer, E., Marotzke, J., and Stammer, D. (2012). An Estimate of the Lorenz Energy Cycle for the World Ocean Based on the 1/10° STORM/NCEP Simulation. *J. Phys. Oceanogr.*, 42:2185–2205, doi:10.1175/JPO-D-12-079.1.

Wang, C. (2006). An overlooked feature of tropical climate: Inter-Pacific-Atlantic variability. *Geophy. Res. Lett.*, 33:L12702, doi:10.1029/2006GL026324.

Wang, C., Zhang, L., Lee, S.-K., Wu, L., and Mechoso, C. R. (2014). A global perspective on CMIP5 climate model biases. *Nature Climate Change*, 4:201–205, doi:10.1038/NCLIMATE2118.

Wang, D., Gouhier, T. C., Menge, B. A., and Ganguly, A. R. (2015). Intensification and spatial homogenization of coastal upwelling under climate change. *Nature*, 518:390–394, doi:10.1038/nature14235.

Wolter, K. and Timlin, M. S., editors (1993). *Monitoring ENSO in COADS with a Seasonally Adjusted Principal Component Index*. Proceedings of the 17th Climate Diagnostics Workshop, Norman, OK, NOAA/NMC/CAC, NSSL, Oklahoma Climate Survec, CIMMS and the School of Meteorology, University of Oklahoma: Norman, OK.

List of Figures

List of Tables

Acknowledgements

First of all, I would like to thank Dr. Eduardo Zorita, my thesis supervisor, and Dr. Birgit Hünicke for their supervision, their help and support in the daily work. Their knowledge about climate research in general, about writing manuscripts, statistics, and about my PhD topic were inspiring and supporting.

My grateful thanks go to Prof. Dr. Kay-Christian Emeis, reviewer of my thesis, my panel chair, and the coordinator of the GENUS (Geochemistry and Ecology of the Namibian Upwelling System) project in the context of which my thesis was conducted. His comments and suggestions during the panel meetings and the GENUS meetings provided fruitful input from another perspective.

I would like to thank Svenja Bierstedt with whom I shared not only my office but also all the things a PhD comes along with. Dealing with new situations together was helpful and fun.

Furthermore, I am thankful for the position offered by the Helmholtz-Zentrum Geesthacht and for the chance to be a PhD student at the School of Integrated Climate System Science (SICSS) of the Cluster of Excellence on Integrated Climate System Analysis and Prediction (CliSAP) in Hamburg.

The GENUS project and thus my thesis were funded by The German Federal Ministry of Education and Research (BMBF, Germany). I would like to thank the GENUS II project members, especially Dr. Anja Eggert and Dr. Martin Schmidt from the Leibniz Institute for Baltic Sea Research Warnemünde (IOW).

Many thanks go to Nele von Pein for proof-reading this work.

Special thanks go to my parents, my family and friends for supporting me and their believe in me and my way. Especialmente estoy muy agradecida a mi esposo, Demetrio, que siempre está a mi lado ayudando, apoyando y respaldándome.

Aus dieser Dissertation hervorgegangene Vorveröffentlichungen

List of Publications

Tim, N., Zorita, E., and Hünicke, B. (2015): Decadal variability and trends of the Benguela upwelling system as simulated in a high-resolution ocean simulation. *Ocean Sci.*, 11:483–502, doi:10.5194/os-11-483-2015.

Tim, N., Zorita, E., Hünicke, B., Yi, X., and Emeis, K.-C. (2015): Imprint of external climate forcing on coastal upwelling in past and future climate. *Ocean Sci. Discuss.*, 12:2899–2930, doi:10.5194/osd-12-2899-2015.

Yi, X., Hünicke, B., Tim, N., and Zorita, E. (2015): The relationship between Arabian Sea upwelling and Indian monsoon revisited. *Ocean Sci. Discuss.*, 12:2683–2704, doi:10.5194/osd-12-2683-2015.

Eidesstattliche Versicherung

Declaration on Oath

Hiermit erkläre ich an Eides statt, dass ich die vorliegende Dissertationsschrift selbst verfasst und keine anderen als die angegebenen Quellen und Hilfsmittel benutzt habe.

I hereby declare, on oath, that I have written the present dissertation by myself and have not used other than the acknowledged resources and aids.

Hamburg, 1. Oktober 2015